Iterative Leakage-Based Precoding for Multiuser-MIMO Systems

Eric Sollenberger

Thesis submitted to the faculty of the Virginia Polytechnic Institute and State University
in partial fulfillment of the requirements for the degree of

Master of Science
In
Electrical Engineering

Michael Buehrer
Carl Dietrich
Harpreet Dhillon

May 5, 2016
Blacksburg, VA

Keywords: multiuser, MIMO, linear precoding, leakage, imperfect CSI, LTE-A

Iterative Leakage-Based Precoding for Multiuser-MIMO Systems

Eric Sollenberger

ABSTRACT

This thesis investigates the application of an iterative leakage-based precoding algorithm to practical multiuser-MIMO systems. We consider the effect of practical impairments including imperfect channel state information, transmit antenna correlation, and time-varying channels. Solutions are derived which improve performance of the algorithm with imperfect channel state information at the transmitter by leveraging knowledge of the second-order statistics of the error. From this work we draw a number of conclusions on how imperfect channel state information may impact the system design including the importance of interference suppression at the receiver and the selection of the number of co-scheduled users. We also demonstrate an efficient approach to improve the convergence of the algorithm when using interference-rejection-combining receivers. Finally, we conduct simulations of an LTE-A system employing the improved algorithm to show its utility for modern communication systems.

Iterative Leakage-Based Precoding for Multiuser-MIMO Systems

Eric Sollenberger

General Audience Abstract

This thesis investigates several aspects of a particular method by which multiple users can share radio resources within a wireless system i.e. they may operate on the same frequency and at the same time. This is a desirable capability in modern wireless systems because it improves the efficiency of radio spectrum usage. Radio spectrum has become a very expensive resource in recent years so achieving high efficiency is crucial. Our investigation led us to propose several modifications to the aforementioned method which demonstrated improved performance under certain practical conditions. We further demonstrated the effects of several common system impairments and provided insight into how these impairments effect the system design. Finally, we demonstrated that using this method provides significant gains when used for the latest cellular technology.

Acknowledgements

To my advisor Dr. R. Michael Buehrer, I thank you for giving me the opportunity to work with you on this thesis. Your insight and guidance have been instrumental in ensuring its quality and to my personal growth as a researcher in the field of wireless communications. I have always left our weekly meetings with a renewed sense of purpose and focus. The course I took with you on MIMO systems brought clarity to this complex subject matter thanks to your superb teaching abilities and willingness to work with your students.

To the members of my committee, Dr. Carl Dietrich and Dr. Dhillon, I thank you for your advice and support over the past two years. Your mentorship has been a great help in navigating my life as a graduate student. My understanding of wireless communications fundamentals and software-defined radio have benefitted greatly from the courses I've taken with you and the discussions we've had.

To my parents, I thank you for your unconditional love and support and the role-models you have been for me. I would not have made it to this point if it weren't for you.

Contents

List of Abbreviations

BD-ZF	Block-diagonal zero-forcing
BER	Bit error rate
BLER	Block error rate
CSIT	Channel state information at the transmitter
CSIR	Channel state information at the receiver
cSLNR	Conventional signal-to-leakage-and-noise ratio
DMRS	Demodulation reference signals
eNB	Evolved Node B
FFT	Fast Fourier transform
HARQ	Hybrid automatic repeat request
IFFT	Inverse fast Fourier transform
IRC	Interference-rejection-combining
iSLNR	Iterative signal-to-leakage-and-noise-ratio
LS	Least squares
LTE-A	Long Term Evolution Advanced
MF	Matched filter
MIMO	Multiple-input-multiple-output
MMSE	Minimum mean square error
MSE	Mean square error
mSLNR	Modified signal-to-leakage-and-noise ratio
MUI	Multiuser-interference
MU-MIMO	Multiuser multiple-input-multiple-output
OFDM	Orthogonal frequency division multiplexing
QAM	Quadrature amplitude modulation
QPSK	Quadrature phase shift keying
RB	Resource block
SINR	Signal-to-interference-and-noise ratio
SLNR	Signal-to-leakage-and-noise ratio
SNR	Signal-to-noise ratio
SU-MIMO	Single-user multiple-input-multiple-output
TM	Transmission mode
UE	User equipment
ZF	Zero-forcing

List of Figures

Chapter 1

Introduction

In recent years there has been significant work done in the area of multi-user multiple-input multiple-output (MU-MIMO) techniques for wireless communication systems. Ideally MU-MIMO will achieve significant system sum-rate gains compared to single-user MIMO (SU-MIMO) by spatially multiplexing multiple users onto a common set of radio resources. Indeed MU-MIMO has already been incorporated into some of the more prominent wireless standards *e.g.*, LTE [1] and IEEE 802.11 [2], and some of the promised gains have been realized. That being said, there are still improvements that can be made to realize the full potential of MU-MIMO. For the downlink, one of the most pressing design challenges is efficiently suppressing the multi-user interference that will naturally occur between co-channel users using the spatial degrees of freedom afforded from having multiple transmit antennas. While it is well known that Dirty Paper Coding (DPC), originally proposed in [3], is the optimal precoding technique in terms of sum-rate, it is typically considered to be prohibitively complex. For this reason, suboptimal but much lower-complexity linear precoding schemes are an attractive alternative.

A number of linear precoding schemes have been proposed based on various optimization criteria. Zero-forcing and block-diagonal zero-forcing [4] constrain the problem to create zero multiuser-interference (MUI). This is accomplished by ensuring that the precoding matrix for each user lies in the null-space of the channel for all other users. While zero MUI sounds good, these schemes give no consideration to the noise present at the receivers which degrades their performance. Regularized zero-forcing schemes have been proposed as a way of accounting for the noise in the low SNR regime [5]. The concept of leakage-based precoding was proposed in [6] and later extended to consider noise using the signal-to-leakage-and-noise ratio (SLNR) metric [7]. The solution presented in [7] is referred to as the conventional SLNR precoding scheme (cSLNR) in this thesis. The SLNR metric is useful in that it is closely related to the signal-to-interference-and-noise ratio (SINR) which ultimately determines the performance of the wireless links, but it

decouples the user precoding matrices which can be problematic for SINR maximization schemes. It also has the benefit of not requiring the number of transmit antennas to be equal to or greater than the total number of receive antennas, whereas the other schemes mentioned do impose such a requirement. The SLNR metric was used in an iterative algorithm (iSLNR) in [8] which considers the receiver processing and provides substantial gains for non-full-rank transmissions. Another iterative approach was described in [9] which considers the MUI imposed on the user in addition to the leaked MUI, though this approach did not show as significant results. These schemes will be discussed in greater detail in a later section.

Interference suppression at the receiver can provide further gains when there is residual MUI after precoding. Receivers with this capability are referred to as interference-aware, whereas other receivers are interference-unaware. Interference-aware receivers include the interference-rejection-combining (IRC) receiver and the Max-log-MAP receiver [10]. Interference-unaware receivers include any of the traditional single-user receiver structures such as the matched-filter (MF), zero-forcing (ZF), and minimum-mean-square-error (MMSE) receivers. To be clear, the single-user ZF and MMSE receivers will suppress interference between multiple streams for a single user, but do not consider interference from other users' streams. The work in [10,11] demonstrated that when precoding matrices are quantized to a finite codebook, the interference-aware receivers provide significant gains over the interference-unaware receivers due to the residual MUI.

The transmitter and receiver techniques discussed above rely on accurate channel state information at the transmitter (CSIT) and at the receiver (CSIR) respectively to achieve good performance. Imperfect CSIT and/or CSIR can lead to significant system performance degradation. Since any practical system will have some degree of CSIT/CSIR error, these are compelling issues to consider. CSIT error can result as a culmination of several factors including channel estimation error, acquisition delay, non-reciprocal hardware, and time-varying channels. For this reason CSIT quality may not necessarily track with SNR. CSIR quality on the other hand, is often considered to track the SNR rather closely, particularly with low Doppler spread.

In this work we focus our attention on application of the iSLNR algorithm in a practical setting, that is, with practical system impairments and using techniques employed by current communications systems. We begin by considering the impairment of imperfect CSIT and CSIR. We then consider transmit antenna correlation and time-varying channels. Finally, we investigate the application of the iSLNR algorithm to an LTE-A system.

1.1 Contributions and Main Findings

In this section we summarize the contributions and main findings presented in this thesis.

- **Conventional SLNR Precoding with Imperfect CSIT**: We derive the solution for the precoding matrix which will maximize the SLNR in the presence of imperfect CSIT. We note that this problem was previously addressed in [7] using the same model for the imperfect CSIT, however our derivation leads us to a slightly different solution which is shown to provide better performance.
- **iSLNR Precoding with Imperfect CSIT**: The iSLNR algorithm will be degraded in two ways due to imperfect CSIT. First, there will be error between the receive filters calculated at the transmitter during the execution of the iSLNR algorithm and those actually employed at the receiver. The calculation of the precoding matrix will also be affected in a manner similar to the cSLNR scheme. By using the MMSE estimate of the receive filters and modifying the precoding matrix calculation we are able to improve performance of the iSLNR algorithm with imperfect CSIT.
- **MMSE Modification of CSIT**: The work in [12, 20] motivated us to investigate potential performance gains that might be realized by applying a linear modification to the CSIT so as to minimize its mean square error with respect to the true channel. We note that the solution presented in [12, 20] is not suitable for a practical system as the modification depends on knowledge of the true channel while the transmitter will only possess an estimate of the channel. We therefore derive the MMSE modification that avoids relying on the true channel, which

turns out to be a simple scalar factor. We apply this modification to both the conventional and iterative SLNR precoding schemes. It was shown to provide some marginal though non-negligible gain to the conventional scheme, though this gain did not translate to the iterative algorithm.

- **iSLNR Precoding with Imperfect CSIR**: It was shown that imperfect CSIR will lead to performance degradation for the iSLNR algorithm which relies on knowledge of the receive filters. At a sufficiently poor quality CSIR, the iSLNR algorithm actually performs worse than the cSLNR solution. Simulations showed that for systems where the number of transmit antennas is greater than or equal to the total number of receive antennas for all users the CSIR quality should be greater than the SNR in order to achieve significant gain using the iSLNR algorithm. For systems where the number of transmit antennas is less than the total number of receive antennas for all users this requirement is not as strict.
- **iSLNR Precoding with Transmit Antenna Correlation**: We investigated the performance of the iSLNR algorithm under varying degrees of transmit antenna correlation assuming a uniformly spaced linear array. It was first shown that increasing transmit antenna correlation will reduce the achieved system sum-rate. These simulations also led us to the only observed instance where the iSLNR algorithm produced non-monotonically increasing sum-rate per iteration. We observed that this situation arises only with IRC receivers and with high transmit antenna correlation. In this specific situation the algorithm provides a substantial gain for the first several iterations, but then begins to diverge, leading to decreasing system sum-rate per iteration.
- **iSLNR Precoding in Time-Varying Channels**: Time-varying channels effectively cause the CSIT quality to degrade over time. Having shown improvements in the iSLNR algorithm by considering imperfect CSIT, we investigate several possible approaches to apply this work to time-varying channels. It was shown that considering the CSIT quality on a per symbol basis will provide better convergence and achieve the best possible solution. Using the mean CSIT quality provides very quick convergence, but limits the sum-rate of

the converged solution. In general there is a tradeoff between achieving quick convergence and achieving the optimal solution.

- **Improved Convergence with IRC Receivers**: We show that convergence of the iSLNR algorithm with IRC receivers can be greatly improved by performing the first few iterations of the algorithm using the ZF receiver structure. Further sum-rate can be gained thereafter by performing additional iterations using the IRC receiver structure.
- **Selecting the Number of Co-Scheduled Users:** We compare the sum-rate achieved using the cSLNR and iSLNR algorithms for different numbers of co-scheduled users. With perfect CSIT the sum-rate is always maximized by co-scheduling the maximum number of users for the iSLNR algorithm. With imperfect CSIT we observe two operating regimes. In the low SNR regime it is better to co-schedule the maximum number of users for the iSLNR algorithm, but in the high SNR regime it is better to co-schedule fewer users. This is because in the high SNR regime the residual MUI due to imperfect CSIT dominates the performance. With fewer users each receiver can suppress the residual MUI but with many users they do not have sufficient degrees of freedom.
- **Application of iSLNR Precoding to LTE-A**: We demonstrate the application of the iSLNR algorithm to the LTE-A framework for downlink MU-MIMO via simulation. This result is useful as it includes the following key aspects of the LTE-A physical layer: (1) OFDM transmission with 3GPP channel models (2) LTE-A specific turbo coding (3) precoding performed with the subcarrier granularity defined by the standard and (4) the LTE-A specific technique for MU-MIMO channel estimation. We demonstrate performance with users employing both the MMSE and LS channel estimates. The MMSE estimate provides better overall performance and allows the iSLNR algorithm to provide greater gain which aligns with our analysis of the effect of CSIR error.

1.2 System Model

This section familiarizes the reader with the notation, terms, and assumptions necessary to discuss the subsequently presented theory related to MU-MIMO systems. First the

mathematical notations used throughout later sections are introduced. Next, the theoretical assumptions made by this work are detailed. Finally, the MU-MIMO system model and its related parameters are described.

1.2.1 Mathematical Annotation

Matrices are represented with boldface capital letters *e.g.* **A**, vectors are represented by boldface lowercase letters *e.g.* $\boldsymbol{a}$, and scalars are represented with non-boldface letters *e.g.*, a or A. The transpose of a matrix is denoted by $\boldsymbol{A}^T$, and the Hermitian of a matrix is denoted by $\boldsymbol{A}^*$. The trace of a matrix is denoted by $Tr[\boldsymbol{A}]$, and the Frobenius norms of vectors and matrices are denoted as $\|\boldsymbol{a}\|$ and $\|\boldsymbol{A}\|$ respectively. The matrix square root is denoted as $\boldsymbol{A}^{1/2}$.

1.2.2 General Assumptions

This section discusses the assumptions made in the analysis throughout this work along with a brief justification for each. Several of these assumptions are made based on the fact that modern wireless technologies predominantly use cyclic-prefixed orthogonal frequency division multiplexing (OFDM) which has some useful properties.

- *Frequency Flat Fading*: It is assumed that each symbol transmitted will experience a channel that can effectively be represented by a single complex coefficient. This is equivalent to saying that the utilized bandwidth is less than the channel coherence bandwidth or that the channel delay spread is much less than the symbol period. This is assumption is often made with the use of OFDM since the bandwidth of each subcarrier is relatively small, certainly within the coherence bandwidth of the channel.

- *Zero Inter-Symbol Interference*: It is assumed that symbols will not bleed into one another. In a single-carrier system this is similar to the previous assumption; that the channel delay spread must be much less than the symbol period. In an OFDM

system this assumption is met by inserting a cyclic prefix which is later discarded, removing and existing inter-symbol interference.

- *Zero Inter-Carrier Interference*: Inter-carrier interference can occur in OFDM systems due to frequency offset of the received signal and/or mobility in a multi-path propagation environment. User mobility will cause each path to have a unique Doppler shift resulting in what is referred to as the Doppler spectrum. This can cause the subcarriers of an OFDM signal to bleed into one another. This work assumes zero inter-carrier interference because MU-MIMO is only considered for low-mobility scenarios in which inter-carrier interference will be minimal.

- *Fixed Transmission Power*: It is assumed that the transmitter will use a fixed total transmission power, which is an obvious restriction for a practical system, but is also important to maintain fair comparisons between systems with different numbers of antennas and users. If doubling the number of transmit antennas doubles the transmit power then results are already skewed in favor of more antennas.

- *Known impairment statistics*: When a particular impairment is being considered, it is assumed that the statistics of this impairment are perfectly known at the transmitter. This includes CSIT error variance, noise power at the receiver, and max Doppler frequency of a time-varying channel.

The following assumptions are made for certain portions of the following analysis and results. In general the text will specify which impairments are currently being considered. Any impairment not mentioned implies that the related assumption has been made. This approach is used so that we can isolate and investigate single impairments at a time to better understand the effect of each individually.

- *Perfect Channel State Information at the Transmitter*: In the sections that do not explicitly state that imperfect CSIT is considered, it should be assumed that CSIT is perfect.

- *Perfect Channel State Information at the Receiverr*: In the sections that do not explicitly state that imperfect CSIR is considered, it should be assumed that CSIR is perfect.

- *Independent Spatial Channels*: In the sections that do not explicitly state that there is non-zero antenna correlation, it should be assumed that the channel is spatially independent.

- *Block Fading Channels*: In the sections that do not explicitly state that the channel is time-varying it should be assumed that the channel is modeled as a static Rayleigh fading channel to capture the statistics of fading.

  In the sections which do consider time-varying channels, we choose a timing structure to emulate the LTE frame so as to establish relevance of the results shown to real-world systems. Specifically, this implies 140 symbols transmitted over a period of 10 ms.

1.2.3 The MU-MIMO System

The MU-MIMO downlink system model consists of a single base station with N transmit antennas and K users. In general the i^{th} user will have M_i receive antennas and will utilize S_i spatial streams for communication, where $S_i \leq M_i$. The transmit symbols are denoted by the column vector $\boldsymbol{s}$ of length $\sum_{i=1}^{K} S_i$. The symbols for the i^{th} user are denoted $\boldsymbol{s}_i$ so the complete symbol vector $\boldsymbol{s}$ is of the form

$$\boldsymbol{s} = \begin{bmatrix} \boldsymbol{s}_1 \\ \boldsymbol{s}_2 \\ \vdots \\ \boldsymbol{s}_K \end{bmatrix} \tag{1}$$

These symbols will be mapped onto the transmit antennas by the precoding matrix $\boldsymbol{W}$ of dimension $N\text{x}\sum_{i=1}^{K} S_i$, which can also be expressed

$$\boldsymbol{W} = [\boldsymbol{W}_1 \boldsymbol{W}_2 \ldots \boldsymbol{W}_K] \tag{2}$$

where $\boldsymbol{W}_i$ is the precoding matrix for the i^{th} user of dimension $N\text{x}S_i$. To meet the fixed transmit power assumption mentioned earlier, each column of $\boldsymbol{W}$ is normalized such that equal power is provided per stream and the total transmit power is unity. We denote the transmit power per stream as

$$P_s = \left\|\boldsymbol{w}_j\right\|^2 = \frac{1}{\sum_{i=1}^{K} S_i} \tag{3}$$

where $\boldsymbol{w}_j$ is the j^{th} column of $\boldsymbol{W}$. The transmission propagates through a MIMO wireless channel which can be expressed as a complex-valued matrix $\boldsymbol{H}$ of dimension $\sum_{i=1}^{K} M_i \text{ x}N$. Each element of $\boldsymbol{H}$ is assumed to be a complex Gaussian random variable with zero mean and variance $\sigma_h^2 = 1$. The channel corresponding to the i^{th} user is denoted $\boldsymbol{H}_i$ and has dimension $M_i\text{x}N$. The full MIMO channel $\boldsymbol{H}$ can then be expressed by the collection of user channels as

$$\boldsymbol{H} = [\boldsymbol{H}_1, \boldsymbol{H}_2, \ldots, \boldsymbol{H}_K]^T \tag{4}$$

When discussing processing at the receiver it can be useful to define an equivalent channel based on the precoding and wireless channel, $\boldsymbol{G} = \boldsymbol{HW}$. The full matrix $\boldsymbol{G}$ is then of the form

$$\boldsymbol{G} = \begin{matrix} \boldsymbol{G}_{11} & \ldots & \boldsymbol{G}_{1K} \\ \vdots & \ddots & \vdots \\ \boldsymbol{G}_{K1} & \ldots & \boldsymbol{G}_{KK} \end{matrix} \tag{5}$$

Where $\boldsymbol{G}_{ij} = \boldsymbol{H}_i \boldsymbol{W}_j$, denoting the equivalent channel from the streams associated with the j^{th} user to the antennas of the i^{th} user. We simplify the notation for the equivalent channel of the desired streams, that is, from the i^{th} user's streams to the i^{th} user's antennas, as $\boldsymbol{G}_i = \boldsymbol{G}_{ii}$. Therefore, the received signal for the i^{th} user, denoted with the length M column vector $\boldsymbol{r}_i$, is given by:

$$\boldsymbol{r}_i = \boldsymbol{H}_i \boldsymbol{W} \boldsymbol{s} + \boldsymbol{n} = \boldsymbol{G}_i \boldsymbol{s}_i + \sum_{j \neq i} \boldsymbol{G}_{ij} \boldsymbol{s}_j + \boldsymbol{n} \tag{6}$$

where $\boldsymbol{n}$ is a length M_i column vector of complex Gaussian noise with zero mean and variance σ_n^2. Each user will perform receiver processing to arrive at a vector of decision statistics $\boldsymbol{z}_i$. A block diagram of the complete system is shown in Figure 1.1.

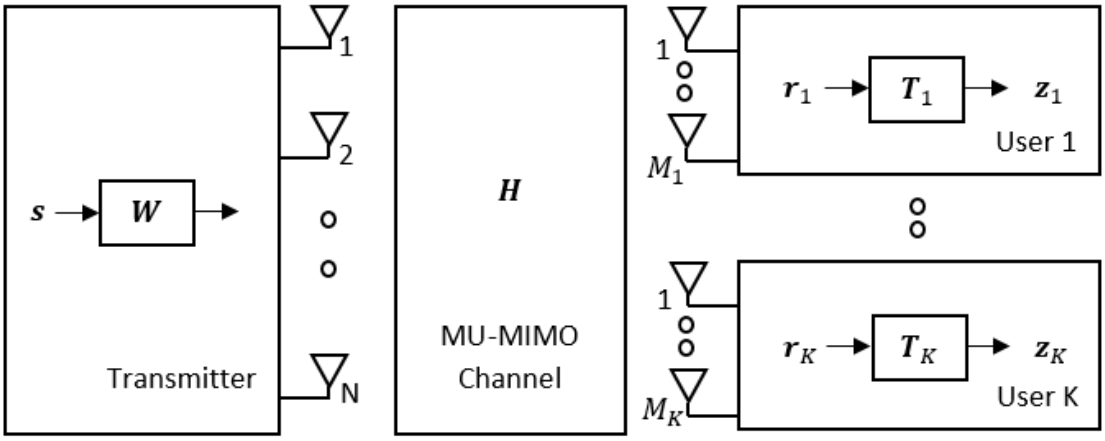

Figure 1.1: MU-MIMO system block diagram

We define the signal-to-noise ratio (SNR) as the total transmit power $P = P_s \sum S_i$ divided by the noise power at each receive antenna σ_n^2. Based on our constraint of unit total transmit power the SNR is equivalently expressed as $\frac{1}{\sigma_n^2}$.

1.2.4 Sum-Rate of the MU-MIMO System

Shannon's bound provides an upper limit on the rate at which reliable data communication can be achieved in a noisy channel, referred to as channel capacity, and given by

$$C = \log_2(1 + \gamma) \tag{7}$$

Where γ is the signal-to-noise ratio at the receiver. This work considers spatial multiplexing in MIMO systems with equal transmit power per stream. We note that equal power per stream is not the capacity achieving scheme in general. Iterative waterfilling techniques are often employed to achieve the system capacity [28], but this consideration

is outside the scope of this work. We instead consider the sum-rate of the system. The sum-rate of a SU-MIMO system employing spatial multiplexing is shown in equation 8.

$$R = \sum_{m=1}^{S} log2(1 + \gamma_m) \tag{8}$$

Where γ_m is the signal-to-interference-and-noise ratio (SINR) of the m^{th} stream, assuming Gaussian interference. In this case the interference is caused by the transmitted streams bleeding into one another, referred to as inter-stream-interference. Assuming the m^{th}stream is precoded at the transmitter using $\boldsymbol{w}_m$ and processed at the receiver using $\boldsymbol{t}_m$, the SINR of the m^{th} stream at the output of the receiver is given by

$$\gamma_m = \frac{\|\boldsymbol{t}_m \boldsymbol{H} \boldsymbol{w}_m\|^2}{M\sigma_n^2 + \sum_{n=1,n\neq m}^{S} \|\boldsymbol{t}_m \boldsymbol{H} \boldsymbol{w}_n\|^2} \tag{9}$$

Where $\boldsymbol{w}_n$ is the vector of precoding weights applied to the $n \neq m^{th}$ stream and is therefore a source of interference.

In a MU-MIMO system the sum-rate expression must include an additional summation across all of the co-scheduled users along with the summation of their possibly unique number of streams [13]. This is the expression which is used to calculate the sum-rate throughout the rest of this work and is shown in equation 10.

$$R = \sum_{i=1}^{K} \sum_{m=1}^{S_i} log2\left(1 + \gamma_{i,m}\right) \tag{10}$$

The SINR for each stream must also consider the interference from co-scheduled users. The SINR for the m^{th} stream of the i^{th} user is then

$$\gamma_{i,m} = \frac{\left\|\boldsymbol{t}_m \boldsymbol{H}_i \boldsymbol{w}_{i,m}\right\|^2}{M_i\sigma_n^2 + \sum_{n=1,n\neq m}^{S} \left\|\boldsymbol{t}_m \boldsymbol{H}_i \boldsymbol{w}_{i,n}\right\|^2 + \sum_{k=1,k\neq i}^{K} \|\boldsymbol{T}_m \boldsymbol{H}_i \boldsymbol{W}_k\|^2} \tag{11}$$

Analysis of MU-MIMO systems often limits users to a single stream each, in which case the SINR for the i^{th} user is

$$\gamma_i = \frac{\|\boldsymbol{t}_m \boldsymbol{H}_i \boldsymbol{W}_i\|^2}{M_i \sigma_n^2 + \sum_{k=1,k\neq i}^{K} \|\boldsymbol{t}_m \boldsymbol{H}_i \boldsymbol{W}_k\|^2} \quad (12)$$

Chapter 2

Background: Conventional MU-MIMO Techniques

Before extending analysis to incorporate practical considerations such as imperfect CSIT and CSIR, antenna correlation, and/or time-varying channels, it's important to develop a firm understanding of the conventional MU-MIMO system concepts including precoding techniques and receiver architectures in ideal conditions. This chapter reviews these concepts as well as the particular algorithm of interest, referred to as the iterative signal-to-leakage-and-noise ratio (iSLNR) algorithm which is expanded upon later in this work.

2.1 Receiver Architectures

Receivers can be classified in several ways; being either linear or non-linear and either interference-aware or interference-unaware. A receiver is linear if it arrives at a set of decision statistics by taking a linear transform of the received signal vector $\boldsymbol{r}$. The applied linear transform is represented by the matrix $\boldsymbol{T}$, which has dimension S_ixM_i, and the length S_i column vector of decision statistics $\boldsymbol{z}$ is given by:

$$\boldsymbol{z} = \boldsymbol{T}\,\boldsymbol{r} \tag{13}$$

Non-linear receivers on the other hand, do not apply linear weights, but perform some non-linear operation to obtain the best estimate of the transmitted symbols. Examples of non-linear receivers include Successive Interference Cancellation (SIC) receivers and Maximum Likelihood (ML) receivers. This work considers linear receivers as they are more commonly used in mobile devices where low-complexity is extremely important.

Interference suppression at the receiver can play an important role in reducing the effect of multiuser interference. Naturally this capability requires the receiver to be interference-aware, having some knowledge of composition of the interfering signals and/or estimates of their statistical properties. There have been a number of papers showing the superiority of interference-aware receivers such as the interference rejection combining (IRC) and Max-Log-MAP receivers, over interference-unaware receivers such as the conventional matched filter (MF) or minimum mean square error (MMSE) receivers [10,11]. Much of

the previous work has focused on the case where precoding is limited to a finite codebook and a specific precoding matrix is chosen based on feedback from the receiver; a common architecture in today's wireless systems. In this case, interference-aware receivers outperform interference-unware receivers due to the quantization of CSIT to a finite codebook which creates significant multiuser interference. That being said, there has been a great deal of effort to move away from the limitation of a finite codebook, possibly exploiting the reciprocity of the wireless channel that exists in a TDD system for CSIT acquisition. For example, release 10 of LTE-A defined Transmission Mode 9, which enables transparent precoding [1]. Transparent precoding implies that the user requires no knowledge of the precoding matrix employed at the base station, this is contrary to the previous Transmission Modes in which the precoding matrix was signaled to the user to enable demodulation. Transparent precoding enables the use of non-codebook-based precoding schemes. The precoding will naturally be accounted for in the channel estimation at the receiver. In this case the transmitter should ideally suppress the multiuser interference sufficiently such that little benefit would be realized from an interference-aware receiver. While this is true under ideal conditions, one of the results of this paper shows that, as from quantization of CSIT to a finite codebook, imperfect CSIT will cause non-trivial residual multiuser interference such that an interference-aware receiver will provide significant performance gains compared to an interference-unaware receiver.

In the next sections we briefly review the conventional linear receiver types. Many of these receiver types are applicable in both the SU-MIMO and MU-MIMO case. Of course in the SU-MIMO case $\boldsymbol{G}_i = \boldsymbol{G}$, but we include the subscript to be clear.

2.1.1 Matched Filter Receiver:

The matched filter (MF) receiver will de-rotate the received symbols to acquire their intended phase. Since it does not apply any amplitude correction, this receiver type is only applicable for phase modulated signals such as QPSK. The MF receiver weights are given by

$$\boldsymbol{T}_{MF} = \boldsymbol{G}_i^{\,*} \tag{14}$$

Note that the MF receiver is only applicable when $\boldsymbol{G}_i$ is assumed to be diagonal. This may indeed be true when precoding is employed at the transmitter so as to diagonalize the channel, but is not true in general.

2.1.2 Zero Forcing Receiver:

The zero forcing (ZF) receiver will completely eliminate all inter-stream-interference without considering the additive noise from the receiver. The weights used by the ZF receiver are given by [14]:

$$\boldsymbol{T}_{ZF} = (\boldsymbol{G}_i^* \, \boldsymbol{G}_i \,)^{-1} \boldsymbol{G}_i^* \tag{15}$$

When the channel magnitude is small the ZF receiver will apply a large gain. This large gain is equally applied to the receiver noise which leads to degraded performance. This effect is known as noise-enhancement.

2.1.3 Minimum Mean Squared Error Receiver:

The minimum mean square error (MMSE) receiver minimizes the total error power that results from inter-stream-interference and noise. This effectively mitigates the issue of noise-enhancement that can occur with the ZF receiver. The MMSE weights are calculated as [14]

$$\boldsymbol{T}_{MMSE} = (\boldsymbol{G}_i^* \, \boldsymbol{G}_i + \sigma_n^2 \, \boldsymbol{I})^{-1} \boldsymbol{G}_i^* \tag{16}$$

2.1.4 Interference Rejection Combining Receiver:

In a system with multiple users there may be additional sources of interference at each receiver due to signals intended for other users. The ZF and MMSE receivers are limited in that they do not make use of any sort of knowledge of the interfering signals to mitigate their impact. The interference rejection combining (IRC) receiver on the other hand is able to suppress the multiuser-interference by utilizing knowledge the interference plus noise covariance matrix $\boldsymbol{R}_n$. The IRC weights are found from [14]

$$\boldsymbol{T}_{IRC} = (\boldsymbol{G}_i^* \boldsymbol{R}_n^{-1} \boldsymbol{G}_i)^{-1} \boldsymbol{G}_i^* \boldsymbol{R}_n^{-1} \tag{17}$$

The interference plus noise covariance matrix is given by

$$\boldsymbol{R}_n = E\{\boldsymbol{\eta}\boldsymbol{\eta}^*\}, \qquad \boldsymbol{\eta} = \boldsymbol{G}_n \boldsymbol{s}_n + \boldsymbol{n} \tag{18}$$

where $\boldsymbol{s}_n$ is the vector of the interfering symbols, $\boldsymbol{G}_n$ is the equivalent channel for the interfering signals to the i^{th} user given by $\boldsymbol{G}_n = \boldsymbol{H}_i \boldsymbol{W}_n$ where $\boldsymbol{W}_n$ is the precoding matrix associated with all interfering streams, and $\boldsymbol{n}$ is a complex Gaussian noise vector with variance σ_n^2. These terms are written out explicitly below.

$$\begin{gathered} \boldsymbol{s}_n = \begin{bmatrix} \boldsymbol{s}_1 \\ \vdots \\ \boldsymbol{s}_{i-1} \\ \boldsymbol{s}_{i+1} \\ \vdots \\ \boldsymbol{s}_K \end{bmatrix} \\ \boldsymbol{W}_n = [\boldsymbol{W}_1, \dots, \boldsymbol{W}_{i-1}, \boldsymbol{W}_{i+1}, \dots, \boldsymbol{W}_K] \\ \boldsymbol{G}_n = \boldsymbol{H}_i \boldsymbol{W}_n \end{gathered} \tag{19}$$

Assuming the elements of $\boldsymbol{s}_n$ have unit average power and a uniformly distributed phase, $\boldsymbol{R}_n$ can be equivalently expressed

$$\boldsymbol{R}_n = \boldsymbol{G}_n \boldsymbol{G}_n^* + \sigma_n^2 \boldsymbol{I} \tag{20}$$

2.2 Conventional MU-MIMO Precoding

This section discusses the conventional MU-MIMO linear precoding techniques and the tradeoffs between them.

2.2.1 Complete Channel Diagonalization

Since it is assumed that the channel is known at the transmitter, the most obvious option is to design the precoding matrix to completely invert the channel, $\boldsymbol{W} = \boldsymbol{H}^{-1}$ which would yield a received vector

$$\boldsymbol{r} = \boldsymbol{H}\boldsymbol{H}^{-1}\boldsymbol{s} + \boldsymbol{n} = \boldsymbol{s} + \boldsymbol{n} \tag{21}$$

The issue with this approach arises from the limitation of finite transmit power. Because of this limitation, the precoding matrix must be scaled by some scalar β such that

$$\|\beta\boldsymbol{H}^{-1}\|^2 = P \tag{22}$$

In our analysis we've assumed that $P = 1$, so $\beta = \frac{1}{\|\boldsymbol{H}^{-1}\|}$. Substituting the precoding matrix into equation 6 gives us

$$\begin{aligned} \boldsymbol{r} &= \boldsymbol{H}\beta\boldsymbol{H}^{-1}\boldsymbol{s} + \boldsymbol{n} \\ \boldsymbol{r} &= \frac{1}{\|\boldsymbol{H}^{-1}\|}\boldsymbol{s} + \boldsymbol{n} \end{aligned} \tag{23}$$

Since the wireless channel will exhibit some fading characteristics, there will surely be instances of deep fades where $\|\boldsymbol{H}\| \ll 1$ which will imply $\|\boldsymbol{H}^{-1}\| \gg 1$, leading to reduced signal power at the receiver and poor performance. This result is analogous to the noise enhancement experienced at a receiver using ZF processing.

Note that in the case of non-square channel matrices this approach uses the pseudo-inverse *i.e.* $\boldsymbol{W} \propto (\boldsymbol{H}^*\boldsymbol{H})^{-1}\boldsymbol{H}^*$.

2.2.2 Block-Diagonal Zero-Forcing

Block-Diagonal Zero-Forcing precoding recognizes that there is no need for the transmitter to separate streams intended for a common user. Doing so is often a redundant operation because the receiver will be able to sufficiently separate the streams later with high probability. Instead, it is sufficient to force all multiuser-interference terms to zero

by ensuring that the equivalent channel matrix is block diagonal. To remind the reader, the equivalent channel is given by

$$\boldsymbol{G} = \begin{matrix} \boldsymbol{G}_{11} & \dots & \boldsymbol{G}_{1K} \\ \vdots & \ddots & \vdots \\ \boldsymbol{G}_{K1} & \dots & \boldsymbol{G}_{KK} \end{matrix} \tag{24}$$

Where G_{ij} is the equivalent channel from the j^{th} user's data stream(s) to the i^{th} user's receive antenna(s). The multiuser-interference terms are therefore $\boldsymbol{G}_{ij} \forall i \neq j$. So by forcing all multi-user interference terms to zero the equivalent channel will be of the form

$$\boldsymbol{G} = \begin{matrix} \boldsymbol{G}_{11} & \dots & \boldsymbol{0} \\ \vdots & \ddots & \vdots \\ \boldsymbol{0} & \dots & \boldsymbol{G}_{KK} \end{matrix} \tag{25}$$

which is block-diagonal. Clearly for this to be true, $\boldsymbol{W}_i$ must be in the null-space of $\boldsymbol{H}_j$ for all $i \neq j$. The advantage of this method is that it is less restrictive than complete diagonalization of the channel, so the average SNR at the receiver will be improved. Of course, when $M_i = 1 \; \forall \; i$, this method simplifies to complete channel diagonalization.

Once the nullspace constraint has been met, the problem has effectively been decomposed into several SU-MIMO sub problems for which traditional SU-MIMO precoding solutions can be used. The precoding matrix for the i^{th} user is then given by

$$\boldsymbol{W}_i = \boldsymbol{Y}_i \boldsymbol{X}_i \tag{26}$$

Where $\boldsymbol{Y}_i$ is chosen such that $\boldsymbol{H}_j \boldsymbol{Y}_i = \boldsymbol{0} \; \forall \; j \neq i$, and $\boldsymbol{X}_i$ is chosen to maximize the SNR for the i^{th} user using traditional SU-MIMO techniques such as eigen-beamforming. The SNR for the i^{th} user is given

$$SNR_i = \frac{\|\boldsymbol{H}_i \boldsymbol{Y}_i \boldsymbol{X}_i\|^2}{M_i \sigma_n^2} \tag{27}$$

So $\boldsymbol{X}_i$ must be chosen to maximize $\|\boldsymbol{H}_i\boldsymbol{Y}_i\boldsymbol{X}_i\|^2 = Tr[\boldsymbol{X}_i^*\boldsymbol{Y}_i^*\boldsymbol{H}_i^*\boldsymbol{H}_i\boldsymbol{Y}_i\boldsymbol{X}_i]$ given $\boldsymbol{H}_i$ and $\boldsymbol{Y}_i$. This can be accomplished using eigendecomposition from which we know there exists a $\boldsymbol{Q}$ and Λ such that

$$\boldsymbol{Q}^*\boldsymbol{Y}_i^*\boldsymbol{H}_i^*\boldsymbol{H}_i\boldsymbol{Y}_i\boldsymbol{Q} = \Lambda \tag{28}$$

where the columns of $\boldsymbol{Q}$ are the right eigenvectors of $\boldsymbol{Y}_i^*\boldsymbol{H}_i^*\boldsymbol{H}_i\boldsymbol{Y}_i$, and $\boldsymbol{\Lambda}$ is a diagonal matrix with elements in descending order *i.e.* $\lambda_1 \geq \cdots \lambda_{M_i} \geq 0$, and where λ_i is the eigenvalue associated with eigenvector in the i^{th} column of $\boldsymbol{Q}$. To maximize the expression in equation 28 and maintaining separable streams the precoding matrix $\boldsymbol{W}_i$ must be constructed using the S_i eigenvectors associated with the largest eigenvalues *i.e.* the S_i left-most columns of $\boldsymbol{Q}$.

Figure 2.1 shows a comparison of the bit error rates using complete channel diagonalization and block-diagonalization in a 9x(3x3) system with 3 streams per user. Block-diagonalization clearly offers improved performance in the lower SNR regime by reducing noise enhancement compared to complete channel diagonalization as described earlier. As a baseline we've also included the error rate for a 1x1 system where the transmit power is normalized to be equal to the per stream transmit power of the 9x(3x3) system. In this case we observe that the performance is identical to the MU-MIMO system with ZF precoding.

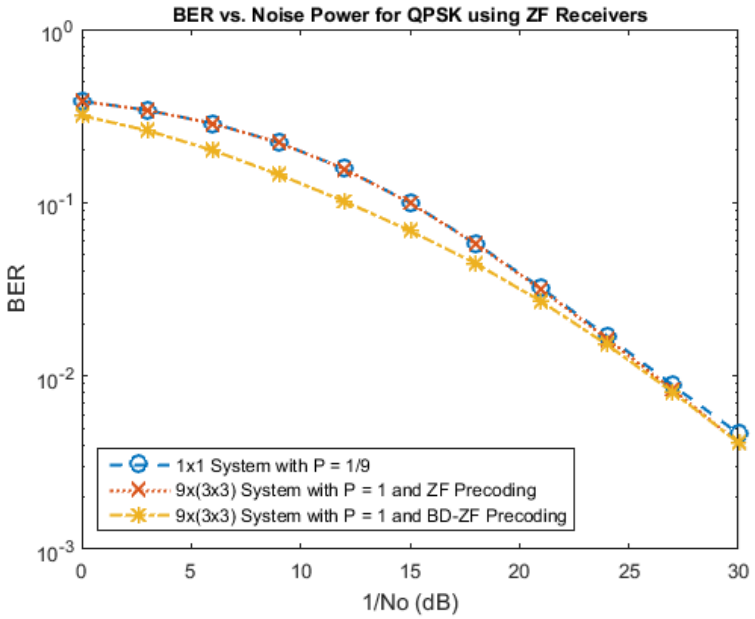

Figure 2.1: BER using ZF and BD-ZF precoding schemes

2.2.3 Signal-to-Leakage-and Noise Ratio Precoding

It should be obvious that complete removal of all multiuser-interference is not an optimal solution. Just as a ZF equalizer is suboptimal due to noise-enhancement, so too block-diagonalization suffers from not considering the noise power at the receiver. A solution which maximizes the per user SINR given by

$$SINR_i = \frac{\|\boldsymbol{H}_i \boldsymbol{W}_i\|^2}{M_i \sigma_n^2 + \sum_{k=1,k\neq i}^{K} \|\boldsymbol{H}_i \boldsymbol{W}_k\|^2} \tag{29}$$

would clearly be better, but is a very challenging optimization problem since the i^{th} user's SINR is coupled to all k^{th} user's precoding matrix for $k \neq i$. With this in mind, the authors of [7] proposed the conventional signal-to-leakage-and-noise ratio precoding scheme (cSLNR) which simplifies the optimization problem by considering the multiuser-interference leaked from the i^{th} user onto all $k \neq i$ users rather than the total multiuser-interference imposed on the i^{th} user. This results in improved SINR overall compared to block-diagonalization. The desired signal power at user i is given by

$\|\boldsymbol{H}_i\boldsymbol{W}_i\|^2$ and the MUI imposed on all other users by this precoding is then $\sum_{k=1,k\neq i}^{K}\|\boldsymbol{H}_k\boldsymbol{W}_i\|^2$. So the SLNR is given by:

$$SLNR = \frac{\|\boldsymbol{H}_i\boldsymbol{W}_i\|^2}{M_i\sigma_n^2 + \left\|\widetilde{\boldsymbol{H}}_i\boldsymbol{W}_i\right\|^2} \tag{30}$$

Where $\widetilde{\boldsymbol{H}}_i = [\boldsymbol{H}_1 \dots \boldsymbol{H}_{i-1}\boldsymbol{H}_{i+1} \dots \boldsymbol{H}_K]^T$ is the so called 'leakage channel'. Note that the SLNR is merely a metric used to approximate the problem of maximizing SINR. It is the SINR at each user that ultimately determines their performance and therefore that of the system as a whole. Expanding equation 30 gives

$$SLNR = \frac{Tr[\boldsymbol{W}_i^*\boldsymbol{H}_i^*\boldsymbol{H}_i\boldsymbol{W}_i]}{M_i\sigma_n^2\boldsymbol{I} + Tr\left[\boldsymbol{W}_i^*\widetilde{\boldsymbol{H}}_i^*\widetilde{\boldsymbol{H}}_i\boldsymbol{W}_i\right]} \tag{31}$$

Noting that $Tr[\boldsymbol{W}_i^*\boldsymbol{W}_i] = S_iP_s$ this can be equivalently expressed

$$= \frac{Tr[\boldsymbol{W}_i^*\boldsymbol{H}_i^*\boldsymbol{H}_i\boldsymbol{W}_i]}{Tr\left[\boldsymbol{W}_i^*\left(\widetilde{\boldsymbol{H}}_i^*\widetilde{\boldsymbol{H}}_i + \frac{M_i}{S_iP_s}\sigma_n^2\boldsymbol{I}\right)\boldsymbol{W}_i\right]} \tag{32}$$

Equation 32 is of the familiar Rayleigh Quotient form, $\boldsymbol{H}_i^*\boldsymbol{H}_i$ being Hermitian and $\frac{M_i}{S_iP_s}\sigma_n^2\boldsymbol{I} + \widetilde{\boldsymbol{H}}_i^*\widetilde{\boldsymbol{H}}_i$ being Hermitian and positive-definite. It can therefore be expressed as

$$\begin{gathered}\boldsymbol{Q}^*\boldsymbol{H}_i^*\boldsymbol{H}_i\boldsymbol{Q} = \boldsymbol{\Lambda} \\ \boldsymbol{Q}^*\left(\frac{M_i}{S_iP_s}\sigma_n^2\boldsymbol{I} + \widetilde{\boldsymbol{H}}_i^*\widetilde{\boldsymbol{H}}_i\right)\boldsymbol{Q} = \boldsymbol{I}\end{gathered} \tag{33}$$

Where the columns of $\boldsymbol{Q}$ are the right generalized eigenvectors of the pair $\left\{\boldsymbol{H}_i^*\boldsymbol{H}_i, \frac{M_i}{S_iP_s}\sigma_n^2\boldsymbol{I} + \widetilde{\boldsymbol{H}}_i^*\widetilde{\boldsymbol{H}}_i\right\}$, and $\boldsymbol{\Lambda}$ is a diagonal matrix with elements $\lambda_1 \geq \cdots \lambda_M \geq 0$, where λ_i is the eigenvalue associated with eigenvector in the i^{th} column of $\boldsymbol{Q}$. For a single stream per user the SLNR is then maximized by selecting $\boldsymbol{W}_i$ to be the eigenvector

associated with the largest eigenvalue *e.g.* the left-most column of $\boldsymbol{Q}$. Through the rest of the paper we see this same eigendecomposition problem many times with minor differences. In each case we apply the same approach and write the solution compactly in the following manner to ease notation.

$$\boldsymbol{W}_i \propto max\ eigenvector\left(\left(\widetilde{\boldsymbol{H}}_i^*\widetilde{\boldsymbol{H}}_i + \frac{M_i}{S_i P_s}\sigma_n^2\boldsymbol{I}\right)^{-1}\boldsymbol{H}_i^*\boldsymbol{H}_i\right) \tag{34}$$

The extension to multiple streams is quite natural. In order for the streams to be decoupled at the i^{th} user we require that $\boldsymbol{W}_i^*\boldsymbol{H}_i^*\boldsymbol{H}_i\boldsymbol{W}_i$ is diagonal. For a user with S_i streams, the columns of $\boldsymbol{W}_i$ should therefore be proportional to the eigenvectors corresponding to the S_i largest eigenvalues of the pair $\left\{\boldsymbol{H}_i^*\boldsymbol{H}_i, \frac{M_i}{S_i P_s}\sigma_n^2\boldsymbol{I} + \widetilde{\boldsymbol{H}}_i^*\widetilde{\boldsymbol{H}}_i\right\}$ which we write as

$$\boldsymbol{W}_i \propto S_i\, max\ eigenvectors\left(\left(\widetilde{\boldsymbol{H}}_i^*\widetilde{\boldsymbol{H}}_i + \frac{M_i}{S_i P_s}\sigma_n^2\boldsymbol{I}\right)^{-1}\boldsymbol{H}_i^*\boldsymbol{H}_i\right) \tag{35}$$

Figure 2.2 shows a comparison of error rates between the SLNR and BD-ZF precoding schemes for a 9x(3x3) system with three streams per user. You can see that SLNR precoding provides better performance since it accounts for noise at the receiver, whereas BD-ZF precoding does not.

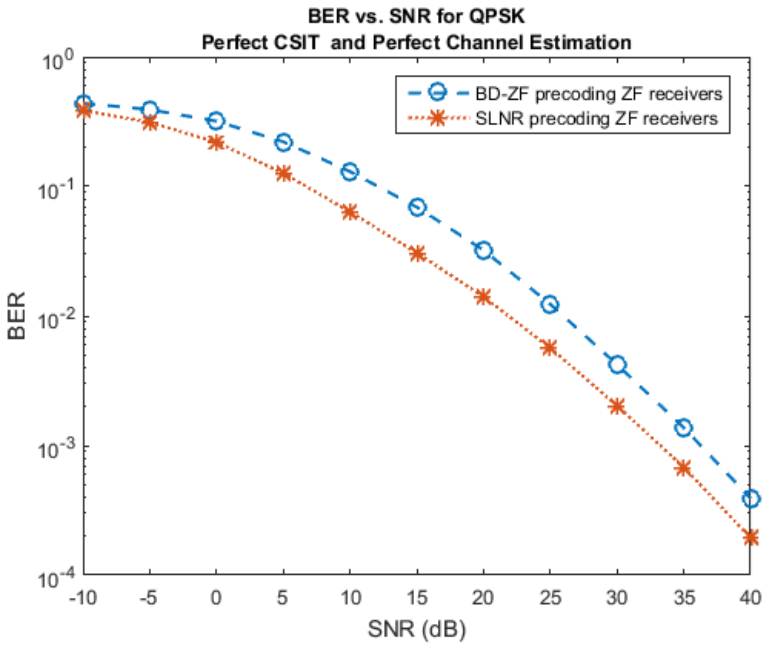

Figure 2.2: BER using BD-ZF and SLNR precoding schemes

SLNR precoding also has the added benefit that it can be applied in systems where the number of transmit antennas is less than the sum of receive antennas. This is not true for the ZF schemes which require sufficient degrees of freedom to completely remove the multiuser-interference. Figure 2.3 shows the error rate of a 4x(3x3) system using SLNR precoding with a single stream per user. Note that while such an operating point is possible with SLNR precoding, it results in an error floor due to the transmitter's inability to completely remove the multiuser-interference as a result of its limited degrees of freedom.

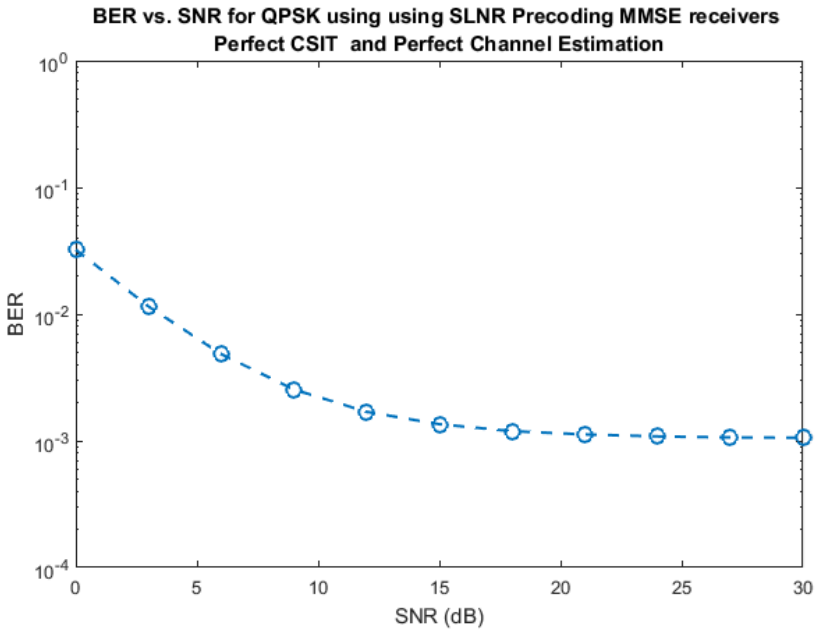

Figure 2.3: BER error floor using SLNR precoding with $N < \sum_{i=1}^{K} M_i$

2.3 Iterative Signal-to-Leakage-and-Noise Ratio Precoding

The work in [8] proposed an iterative SLNR precoding scheme (iSLNR) that was shown to provide substantial gains in sum-rate and error rate assuming a known linear receiver structure. The algorithm begins by calculating an initial precoding matrix $\boldsymbol{W}$ using the cSLNR scheme. It then calculates the linear receive processing matrix $\widehat{\boldsymbol{T}}_i$ for each user i using the expression for the appropriate linear receiver type as given in equations 15-17. The hat notation is used to signify that this quantity is estimated at the transmitter and is differentiated from the receive processing matrix actually used at the receiver which is denoted $\boldsymbol{T}_i$. This is an important distinction because it implies that there is no additional feedback overhead to pass the precoding and/or receive combining matrices between the base station and the user. This is in contrast to a number of proposed solutions which perform a joint transmitter/receiver design optimization and then distribute the processing matrices to the receivers [15-17]. Each row of $\widehat{\boldsymbol{T}}_i$ is scaled to have unit norm. The normalized receiver processing is then given by

$$\breve{\boldsymbol{T}}_i = \boldsymbol{B}_i \widehat{\boldsymbol{T}}_i \tag{36}$$

Where $\boldsymbol{B}_i$ is a diagonal matrix with elements $b_{jj} = \frac{1}{\|\hat{\boldsymbol{t}}_{i,j}\|}$, with $\hat{\boldsymbol{t}}_{i,j}$ being the j^{th} row of $\widehat{\boldsymbol{T}}_i$. Using the normalized receiver processing calculated at the transmitter, the algorithm then defines an effective channel $\breve{\boldsymbol{H}}_i$ for each user i, which is given by

$$\breve{\boldsymbol{H}}_i \triangleq \begin{bmatrix} \breve{\boldsymbol{T}}_i \\ \boldsymbol{0} \end{bmatrix} \boldsymbol{H}_i \tag{37}$$

The zero rows are included to maintain the dimension of $\breve{\boldsymbol{H}}_i$ as being equal to the dimension of $\boldsymbol{H}_i$. This is necessary when $S_i < M_i$, which is a requirement for the iSLNR algorithm to provide performance improvement to the system. When $S_i = M_i$, the iSLNR algorithm collapses to the cSLNR scheme.

With the effective channel for each user at hand, the algorithm then recalculates the precoding matrices using a modified definition of the SLNR metric (mSLNR) which relies on the effective leakage channel, defined as

$$\bar{\boldsymbol{H}}_i \triangleq \left[\breve{\boldsymbol{H}}_1, \dots, \breve{\boldsymbol{H}}_{i-1}, \breve{\boldsymbol{H}}_{i+1}, \dots, \breve{\boldsymbol{H}}_K\right]^T \tag{38}$$

The modified SLNR metric is then

$$mSLNR = \frac{\|\boldsymbol{H}_i \boldsymbol{W}_i\|^2}{S_i \sigma_n^2 + \|\bar{\boldsymbol{H}}_i \boldsymbol{W}_i\|^2} \tag{39}$$

Note that the noise power is scaled by the number of streams S_i rather than the number of antennas M_i as in the cSLNR metric. This is to ensure that the noise and leakage powers are considered equally. In this mSLNR metric the leakage power is considered at the output of the normalized receiver processing. The total noise at this point will therefore be proportional to the number of streams rather than the number of antennas. We further note the importance of normalizing each row of the receiver processing matrix $\widehat{\boldsymbol{T}}$, which is necessary to maintain proportionality between the noise and leakage.

The solution for the $\boldsymbol{W}_i$ which will maximize the expression given in equation 39 is found using eigendecomposition as in the derivation of eqs. 34 and 35 and is given by

$$\boldsymbol{W}_i \propto S_i \max eigenvectors \left(\left(\bar{\boldsymbol{H}}_i^* \bar{\boldsymbol{H}}_i + \frac{1}{P_s} \sigma_n^2 \boldsymbol{I} \right)^{-1} \boldsymbol{H}_i^* \boldsymbol{H}_i \right) \tag{40}$$

This updated precoding matrix is then used to recalculate the normalized receiver processing matrices $\breve{\boldsymbol{T}}_{\boldsymbol{i}}$ and update the effective leakage channels $\bar{\boldsymbol{H}}_i$. The algorithm continues to alternate between calculating the precoding matrix and updating the effective leakage channels for however many iterations are to be performed, denoted n_{iter}. In summary, the iSLNR algorithm uses the following approach.

iSLNR Algorithm

1. compute initial precoding matrix $\boldsymbol{W}$ using the cSLNR scheme
2. calculate $\widehat{\boldsymbol{T}}_j \forall\, j$ based on known receiver type
3. update $\breve{\boldsymbol{H}}_j \;\forall\, j$
4. for $i \leftarrow 1, n_{iter}$ do
5. for $j \leftarrow 1, K$ do
6. compute $\boldsymbol{W}_j$ using mSLNR (eq. 40)
7. calculate $\widehat{\boldsymbol{T}}_j \forall\, j$ based on known receiver type
8. update $\breve{\boldsymbol{H}}_j \;\forall\, j$
9. end for
10. end for

This technique can be applied for any linear receiver structure, though the work in [8] discussed MF and IRC receivers. One of the main conclusions drawn was that IRC receivers can provide slight performance gains but requires many more iterations to converge to the optimal solution, therefore the better performance-complexity tradeoff is to use MF receivers. In this paper we consider ZF and IRC receivers. We make this

distinction so that we can investigate error rates using higher order modulations, where the MF receiver would not be applicable. As stated previously the MF receiver only corrects the phase rotation of the received symbol, not its amplitude. This means that the MF receiver cannot be used with amplitude modulated signals *i.e.* quadrature-amplitude-modulation (QAM). The ZF and IRC receiver weights were provided in equations 15 and 17.

Figure 2.4 shows the achieved sum-rate of a 4x(2x2) system employing iSLNR in an idealized setting. This is included to verify the expected result based on the work in [8]; that with perfect CSIT, perfect CSIR, a time-invariant channel, and $N \geq \sum_{i=1}^{K} M_i$, there is very little difference in the converged sum-rate using ZF or IRC receivers. In addition, the solution converges much more slowly using the IRC receiver.

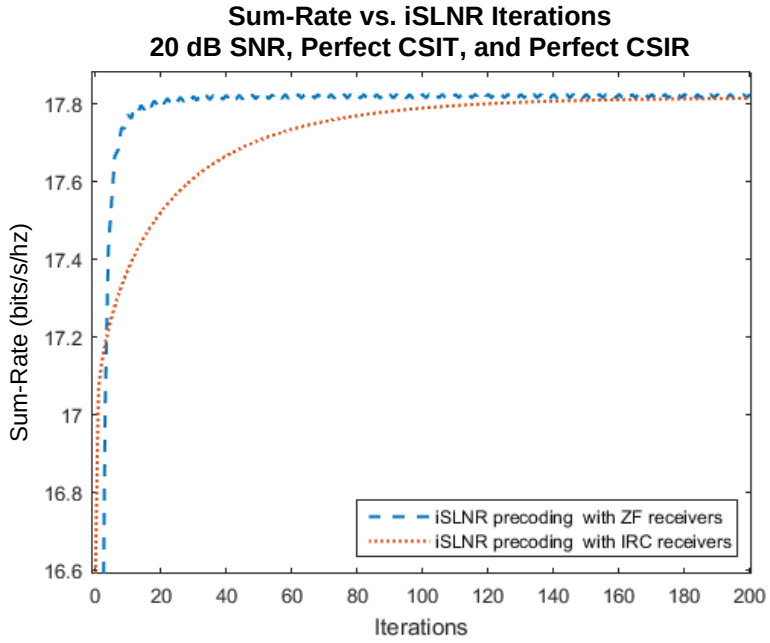

Figure 2.4: Sum-rate achieved using iSLNR in a 4x(2x2) system with 20 dB SNR

In Figures 2.5 and 2.6 we show sum-rate of a 4x(2x4) system employing iSLNR with perfect CSIT. Because $N < \sum_{i=1}^{K} M_i$, the transmitter is not able to suppress the multiuser interference as effectively. As a result, the IRC receiver provides some sum-rate gain by further suppressing the residual multiuser interference at the receiver. This is shown more clearly in Figure 2.6 where we've zoomed in more closely to see the convergence

behavior of the algorithm. Using the standard iSLNR algorithm this comes at the expense of a large number of iterations; the IRC receiver does not surpass the ZF receiver until after roughly 50 iterations and requires on the order of 100 iterations to have reached a converged state. Also note the drastic increase in sum-rate (~100%) between the cSLNR (the zeroth iSLNR iteration) and the converged iSLNR solutions. This is due to the effective decrease in required transmit degrees of freedom that results from using this algorithm, as explained in [8]. It was shown in [18] that sufficient degrees of freedom exist for the SLNR scheme to drive the leakage power to zero at asymptotic high SNR if $\sum_{j\neq i} M_i < N_t$ is satisfied. This is because in the cSLNR scheme we have $rank\left(\widetilde{\boldsymbol{H}}_i^* \widetilde{\boldsymbol{H}}_i\right) = \sum_{j\neq i} M_i$. In the mSLNR scheme we instead have $rank(\overline{\boldsymbol{H}}_i^* \overline{\boldsymbol{H}}_i) = \sum_{j\neq i} S_i$. The leakage power from user i will therefore converge to zero at asymptotic high SNR when $\sum_{j\neq i} S_i < N_t$ is satisfied. This requirement is less stringent which means more degrees of freedom may be obtained.

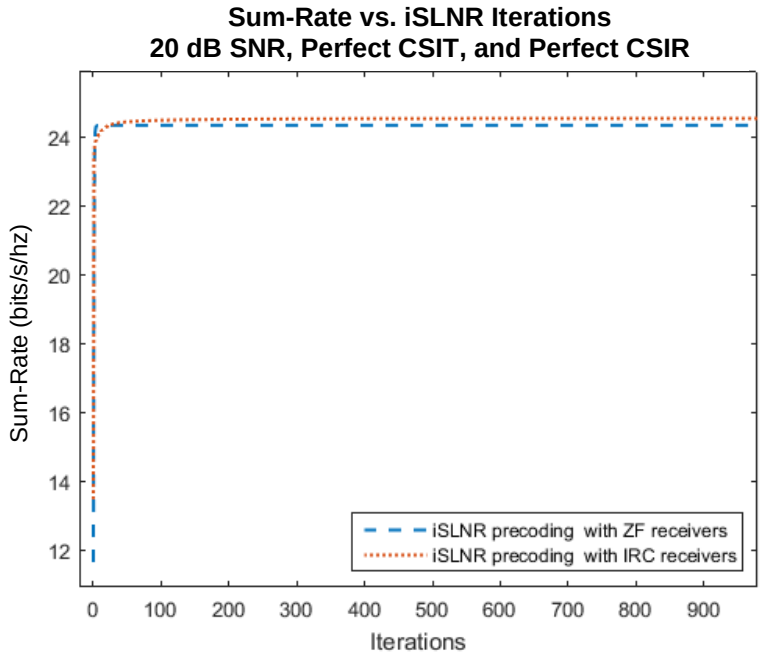

Figure 2.5: Sum-rate achieved using iSLNR in a 4x(2x4) system with 20 dB SNR

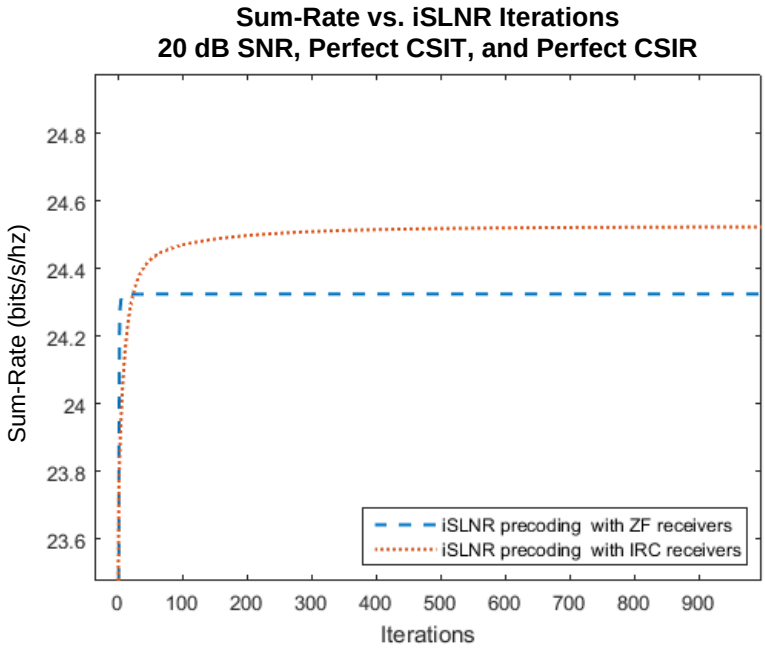

Figure 2.6: Convergence behavior for sum-rate achieved using iSLNR in a 4x(2x4) system with 20 dB SNR

We also observe that a greater number of iterations are required for convergence at higher SNR. This is illustrated in Figures 2.7 and 2.8 which show convergence of the iSLNR scheme for a 9x(3x3) system using IRC receivers operating at 0 dB and 30 dB SNR respectively. You can see that at 0 dB SNR there is no significant gain after about 3 iterations, whereas at 30 dB SNR there is non-negligible gain for on the order of hundreds of iterations.

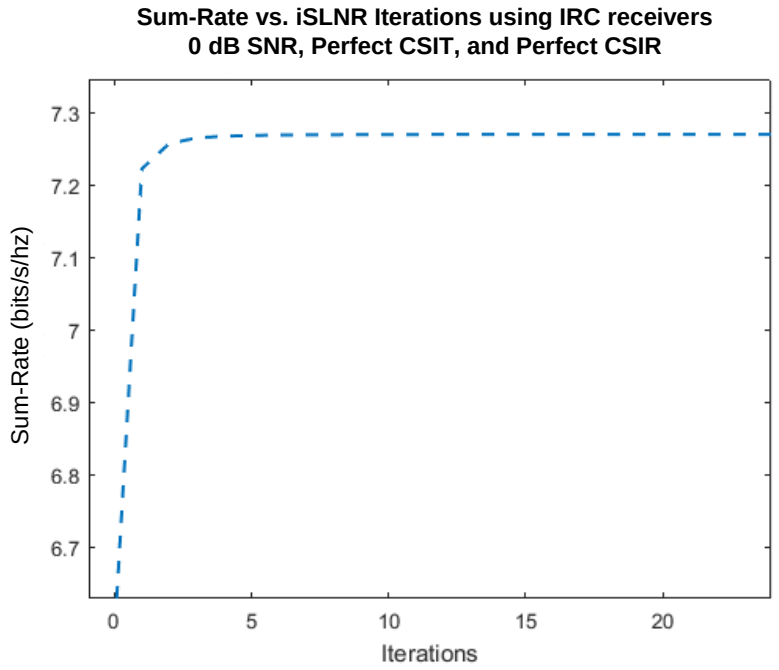

Figure 2.7: Sum-rate of 9x(3x3) system using iSLNR precoding with IRC receivers at 0 dB SNR

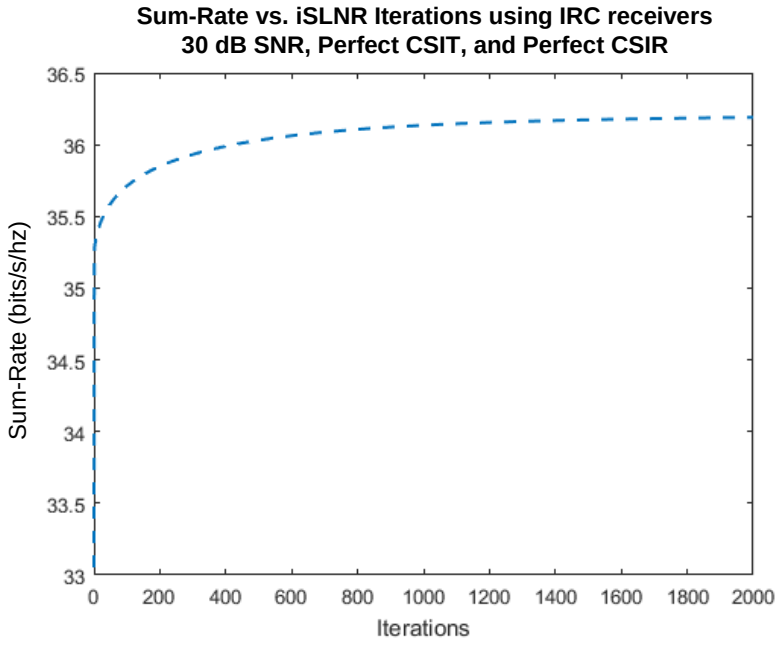

Figure 2.8: Sum-rate of 9x(3x3) system using iSLNR precoding with IRC receivers at 30 dB SNR

In Figures 2.9 and 2.10 we examine the BER achieved in a 4x(2x4) system using ZF and IRC receivers respectively. You can see that the first several iterations significantly reduce

the error floor that exists using the cSLNR precoding. Again, this is due to the effective increase in degrees of freedom at the transmitter. As before, we observe that more iterations are required at higher SNR to achieve convergence.

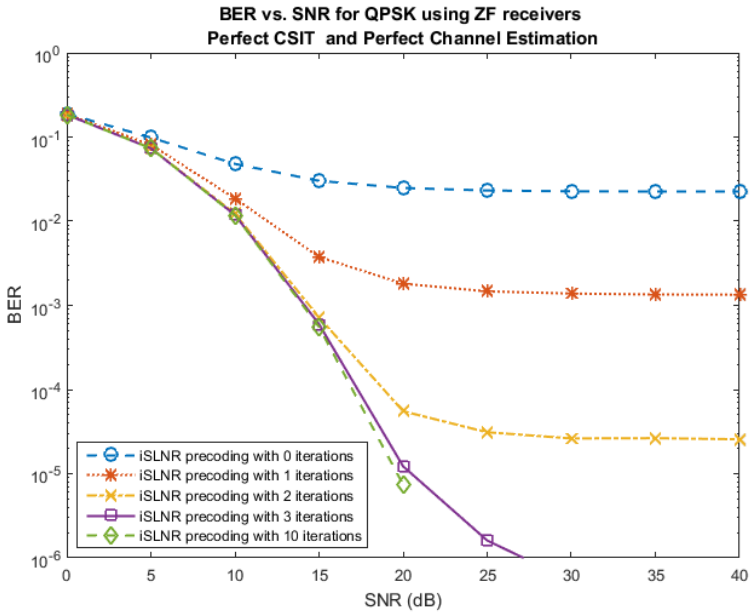

Figure 2.9: BER for a 4x(2x4) system using iSLNR and ZF receivers

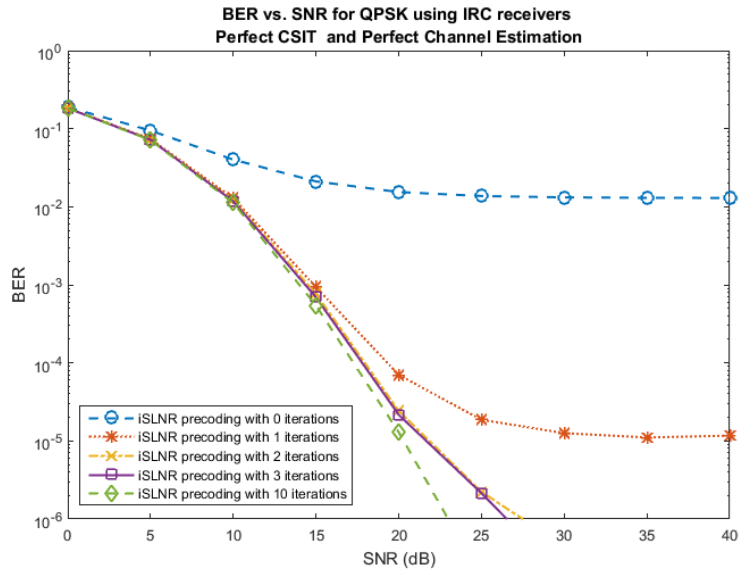

Figure 2.10: BER for a 4x(2x4) system using iSLNR and IRC receivers

2.4 Chapter Summary

In this chapter we reviewed the conventional MU-MIMO concepts including receiver structures and precoding techniques. We explained the motivation to introduce the BD-ZF scheme rather than the complete channel diagonalization of the ZF scheme and showed the error rate performance gain achieved. We further explained how SLNR is a useful approximation for SINR as it captures the figures of merit without the coupling issue that exists when attempting to directly maximize SINR. The error rate performance of SLNR precoding was compared to BD-ZF precoding and shown to be superior. Finally, we reviewed the iSLNR precoding algorithm which iteratively maximizes a modified definition of the SLNR metric wherein the leakage channel is considered at the output of the receiver. This approach was shown to provide significant gains in error rate and sum-rate, and to reduce the required degrees of freedom at the transmitter. All of this analysis was performed in an ideal scenario. In the next chapters we'll investigate the impact of several practical impairments on system performance and ways to mitigate them.

Chapter 3

Imperfect Channel State Information

In the previous chapter we reviewed several approaches to calculating the precoding matrices of a MU-MIMO system and demonstrated the performance achieved using these techniques under ideal conditions. For a practical system however, we must consider the presence of non-idealities if we are to achieve the best possible system performance. Both the transmit and receive techniques discussed require knowledge of the channel and are negatively impacted when that knowledge is imperfect. There have been a number of papers written describing methods to deal with imperfect channel state information at the transmitter (CSIT) in the aforementioned precoding techniques [19-22]. No such work exists specifically for the iSLNR algorithm however, which proved to be a very effective precoding scheme for MU-MIMO systems. It is therefore the ultimate goal of this chapter to investigate how this algorithm should be designed with imperfect CSIT. We also note that the iSLNR algorithm relies on knowledge of the receiver processing to provide gain to the system. In practice the receivers will have imperfect channel state information which will impact their processing, so we must also investigate the performance of the iSLNR algorithm with imperfect CSIR.

Before directly approaching the iSLNR algorithm with imperfect CSIT, we must make sure that we fully understand the cSLNR precoding scheme with imperfect CSIT. This chapter is structured into four sections. The first section investigates cSLNR precoding with imperfect CSIT, the second section investigates the iSLNR algorithm with imperfect CSIT, the third section investigates iSLNR precoding with imperfect CSIR, and finally the last section summarizes our conclusions.

3.1 SLNR Precoding Considering CSIT Error

In practice the CSIT used for precoding will have some associated error with respect to the true MIMO channel $\boldsymbol{H}$, which will degrade system performance. The motivation of the following work is therefore to minimize these degradations. We model the CSIT error

as the matrix $\mathbf{\Gamma}$, whose elements are independent and identically distributed complex Gaussian random variables with zero mean and variance σ_c^2. When a system is said to have x dB CSIT, the implication is that $x = 10log10\left(\frac{1}{\sigma_c^2}\right)$ since the variance of each element of the MIMO channel is unity. In general the dimensions of $\mathbf{\Gamma}$ should be inferred from context as it is used in several expressions *e.g.*, for a particular user's channel or for leakage channels. Hereafter we denote quantities that are estimated at the transmitter using $\widehat{(\cdot)}$, so the estimates available at the transmitter for the i^{th} user's channel and leakage channel are given by

$$\widehat{\boldsymbol{H}}_i = \boldsymbol{H}_i + \mathbf{\Gamma}_{\mathrm{i}} \tag{41}$$

$$\widehat{\widetilde{\boldsymbol{H}}}_i = \widetilde{\boldsymbol{H}}_i + \tilde{\mathbf{\Gamma}}_i \tag{42}$$

In the following analysis it is assumed that the transmitter has perfect knowledge of the second order statistics of the CSIT error, σ_c^2.

3.1.1 Revisiting the Existing SLNR Solution

In [7] the authors derived the solution for the precoding matrix which will maximize the SLNR with imperfect CSIT using the same error model as we've described above. They began from the SLNR expression conditioned on the i^{th} user channel estimate $\widehat{\boldsymbol{H}}_i$ and the leakage channel estimate $\widehat{\widetilde{\boldsymbol{H}}}_i$ at the transmitter.

$$SLNR = \frac{E\left\{Tr[\boldsymbol{W}_i^* \boldsymbol{H}_i^* \boldsymbol{H}_i \boldsymbol{W}_i] \mid \widehat{\boldsymbol{H}}_i\right\}}{M_i \sigma_n^2 + E\left\{Tr\left[\boldsymbol{W}_i^* \widetilde{\boldsymbol{H}}_i^* \widetilde{\boldsymbol{H}}_i \boldsymbol{W}_i\right] \mid \widehat{\widetilde{\boldsymbol{H}}}_i\right\}} \tag{43}$$

The authors then used equations 41 and 42 to substitute $\widehat{\boldsymbol{H}}_i - \mathbf{\Gamma}_i$ for $\boldsymbol{H}$ and $\widehat{\widetilde{\boldsymbol{H}}}_i - \tilde{\mathbf{\Gamma}}_i$ for $\widetilde{\boldsymbol{H}}_i$.

$$= \frac{E\left\{Tr\left[\boldsymbol{W}_i^* \left(\widehat{\boldsymbol{H}}_i - \mathbf{\Gamma}_i\right)^* \left(\widehat{\boldsymbol{H}}_i - \mathbf{\Gamma}_i\right) \boldsymbol{W}_i\right] \mid \widehat{\boldsymbol{H}}_i\right\}}{M_i \sigma_n^2 + E\left\{Tr\left[\boldsymbol{W}_i^* \left(\widehat{\widetilde{\boldsymbol{H}}}_i - \tilde{\mathbf{\Gamma}}_i\right)^* \left(\widehat{\widetilde{\boldsymbol{H}}}_i - \tilde{\mathbf{\Gamma}}_i\right) \boldsymbol{W}_i\right] \mid \widehat{\widetilde{\boldsymbol{H}}}_i\right\}} \tag{44}$$

Expanding this expression they arrived at the following solution to maximize the SLNR in the presence of CSIT error (we avoid going through this derivation as we will shortly show a very similar one).

$$\boldsymbol{W}_i \propto S_i \max eigenvectors\ of$$

$$\left(\left(\widehat{\widehat{\boldsymbol{H}}}_i^* \widehat{\widehat{\boldsymbol{H}}}_i + \left(\sum_{j=1, j\neq i}^{K} M_j\, \sigma_c^2 + \frac{M_i}{S_i P_s} \sigma_n^2 \right) \boldsymbol{I} \right)^{-1} \left(\widehat{\boldsymbol{H}}_i^* \widehat{\boldsymbol{H}}_i + M_i \sigma_c^2 \boldsymbol{I} \right) \right) \tag{45}$$

The issue we see in this derivation is that the distribution of $\boldsymbol{H}_i$ conditioned on $\widehat{\boldsymbol{H}}_i$ has been represented as $\widehat{\boldsymbol{H}}_i - \boldsymbol{\Gamma}_\mathrm{i}$. It can be readily observed that this is not a valid distribution for $\boldsymbol{H}_i$ given $\widehat{\boldsymbol{H}}_i$. From stochastic theory we know that the variance of the difference of two Gaussian random variables is the sum of their variances. So if the expression $\widehat{\boldsymbol{H}}_i - \boldsymbol{\Gamma}$ is taken to represent the distribution of $\boldsymbol{H}_i$, then the variance of each element of $\boldsymbol{H}_i$ will be given by the sum of the variances of the corresponding elements of $\widehat{\boldsymbol{H}}_i$ and $\boldsymbol{\Gamma}$ *i.e.*

$$\begin{aligned} var(h_{mn}) &= var\left(\hat{h}_{mn}\right) + var(\gamma_{mn})\ \forall\ m, n \\ &= (1 + \sigma_c^2) + \sigma_c^2 \\ &= 1 + 2\sigma_c^2 \end{aligned} \tag{46}$$

But we know from the system model that the variance of each element h_{mn} is defined to be unity; something is clearly amiss. This issue is resolved by using the distribution for $\boldsymbol{H}$ conditioned on $\widehat{\boldsymbol{H}}$ as was stated in [19] and which is given by

$$p\left(\boldsymbol{H}|\widehat{\boldsymbol{H}}\right) = \rho_h \widehat{\boldsymbol{H}} + \boldsymbol{\Omega} \tag{47}$$

Where $\rho_h = \frac{\sigma_h^2}{\sigma_h^2 + \sigma_c^2}$ and $\boldsymbol{\Omega}$ is a matrix of i.i.d. complex Gaussian random variables with zero mean and variance $\frac{\sigma_h^2 \sigma_c^2}{\sigma_h^2 + \sigma_c^2}$. Since our channel model assumes $\sigma_h^2 = 1$, we have $\rho_h =$

$\frac{1}{1+\sigma_c^2}$ and $\boldsymbol{\Omega}$ with variance $\frac{\sigma_c^2}{1+\sigma_c^2}$. We note that treating the true channel as a random variable may seem counter-intuitive, but clearly for a given channel estimate there is a continuous distribution of possible values that the true channel could be.

We now return to the original problem of finding the precoding matrix $\boldsymbol{W}_i$ so as to maximize the SLNR in the presence of imperfect CSIT by substituting equation 47 into equation 43 which gives

$$SLNR = \frac{E\{Tr[\boldsymbol{W}_i^*(\rho_h\widehat{\boldsymbol{H}}_i + \boldsymbol{\Omega}_\mathrm{i})^*(\rho_h\widehat{\boldsymbol{H}}_i + \boldsymbol{\Omega}_\mathrm{i})\boldsymbol{W}_i] \mid \widehat{\boldsymbol{H}}_i\}}{M_i\sigma_n^2 + E\left\{Tr\left[\boldsymbol{W}_i^*\left(\rho_h\widehat{\widehat{\boldsymbol{H}}}_i + \widetilde{\boldsymbol{\Omega}}_i\right)^*\left(\rho_h\widehat{\widehat{\boldsymbol{H}}}_i + \widetilde{\boldsymbol{\Omega}}_i\right)\boldsymbol{W}_i\right] \mid \widehat{\widehat{\boldsymbol{H}}}_i\right\}} \quad (48)$$

Expanding this expression we have

$$= \frac{E\{Tr[\boldsymbol{W}_i^*(\rho_h{}^2\widehat{\boldsymbol{H}}_i^*\widehat{\boldsymbol{H}}_i + \rho\widehat{\boldsymbol{H}}_i^*\boldsymbol{\Omega}_\mathrm{i} + \boldsymbol{\Omega}_\mathrm{i}{}^*\rho_h\widehat{\boldsymbol{H}}_i + \boldsymbol{\Omega}_\mathrm{i}{}^*\boldsymbol{\Omega}_\mathrm{i})\boldsymbol{W}_i] \mid \widehat{\boldsymbol{H}}_i\}}{M_i\sigma_n^2 + E\left\{Tr\left[\boldsymbol{W}_i^*\left(\rho_h{}^2\widehat{\widehat{\boldsymbol{H}}}_i^*\widehat{\widehat{\boldsymbol{H}}}_i + \rho_h\widehat{\widehat{\boldsymbol{H}}}_i^*\widetilde{\boldsymbol{\Omega}}_i + \widetilde{\boldsymbol{\Omega}}_i{}^*\rho_h\widehat{\widehat{\boldsymbol{H}}}_i + \widetilde{\boldsymbol{\Omega}}_i{}^*\widetilde{\boldsymbol{\Omega}}_i\right)\boldsymbol{W}_i\right] \mid \widehat{\widehat{\boldsymbol{H}}}_i\right\}} \quad (49)$$

We exchange the trace and expectation operators which is possible since the trace is a linear operator.

$$= \frac{Tr[\boldsymbol{W}_i^*(E\{\rho_h{}^2\widehat{\boldsymbol{H}}_i^*\widehat{\boldsymbol{H}}_i + \rho_h\widehat{\boldsymbol{H}}_i^*\boldsymbol{\Omega}_\mathrm{i} + \boldsymbol{\Omega}_\mathrm{i}{}^*\rho_h\widehat{\boldsymbol{H}}_i + \boldsymbol{\Omega}_\mathrm{i}{}^*\boldsymbol{\Omega}_\mathrm{i} \mid \widehat{\boldsymbol{H}}_i\})\boldsymbol{W}_i]}{M_i\sigma_n^2 + Tr\left[\boldsymbol{W}_i^*\left(E\left\{\rho_h{}^2\widehat{\widehat{\boldsymbol{H}}}_i^*\widehat{\widehat{\boldsymbol{H}}}_i + \rho_h\widehat{\widehat{\boldsymbol{H}}}_i^*\widetilde{\boldsymbol{\Omega}}_i + \widetilde{\boldsymbol{\Omega}}_i{}^*\rho_h\widehat{\widehat{\boldsymbol{H}}}_i + \widetilde{\boldsymbol{\Omega}}_i{}^*\widetilde{\boldsymbol{\Omega}}_i \mid \widehat{\widehat{\boldsymbol{H}}}_i\right\}\right)\boldsymbol{W}_i\right]} \quad (50)$$

Now we simplify each term in the expectation based on independence between $\widehat{\boldsymbol{H}}_i$ and $\boldsymbol{\Omega}_\mathrm{i}$, independence between $\widehat{\widehat{\boldsymbol{H}}}_i$ and $\widetilde{\boldsymbol{\Omega}}_i$, and the condition on $\widehat{\boldsymbol{H}}_i$ and $\widehat{\widehat{\boldsymbol{H}}}_i$.

$$= \frac{Tr[\boldsymbol{W}_i^*(\rho_h{}^2\widehat{\boldsymbol{H}}_i^*\widehat{\boldsymbol{H}}_i + M_i\rho_h\sigma_c^2\boldsymbol{I})\boldsymbol{W}_i]}{M_i\sigma_n^2 + Tr\left[\boldsymbol{W}_i^*\left(\rho_h{}^2\widehat{\widehat{\boldsymbol{H}}}_i^*\widehat{\widehat{\boldsymbol{H}}}_i + \sum_{k=1,k\neq i}^{K} M_k\,\rho_h\sigma_c^2\boldsymbol{I}\right)\boldsymbol{W}_i\right]} \quad (51)$$

Noting that $Tr[\boldsymbol{W}_i^*\boldsymbol{W}_i] = S_iP_s$ we have

$$= \frac{Tr\left[\boldsymbol{W}_i^*\left({\rho_h}^2 \widehat{\boldsymbol{H}}_i^* \widehat{\boldsymbol{H}}_i + M_i \rho_h \sigma_c^2 \boldsymbol{I}\right)\boldsymbol{W}_i\right]}{Tr\left[\boldsymbol{W}_i^*\left({\rho_h}^2 \widehat{\widehat{\boldsymbol{H}}}_i^* \widehat{\widehat{\boldsymbol{H}}}_i + \left(\sum_{j=1,j\neq i}^{K} M_j \, \rho_h \sigma_c^2 + \frac{M_i}{S_i P_s}\sigma_n^2\right)\boldsymbol{I}\right)\boldsymbol{W}_i\right]} \tag{52}$$

By following the same approach used to derive the solution of the cSLNR precoding via eigendecomposition and substituting the value of ρ_h into the expression, the precoding matrix which will maximize SLNR in the presence of the imperfect CSIT defined by our model is given by

$$\boldsymbol{W}_i \propto S_i \max eigenvectors\ of$$
$$\left(\left(\frac{\widehat{\widehat{\boldsymbol{H}}}_i^* \widehat{\widehat{\boldsymbol{H}}}_i}{(1+\sigma_c^2)^2} + \left(\sum_{j=1,j\neq i}^{K} M_j \frac{\sigma_c^2}{1+\sigma_c^2} + \frac{M_i}{S_i P_s}\sigma_n^2\right)\boldsymbol{I}\right)^{-1}\left(\frac{\widehat{\boldsymbol{H}}_i^* \widehat{\boldsymbol{H}}_i}{(1+\sigma_c^2)^2} + \frac{M_i \sigma_c^2}{1+\sigma_c^2}\boldsymbol{I}\right)\right) \tag{53}$$

Under the assumption of equal power per stream and unit total transmit power the result is then normalized such that

$$\|\boldsymbol{w}_s\|^2 = \frac{1}{\sum_{i=1}^{K} S_i} \quad \forall\, s \tag{54}$$

Where $\boldsymbol{w}_s$ is the s^{th} column in $\boldsymbol{W}$.

Figure 3.1 shows a comparison between the bit error rates achieved by a 9x(3x3) system using the SLNR precoding scheme without considering imperfect CSIT, the previously proposed SLNR precoding scheme considering imperfect CSIT, and our newly derived SLNR precoding scheme considering imperfect CSIT. In this simulation the CSIT is 5 dB. The first observation from these results is that both of the schemes considering the CSIT error statistics perform significantly better than the scheme which does not. At an error rate of 1e-3 there is approximately 6 dB of gain. We also observe that the newly derived approach provides better error rate performance than the previously proposed solution as it more accurately accounts for the distribution of $\boldsymbol{H}_i$ given $\widehat{\boldsymbol{H}}_i$. The difference in performance is somewhat marginal; about 0.6 dB at an error rate of 1e-3, but we want

to be rigorous in our analysis and understanding before moving on to the iSLNR algorithm.

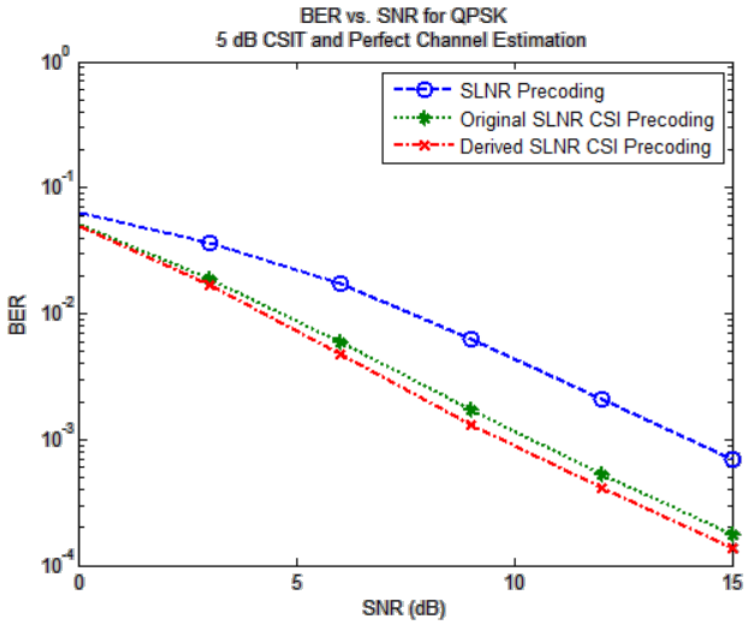

Figure 3.1: BER comparison between SLNR precoding considering CSIT error using the existing solution and the newly derived solution for a 9x(3x3) system

3.1.2 MMSE Modification of CSIT for SLNR Precoding

While reviewing the literature for possible approaches to improve performance of the SLNR precoding scheme with imperfect CSIT, we came across the work in [12]. In this paper it was shown that the impact of CSIT error can be further reduced by modifying the user and leakage channel estimates $\widehat{\boldsymbol{H}}_i$ and $\widehat{\widetilde{\boldsymbol{H}}}_i$ so as to minimize their mean square error to the true user and leakage channels $\boldsymbol{H}_i$ and $\widetilde{\boldsymbol{H}}_i$**.** This same approach was also used in [20]. We therefore continue our analysis by reviewing this work to determine whether or not it should be leveraged in our ultimate approach for the iSLNR algorithm with imperfect CSIT. In the following discussion we generalize the MMSE modification to the channel estimate $\widehat{\boldsymbol{H}}$. Note that the analysis is equivalent and applied in the same manner to both the user channel estimate $\widehat{\boldsymbol{H}}_i$ and the leakage channel estimate $\widehat{\widetilde{\boldsymbol{H}}}_i$.

We denote the MMSE modified quantities using $(\cdot)'$. The approach in [12] was to apply a linear transform matrix A as follows.

$$\boldsymbol{H}' \triangleq \widehat{\boldsymbol{H}}\boldsymbol{A} \tag{55}$$

The mean square error of the channel estimate from the true channel is given by

$$MSE = E\{\|\boldsymbol{H}' - \boldsymbol{H}\|^2\} \tag{56}$$

It was then shown that the matrix $\boldsymbol{A}$ which will minimize the mean square error is

$$\boldsymbol{A} = (M\sigma_c^2\boldsymbol{I} + \boldsymbol{H}^*\boldsymbol{H})\boldsymbol{H}^*\boldsymbol{H} \tag{57}$$

It was further shown that using this approach reduces the CSIT error variance and the modified CSIT error variance is then given by

$$\sigma_c^{2\prime} = \frac{\sigma_c^2}{r}\sum_{i=1}^{r}\frac{\lambda_i}{\lambda_i + \sigma_c^2} \tag{58}$$

where r is the rank and λ_i is the i^{th} eigenvalue of the transmit covariance matrix. The modified CSIT and modified error variances are then substituted directly into the original solution for the SLNR precoding matrix under imperfect CSIT (given in equation 45) as follows

$$\boldsymbol{W}_i \propto S_i \max eigenvectors\ of$$

$$\left(\left(\widetilde{\boldsymbol{H}}_i'^{*}\widetilde{\boldsymbol{H}}_i' + \left(\sum_{j=1, j\neq i}^{K} M_j\,\sigma_c^{2\prime} + \frac{M_i}{S_i P_s}\sigma_n^2\right)\boldsymbol{I}\right)^{-1}\left(\boldsymbol{H}_i'^{*}\boldsymbol{H}_i' + \sigma_c^{2\prime}\boldsymbol{I}\right)\right) \tag{59}$$

The issue we note with this approach is that the expression for $\boldsymbol{A}$ given in equation 57 depends on the actual channel $\boldsymbol{H}$ rather than the estimated channel $\widehat{\boldsymbol{H}}$. This presents an issue because the transmitter will only have knowledge of $\widehat{\boldsymbol{H}}$ in practice. Indeed if the transmitter has knowledge of $\boldsymbol{H}$**,** then it already possesses an error free channel estimate and the entire problem is effectively avoided by using $\boldsymbol{H}$ directly. So in practice the approach used in [12,20] is only useful if $\widehat{\boldsymbol{H}}$ can be substituted for $\boldsymbol{H}$ as in

$$\boldsymbol{A} = \left(M\sigma_c^2\boldsymbol{I} + \widehat{\boldsymbol{H}}^*\widehat{\boldsymbol{H}}\right)\widehat{\boldsymbol{H}}^*\widehat{\boldsymbol{H}} \tag{60}$$

As we'll show later, the more practical solution in equation 60 will still manage to reduce the CSIT MSE, but it will not minimize it. In addition, we note that the authors of [12] reused the solution proposed in [7] for SLNR precoding with imperfect CSIT whereas we have shown that the newly derived solution results in better performance.

While there are certain issues with the particular approach used to minimize the mean square error shown in [12], it still seems reasonable that the SLNR precoding might benefit from modifying the CSIT to meet the MMSE criteria. So rather than using the solution proposed in [12] directly, we instead move to derive the MMSE modification which will rely only on knowledge of $\widehat{\boldsymbol{H}}$ and the second-order statistics of the CSIT error, σ_c^2. We begin in a similar fashion with the expression for the MSE between the modified channel estimate $\boldsymbol{H}'$ and the actual channel $\boldsymbol{H}$, conditioned on the unmodified channel estimate $\widehat{\boldsymbol{H}}$.

$$MSE = E\{\|\boldsymbol{H}' - \boldsymbol{H}\|^2 \mid \widehat{\boldsymbol{H}}\}$$

$$= E\left\{\left\|\widehat{\boldsymbol{H}}\boldsymbol{A} - \boldsymbol{H}\right\|^2 \mid \widehat{\boldsymbol{H}}\right\}$$

$$= E\{Tr[(\widehat{\boldsymbol{H}}\boldsymbol{A} - \boldsymbol{H})^*(\widehat{\boldsymbol{H}}\boldsymbol{A} - \boldsymbol{H})] \mid \widehat{\boldsymbol{H}}\}$$

$$= E\{Tr[\boldsymbol{A}^*\widehat{\boldsymbol{H}}^*\widehat{\boldsymbol{H}}\boldsymbol{A} - \boldsymbol{A}^*\widehat{\boldsymbol{H}}^*\boldsymbol{H} - \boldsymbol{H}^*\widehat{\boldsymbol{H}}\boldsymbol{A} + \boldsymbol{H}^*\boldsymbol{H}] \mid \widehat{\boldsymbol{H}}\} \quad (61)$$

The trace of a matrix is a linear operator and so may be exchanged with the expectation.

$$= Tr[\boldsymbol{A}^*\widehat{\boldsymbol{H}}^*\widehat{\boldsymbol{H}}\boldsymbol{A} - \boldsymbol{A}^*\boldsymbol{E}\{\widehat{\boldsymbol{H}}^*\boldsymbol{H}|\ \widehat{\boldsymbol{H}}\} - E\{\boldsymbol{H}^*\widehat{\boldsymbol{H}}|\ \widehat{\boldsymbol{H}}\}\boldsymbol{A} + E\{\boldsymbol{H}^*\boldsymbol{H}|\ \widehat{\boldsymbol{H}}\}] \quad (62)$$

As in section 3.1.1 we utilize the distribution of $\boldsymbol{H}$ conditioned on $\widehat{\boldsymbol{H}}$ given below

$$p(\boldsymbol{H}|\widehat{\boldsymbol{H}}) = \rho_h\widehat{\boldsymbol{H}} + \boldsymbol{\Omega} \quad (63)$$

Substituting this expression into equation 62 we have

$$= Tr[\boldsymbol{A}^*\widehat{\boldsymbol{H}}^*\widehat{\boldsymbol{H}}\boldsymbol{A} - \boldsymbol{A}^*\boldsymbol{E}\{\widehat{\boldsymbol{H}}^*(\rho_h\widehat{\boldsymbol{H}} + \boldsymbol{\Omega})|\ \widehat{\boldsymbol{H}}\} - E\{(\rho_h\widehat{\boldsymbol{H}} + \boldsymbol{\Omega})^*\widehat{\boldsymbol{H}}|\ \widehat{\boldsymbol{H}}\}\boldsymbol{A}$$

$$+ E\{(\rho_h\widehat{\boldsymbol{H}} + \boldsymbol{\Omega})^*(\rho_h\widehat{\boldsymbol{H}} + \boldsymbol{\Omega})|\ \widehat{\boldsymbol{H}}\}]$$

which simplifies to

$$= Tr\left[\boldsymbol{A}^{*}\widehat{\boldsymbol{H}}^{*}\widehat{\boldsymbol{H}}\boldsymbol{A} - \rho_h\boldsymbol{A}^{*}\widehat{\boldsymbol{H}}^{*}\widehat{\boldsymbol{H}} - \rho_h\widehat{\boldsymbol{H}}^{*}\widehat{\boldsymbol{H}}\boldsymbol{A} + \rho_h{}^{\boldsymbol{2}}\widehat{\boldsymbol{H}}^{*}\widehat{\boldsymbol{H}} + M\rho_h\boldsymbol{I}\right] \tag{64}$$

In order to minimize this MSE, we take the gradient with respect to $\boldsymbol{A}$ and set it equal to zero.

$$\nabla_{\boldsymbol{A}}(MSE) = 2\boldsymbol{A}^{*}\widehat{\boldsymbol{H}}^{*}\widehat{\boldsymbol{H}} - \rho_h\widehat{\boldsymbol{H}}^{*}\widehat{\boldsymbol{H}} - \rho_h\widehat{\boldsymbol{H}}^{*}\widehat{\boldsymbol{H}} = \boldsymbol{0}$$

$$= 2\boldsymbol{A}^{*}\widehat{\boldsymbol{H}}^{*}\widehat{\boldsymbol{H}} - 2\rho_h\widehat{\boldsymbol{H}}^{*}\widehat{\boldsymbol{H}} = \boldsymbol{0} \tag{65}$$

from which we arrive at

$$\boldsymbol{A} = \rho_h\widehat{\boldsymbol{H}}^{*}\widehat{\boldsymbol{H}}\left(\widehat{\boldsymbol{H}}^{*}\widehat{\boldsymbol{H}}\right)^{-1}$$

$$\boldsymbol{A} = \rho_h\boldsymbol{I} \tag{66}$$

So the candidate $\boldsymbol{A}$, to minimize the mean square error of the CSIT error is given in equation 66. We then derive the Hessian of the MSE with respect to $\boldsymbol{A}$

$$\nabla_{\boldsymbol{A}}^{\boldsymbol{2}}(MSE) = 2\widehat{\boldsymbol{H}}^{*}\widehat{\boldsymbol{H}} \tag{67}$$

which is trivially noted to be a positive semi-definite matrix, making $\boldsymbol{A}$ the global minimizer of the MSE.

From equation 66 we see that only a scalar modification is needed to minimize the mean square error of the channel estimate. We therefore redefine the modified CSIT using a scalar modification as

$$\boldsymbol{H}' \triangleq \alpha\widehat{\boldsymbol{H}} \tag{68}$$

and the particular α which will minimize the mean square error is $\alpha_{MMSE} \triangleq \rho_h = \frac{1}{1+\sigma_c^2}$.

The resulting CSIT error covariance after applying an arbitrary scalar α will be given by

$$\begin{aligned}
\boldsymbol{R}_c &= E\{(\boldsymbol{H}' - \boldsymbol{H})^*(\boldsymbol{H}' - \boldsymbol{H})\} \\
&= E\{(\alpha(\boldsymbol{H} + \boldsymbol{\Gamma}) - \boldsymbol{H})^*(\alpha(\boldsymbol{H} + \boldsymbol{\Gamma}) - \boldsymbol{H})\} \\
&= E\begin{Bmatrix} \alpha^2\boldsymbol{H}^*\boldsymbol{H} + \alpha^2\boldsymbol{H}^*\boldsymbol{\Gamma} - \alpha\boldsymbol{H}^*\boldsymbol{H}_{t_1} + \alpha^2\boldsymbol{\Gamma}^*\boldsymbol{H} \\ +\alpha^2\boldsymbol{\Gamma}^*\boldsymbol{\Gamma} - \alpha\boldsymbol{\Gamma}^*\boldsymbol{H} - \alpha\boldsymbol{H}^*\boldsymbol{H} - \alpha\boldsymbol{H}^*\boldsymbol{\Gamma} + \boldsymbol{H}^*\boldsymbol{H} \end{Bmatrix} \\
&= \left(1 - 2\alpha + \alpha^2(1 + \sigma_c^2)\right)\boldsymbol{I}
\end{aligned} \tag{69}$$

By applying α_{MMSE} the CSIT error covariance will be

$$\begin{aligned}
\boldsymbol{R}_c &= \left(1 - 2\frac{1}{(1+\sigma_c^2)} + \left(\frac{1}{(1+\sigma_c^2)}\right)^2 (1+\sigma_c^2)\right)\boldsymbol{I} \\
&= \left(1 - \frac{1}{(1+\sigma_c^2)}\right)\boldsymbol{I} \\
&= \frac{\sigma_c^2}{(1+\sigma_c^2)}\boldsymbol{I}
\end{aligned} \tag{70}$$

We then define this to be the CSIT error variance after the MMSE scaling.

$$\sigma_c^{2\prime} \triangleq \frac{\sigma_c^2}{(1+\sigma_c^2)} \tag{71}$$

The effect of the MMSE scaling is investigated via simulation. Figure 3.2 shows the CSIT MSE with and without the MMSE modification in a 6x(2x3) system. We also include the solution from [12] using the actual channel and the imperfect channel estimate as stated in equations 57 and 60. You can see that the solution presented in [12] which uses the actual channel $\boldsymbol{H}$ does the best in terms of reducing the MSE, but as mentioned earlier it is impractical to assume knowledge of $\boldsymbol{H}$. Applying the solution

presented in [12] using the imperfect CSIT will still reduce the MSE to some degree, but ultimately the scalar modification we derived above is the best solution since it minimizes the MSE without relying on knowledge of $\boldsymbol{H}$.

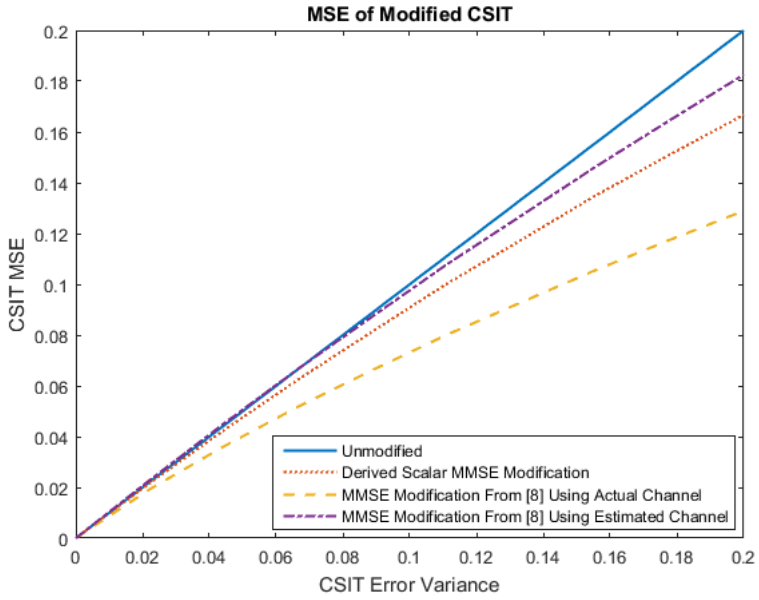

Figure 3.2: MMSE Modified CSIT Mean Square Error

Now that we have derived the practical MMSE modification for the CSIT, we investigate the effect of using the modified CSIT directly in place of the unmodified CSIT as [12] suggests, by directly substituting the modified user channel $\boldsymbol{H}_i'$, the modified leakage channel $\widetilde{\boldsymbol{H}}_i'$, and the modified error variance $\sigma_c^{2\prime}$ into the newly derived solution for SLNR precoding with imperfect CSIT given in equation 53. The SLNR precoding matrix is then calculated as in equation 72

$$\boldsymbol{W}_i \propto S_i \max eigenvectors$$

$$\left(\left(\frac{\widetilde{\boldsymbol{H}}_i'^{*}\widetilde{\boldsymbol{H}}_i'}{(1+\sigma_c^{2\prime})^2}+\left(\left(\sum_{j=1,j\neq i}^{K} M_j\right)\frac{\sigma_c^{2\prime}}{1+\sigma_c^{2\prime}}+\frac{M_i}{S_i P_s}\sigma_n^2\right)\boldsymbol{I}\right)^{-1}\left(\frac{\boldsymbol{H}_i'^{*}\boldsymbol{H}_i'}{(1+\sigma_c^{2\prime})^2}+\frac{\sigma_c^{2\prime}}{1+\sigma_c^{2\prime}}\boldsymbol{I}\right)\right) \qquad (72)$$

Figure 3.3 shows the bit error rate of a 9x(3x3) system operating with 5 dB CSIT using the derived SLNR precoding scheme which considers CSIT error, both with the unmodified CSIT and with the MMSE modified CSIT. The previously derived SLNR precoding scheme with imperfect CSIT is also included. From these results we observe that the practical MMSE modification provides a marginal gain, less than was shown by the results in [12]. In this case, at an error rate of 1e-3 it provides about 0.4 dB of gain compared to the newly derived SLNR precoding with imperfect CSIT and about 1 dB compared to the original SLNR precoding with imperfect CSIT from [7].

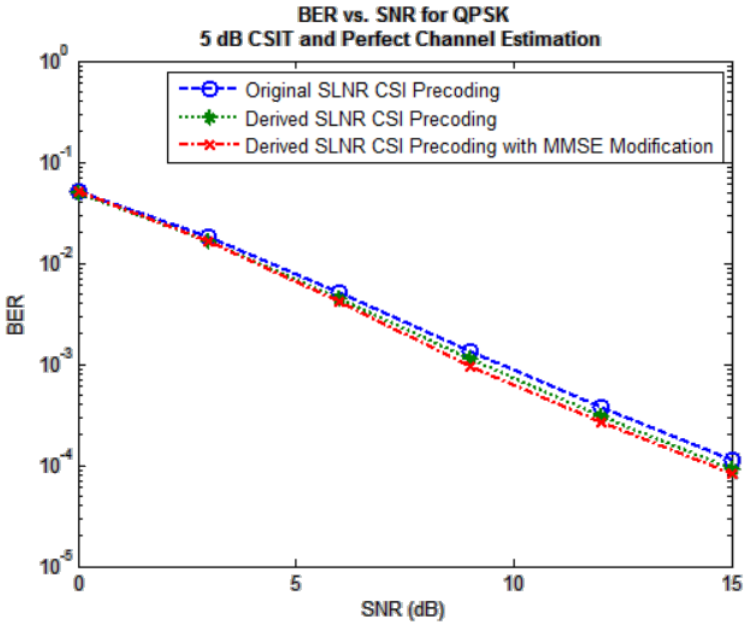

Figure 3.3: Bit error rate with MMSE modification of CSIT

3.2 iSLNR Precoding Considering CSIT Error

Now that we have considered how we may best mitigate the effects of imperfect CSIT using the non-iterative SLNR precoding scheme, we will continue on to apply similar analysis to the iterative algorithm. As explained in chapter two, the iSLNR algorithm relies on calculating the receiver processing for each user to then update effective leakage channels and recalculate the precoding matrices. We must then consider the effects of imperfect CSIT both in the calculation of receiver processing and precoding matrices in order to achieve the best possible performance using this algorithm with imperfect CSIT.

3.2.1 Receiver Calculation with Imperfect CSIT

With perfect CSIT and CSIR, the receive filters are calculated without error using equation 15 for ZF receivers and equations 17 and 20 for IRC receivers. With imperfect CSIT this is no longer true, which motivates us to investigate the calculation of receive filters in the iSLNR algorithm with imperfect CSIT. Note that in the following derivations we have dropped the user index to ease notation, though the reader should note that all quantities are specific to a particular user.

We begin by considering the interference plus noise covariance matrix given in equation 18 which is required to calculate the IRC receiver structure. With perfect CSIT this expression would be conditioned on the true channel $\boldsymbol{H}$ and the interference precoding matrix $\boldsymbol{W}_n$, which is ultimately how we arrived at the expression in equation 20. In this case the expression is conditioned on the channel estimate $\widehat{\boldsymbol{H}}$ and the interference precoding matrix $\boldsymbol{W}_n$ as shown below.

$$\widehat{\boldsymbol{R}}_n = E\{(\boldsymbol{H}\boldsymbol{W}_n\boldsymbol{s}_n + \boldsymbol{n})(\boldsymbol{H}\boldsymbol{W}_n\boldsymbol{s}_n + \boldsymbol{n})^* \mid \widehat{\boldsymbol{H}}, \boldsymbol{W}_n\} \tag{73}$$

We substitute the distribution of $\boldsymbol{H}$ given $\widehat{\boldsymbol{H}}$ into the equation

$$= E\left\{\left(\left(\rho_h\widehat{\boldsymbol{H}} + \boldsymbol{\Omega}\right)\boldsymbol{W}_n\boldsymbol{s}_n + \boldsymbol{n}\right)\left(\left(\rho_h\widehat{\boldsymbol{H}} + \boldsymbol{\Omega}\right)\boldsymbol{W}_n\boldsymbol{s}_n + \boldsymbol{n}\right)^* \mid \widehat{\boldsymbol{H}}, \boldsymbol{W}_n\right\} \tag{74}$$

Where again $\rho_h = \frac{1}{1+\sigma_c^2}$ and the elements of $\boldsymbol{\Omega}$ are i.i.d. complex Gaussian random variables with zero mean and variance $\frac{\sigma_c^2}{1+\sigma_c^2}$. We expand this expression as follows.

$$\begin{aligned} = E\Big\{&\left(\left(\rho_h\widehat{\boldsymbol{H}} + \boldsymbol{\Omega}\right)\boldsymbol{W}_n\boldsymbol{s}_n\right)\left(\left(\rho_h\widehat{\boldsymbol{H}} + \boldsymbol{\Omega}\right)\boldsymbol{W}_n\boldsymbol{s}_n\right)^* + \left(\left(\rho_h\widehat{\boldsymbol{H}} + \boldsymbol{\Omega}\right)\boldsymbol{W}_n\boldsymbol{s}_n\right)\boldsymbol{n}^* \\ &+ \boldsymbol{n}\left(\left(\rho_h\widehat{\boldsymbol{H}} + \boldsymbol{\Omega}\right)\boldsymbol{W}_n\boldsymbol{s}_n\right)^* + \boldsymbol{n}\boldsymbol{n}^* \mid \widehat{\boldsymbol{H}}, \boldsymbol{W}_n\Big\} \end{aligned} \tag{75}$$

By noting that the noise term is independent of all other terms and has zero mean we can simplify.

$$= E\left\{\left(\left(\rho_h\widehat{\boldsymbol{H}} + \boldsymbol{\Omega}\right)\boldsymbol{W}_n\boldsymbol{s}_n\right)\left(\left(\rho_h\widehat{\boldsymbol{H}} + \boldsymbol{\Omega}\right)\boldsymbol{W}_n\boldsymbol{s}_n\right)^* \mid \widehat{\boldsymbol{H}}, \boldsymbol{W}_n\right\} + E\{\boldsymbol{n}\boldsymbol{n}^*\} \tag{76}$$

We then continue by expanding the expression on the left.

$$\begin{aligned} = E\{&\rho_h^2\widehat{\boldsymbol{H}}\boldsymbol{W}_n\boldsymbol{s}_n\boldsymbol{s}_n^*\boldsymbol{W}_n^*\widehat{\boldsymbol{H}}^* + \rho_h\widehat{\boldsymbol{H}}\boldsymbol{W}_n\boldsymbol{s}_n\boldsymbol{s}_n^*\boldsymbol{W}_n^*\boldsymbol{\Omega}^* + \rho_h\boldsymbol{\Omega}\boldsymbol{W}_n\boldsymbol{s}_n\boldsymbol{s}_n^*\boldsymbol{W}_n^*\widehat{\boldsymbol{H}}^* \\ &+ \boldsymbol{\Omega}\boldsymbol{W}_n\boldsymbol{s}_n\boldsymbol{s}_n^*\boldsymbol{W}_n^*\boldsymbol{\Omega}^* \mid \widehat{\boldsymbol{H}}, \boldsymbol{W}_n\} + E\{\boldsymbol{n}\boldsymbol{n}^*\} \end{aligned} \tag{77}$$

We can again simplify by noting that $\widehat{\boldsymbol{H}}$ and $\boldsymbol{\Omega}$ are independent and by treating $\boldsymbol{s}_n$ as a random variable with unit power and uniformly distributed phase. This results in the following expression.

$$= E\{\rho_h^2\widehat{\boldsymbol{H}}\boldsymbol{W}_n\boldsymbol{W}_n^*\widehat{\boldsymbol{H}}^* + \boldsymbol{\Omega}\boldsymbol{W}_n\boldsymbol{W}_n^*\boldsymbol{\Omega}^* \mid \widehat{\boldsymbol{H}}, \boldsymbol{W}_n\} + E\{\boldsymbol{n}\boldsymbol{n}^*\} \tag{78}$$

Since $\widehat{\boldsymbol{H}}$ and $\boldsymbol{W}_n$ are given quantities, the expectation can be removed.

$$= \rho_h^2\widehat{\boldsymbol{H}}\boldsymbol{W}_n\boldsymbol{W}_n^*\widehat{\boldsymbol{H}}^* + E\{\boldsymbol{\Omega}\boldsymbol{W}_n\boldsymbol{W}_n^*\boldsymbol{\Omega}^*\} + E\{\boldsymbol{n}\boldsymbol{n}^*\} \tag{79}$$

The $E\{\boldsymbol{n}\boldsymbol{n}^*\}$ term is very easily seen to be $\sigma_n^2\boldsymbol{I}$, though it's maybe not quite as obvious how the $E\{\boldsymbol{\Omega}\boldsymbol{W}_n\boldsymbol{W}_n^*\boldsymbol{\Omega}^*\}$ term simplifies. We therefore show it explicitly here using an example scenario to avoid the more complex notation needed to make the expressions general. We consider a 6x(2x4) system with a single stream per user. In this case, for user 1 we have

$$\boldsymbol{\Omega}\boldsymbol{W}_n = \begin{bmatrix} \omega_{11} & \omega_{12} & \omega_{13} & \omega_{14} & \omega_{15} & \omega_{16} \\ \omega_{21} & \omega_{22} & \omega_{23} & \omega_{24} & \omega_{25} & \omega_{26} \end{bmatrix} \begin{bmatrix} w_{21} & w_{31} & w_{41} \\ w_{22} & w_{32} & w_{42} \\ w_{23} & w_{33} & w_{43} \\ w_{24} & w_{34} & w_{44} \\ w_{25} & w_{35} & w_{45} \\ w_{26} & w_{36} & w_{46} \end{bmatrix}$$

$$= \begin{bmatrix} \sum_{k=1}^{6} \omega_{1k} w_{2k} & \sum_{k=1}^{6} \omega_{1k} w_{3k} & \sum_{k=1}^{6} \omega_{1k} w_{4k} \\ \sum_{k=1}^{6} \omega_{2k} w_{2k} & \sum_{k=1}^{6} \omega_{2k} w_{3k} & \sum_{k=1}^{6} \omega_{2k} w_{4k} \end{bmatrix}$$

$$= \sum_{k=1}^{6} \begin{bmatrix} \omega_{1k} w_{2k} & \omega_{1k} w_{3k} & \omega_{1k} w_{4k} \\ \omega_{2k} w_{2k} & \omega_{2k} w_{3k} & \omega_{2k} w_{4k} \end{bmatrix} \tag{80}$$

Using this expression we can rewrite $E\{\boldsymbol{\Omega} \boldsymbol{W}_n \boldsymbol{W}_n^* \boldsymbol{\Omega}^*\}$ as

$$E\{\boldsymbol{\Omega} \boldsymbol{W}_n \boldsymbol{W}_n^* \boldsymbol{\Omega}^*\} = E\left\{ \sum_{j=1}^{6} \begin{bmatrix} \omega_{1j} w_{2j} & \omega_{1j} w_{3j} & \omega_{1j} w_{4j} \\ \omega_{2j} w_{2j} & \omega_{2j} w_{3j} & \omega_{2j} w_{4j} \end{bmatrix} \sum_{k=1}^{6} \begin{bmatrix} \omega_{1k}^* w_{2k}^* & \omega_{2k}^* w_{2k}^* \\ \omega_{1k}^* w_{3k}^* & \omega_{2k}^* w_{3k}^* \\ \omega_{1k}^* w_{4k}^* & \omega_{2k}^* w_{4k}^* \end{bmatrix} \right\} \tag{81}$$

We define the matrix $C = E\{\boldsymbol{\Omega} \boldsymbol{W}_n \boldsymbol{W}_n^* \boldsymbol{\Omega}^*\} = \begin{bmatrix} b_{11} & b_{12} \\ b_{21} & b_{22} \end{bmatrix}$ so we can reasonably write out each element as below.

$$\begin{aligned} c_{11} &= E\left\{ \sum_{i=2}^{4} \left(\sum_{k=1}^{6} \omega_{1k} w_{ik} \sum_{k=1}^{6} \omega_{1k}^* w_{ik}^* \right) \right\} \\ c_{12} &= E\left\{ \sum_{i=2}^{4} \left(\sum_{k=1}^{6} \omega_{1k} w_{ik} \sum_{k=1}^{6} \omega_{2k}^* w_{ik}^* \right) \right\} \\ c_{21} &= E\left\{ \sum_{i=2}^{4} \left(\sum_{k=1}^{6} \omega_{2k} w_{ik} \sum_{k=1}^{6} \omega_{1k}^* w_{ik}^* \right) \right\} \\ c_{22} &= E\left\{ \sum_{i=2}^{4} \left(\sum_{k=1}^{6} \omega_{2k} w_{ik} \sum_{k=1}^{6} \omega_{2k}^* w_{ik}^* \right) \right\} \end{aligned} \tag{82}$$

Independence between ω_{ij} and w_{mn} implies

$$E\{\omega_{ij} \omega_{ij}^* w_{mn} w_{mn}^*\} = E\{\omega_{ij} \omega_{ij}^*\} E\{w_{mn} w_{mn}^*\} \; \forall \; i, j, m, \text{and } n \tag{83}$$

With the elements of $\boldsymbol{\Omega}$ being i.i.d. we also have

$$E\{\omega_{ij} \omega_{mn}^*\} = 0 \; \forall \; i \neq m \text{ or } j \neq n \tag{84}$$

Using the conditions in equations 83 and 84 we can simplify $\boldsymbol{C}$ to the following

$$\boldsymbol{C} = \begin{bmatrix} \sum_{i=2}^{4}\sum_{k=1}^{6} E\{\omega_{1k}\omega_{1k}^{*}\} w_{ik}w_{ik}^{*} & 0 \\ 0 & \sum_{i=2}^{4}\sum_{k=1}^{6} E\{\omega_{2k}\omega_{2k}^{*}\} w_{ik}w_{ik}^{*} \end{bmatrix} \quad (85)$$

Noting that $E\{\omega_{ij}\omega_{ij}^{*}\} = \frac{\sigma_c^2}{1+\sigma_c^2}\ \forall\ i,j$ this simplifies to

$$\boldsymbol{C} = \begin{bmatrix} \frac{\sigma_c^2}{1+\sigma_c^2}\sum_{i=2}^{4}\sum_{k=1}^{6} w_{ik}w_{ik}^{*} & 0 \\ 0 & \frac{\sigma_c^2}{1+\sigma_c^2}\sum_{i=2}^{4}\sum_{k=1}^{6} w_{ik}w_{ik}^{*} \end{bmatrix}$$

$$= \left(\frac{\sigma_c^2}{1+\sigma_c^2}\sum_{i=2}^{4}\sum_{k=1}^{6} w_{ik}w_{ik}^{*}\right)\boldsymbol{I} \quad (86)$$

In this work we have assumed equal power per stream given by P_s. This implies that

$$\sum_{k=1}^{6} w_{ik}w_{ik}^{*} = P_s\ \forall\ i \quad (87)$$

So the matrix $\boldsymbol{C}$ simplifies further to

$$\boldsymbol{C} = \left(\frac{\sigma_c^2}{1+\sigma_c^2}\sum_{i=2}^{4} P_s\right)\boldsymbol{I}$$

$$= \left(3P_s\frac{\sigma_c^2}{1+\sigma_c^2}\right)\boldsymbol{I} \quad (88)$$

We note that the factor of 3 comes from the total number of interfering streams so the generalized expression in a system with K users and where the j^{th} user has S_j streams is given by

$$\boldsymbol{C} = E\{\boldsymbol{\Omega W}_n \boldsymbol{W}_n^* \boldsymbol{\Omega}^*\} = \left(P_s \sum\nolimits_{j=1, j\neq i}^{K} S_j\right) \frac{\sigma_c^2}{1+\sigma_c^2} \boldsymbol{I} \tag{89}$$

With this result in mind, we return to simplifying the expression for the interference plus noise covariance matrix where we left off at equation 79. The final expression is given by

$$\widehat{\boldsymbol{R}}_n = \frac{\widehat{\boldsymbol{H}} \boldsymbol{W}_n \boldsymbol{W}_n^* \widehat{\boldsymbol{H}}^*}{(1+\sigma_c^2)^2} + \left(\left(P_s \sum_{k\neq i}^{K} S_k\right) \frac{\sigma_c^2}{1+\sigma_c^2} + \sigma_n^2\right) \boldsymbol{I} \tag{90}$$

With a single stream per user and total transmit power $P = 1$, this of course simplifies to

$$\widehat{\boldsymbol{R}}_n = \frac{\widehat{\boldsymbol{H}} \boldsymbol{W}_n \boldsymbol{W}_n^* \widehat{\boldsymbol{H}}^*}{(1+\sigma_c^2)^2} + \left(\frac{(K-1)}{K} \frac{\sigma_c^2}{1+\sigma_c^2} + \sigma_n^2\right) \boldsymbol{I} \tag{91}$$

Now that we have found the expression for the interference plus noise covariance, we look at the expression for the IRC receiver processing matrix provided in equation 17. We note that this equation depends on the true channel $\boldsymbol{H}$ whereas the transmitter only has access to the estimated channel $\widehat{\boldsymbol{H}}$. We therefore desire to minimize the impact of the estimation error on our calculation of $\widehat{\boldsymbol{T}}_{IRC}$. To do this we solve for the $\widehat{\boldsymbol{T}}_{IRC}$ which will minimize the mean square error given by

$$\begin{aligned} MSE &= E\left\{\left\|\widehat{\boldsymbol{T}}_{IRC} - \boldsymbol{T}_{IRC}\right\|^2\right\} \\ &= E\left\{\left(\widehat{\boldsymbol{T}}_{IRC} - \boldsymbol{T}_{IRC}\right)^* \left(\widehat{\boldsymbol{T}}_{IRC} - \boldsymbol{T}_{IRC}\right)\right\} \\ &= \widehat{\boldsymbol{T}}_{IRC}^* \widehat{\boldsymbol{T}}_{IRC} - \widehat{\boldsymbol{T}}_{IRC}^* E\{\boldsymbol{T}_{IRC}\} - E\{\boldsymbol{T}_{IRC}^*\} \widehat{\boldsymbol{T}}_{IRC} + E\{\boldsymbol{T}_{IRC}^* \boldsymbol{T}_{IRC}\} \end{aligned} \tag{92}$$

Taking the gradient with respect to $\widehat{\boldsymbol{T}}_{IRC}$ and setting it to zero we have

$$\nabla_{\boldsymbol{T}_{IRC}}(MSE) = 2\widehat{\boldsymbol{T}}_{IRC} - 2E\{\boldsymbol{T}_{IRC}\} = 0$$

$$\widehat{\boldsymbol{T}}_{IRC} = E\{\boldsymbol{T}_{IRC}\} \tag{93}$$

This is a standard result as described in [23]. We therefore move to simplify this expression for $\widehat{\boldsymbol{T}}_{IRC}$ given the known quantities $\widehat{\boldsymbol{H}}$, $\boldsymbol{W}$, and $\widehat{\boldsymbol{R}}_n$.

$$\widehat{\boldsymbol{T}}_{IRC} = E\{\boldsymbol{T}_{IRC} | \, \widehat{\boldsymbol{H}}, \boldsymbol{W}, \widehat{\boldsymbol{R}}_n\}$$

$$= E\left\{\left(\boldsymbol{W}^* \boldsymbol{H}^* \widehat{\boldsymbol{R}}_n^{-1} \boldsymbol{H}\boldsymbol{W}\right)^{-1} \boldsymbol{W}^* \boldsymbol{H}^* \widehat{\boldsymbol{R}}_n^{-1} | \, \widehat{\boldsymbol{H}}, \boldsymbol{W}, \widehat{\boldsymbol{R}}_n\right\} \tag{94}$$

We again substitute the distribution of $\boldsymbol{H}$ given $\widehat{\boldsymbol{H}}$.

$$= E\left\{\left(\boldsymbol{W}^* \left(\rho_h \widehat{\boldsymbol{H}}^* + \boldsymbol{\Omega}^*\right) \widehat{\boldsymbol{R}}_n^{-1} (\rho_h \widehat{\boldsymbol{H}} + \boldsymbol{\Omega}) \boldsymbol{W}\right)^{-1} \boldsymbol{W}^* \left(\rho_h \widehat{\boldsymbol{H}}^* + \boldsymbol{\Omega}^*\right) \widehat{\boldsymbol{R}}_n^{-1} | \, \widehat{\boldsymbol{H}}, \boldsymbol{W}, \widehat{\boldsymbol{R}}_n\right\} \tag{95}$$

We expand the terms in the inverse and simplify by noting independence between $\widehat{\boldsymbol{H}}$ and $\boldsymbol{\Omega}$.

$$= E\left\{\left(\rho_h{}^2 \boldsymbol{W}^* \widehat{\boldsymbol{H}}^* \widehat{\boldsymbol{R}}_n^{-1} \widehat{\boldsymbol{H}} \boldsymbol{W} + \boldsymbol{W}^* \boldsymbol{\Omega}^* \widehat{\boldsymbol{R}}_n^{-1} \boldsymbol{\Omega} \boldsymbol{W}\right)^{-1} | \, \widehat{\boldsymbol{H}}, \boldsymbol{W}, \widehat{\boldsymbol{R}}_n\right\} \rho_h \boldsymbol{W}^* \widehat{\boldsymbol{H}}^* \widehat{\boldsymbol{R}}_n^{-1} \tag{96}$$

For the i^{th} user we have $\|\boldsymbol{W}\|^2 = S_i P_s$. Substituting this and the value of ρ_h into the solution used to calculate the IRC receiver processing in the iSLNR algorithm with imperfect CSIT yields

$$= \left(\frac{\boldsymbol{W}^* \widehat{\boldsymbol{H}}^* \widehat{\boldsymbol{R}}_n^{-1} \widehat{\boldsymbol{H}} \boldsymbol{W}}{(1+\sigma_c^2)^{\mathbf{2}}} + Tr\left[\widehat{\boldsymbol{R}}_n^{-1}\right] S_i P_s \frac{\sigma_c^2}{1+\sigma_c^2} \boldsymbol{I}\right)^{-1} \frac{\boldsymbol{W}^* \widehat{\boldsymbol{H}}^* \widehat{\boldsymbol{R}}_n^{-1}}{1+\sigma_c^2} \tag{97}$$

Similarly the calculation of the receiver processing using ZF receivers will be given by its expectation in order to minimize the mean square error. Expanding this expression as before we have

$$\widehat{\boldsymbol{T}}_{ZF} = E\{T_{ZF}\}$$

$$= E\left\{(\boldsymbol{W}^* \boldsymbol{H}^* \boldsymbol{H}\boldsymbol{W})^{-1} \boldsymbol{W}^* \boldsymbol{H}^* \, | \, \widehat{\boldsymbol{H}}, \boldsymbol{W}\right\}$$

$$= E\left\{\left(\boldsymbol{W}^* \left(\rho_h \widehat{\boldsymbol{H}}^* + \boldsymbol{\Omega}^*\right)\left(\rho_h \widehat{\boldsymbol{H}} + \boldsymbol{\Omega}\right) \boldsymbol{W}\right)^{-1} \boldsymbol{W}^* \left(\rho_h \widehat{\boldsymbol{H}}^* + \boldsymbol{\Omega}^*\right) | \, \widehat{\boldsymbol{H}}, \boldsymbol{W}\right\}$$

$$= E\left\{\left(\rho_h{}^2 \boldsymbol{W}^* \widehat{\boldsymbol{H}}^* \widehat{\boldsymbol{H}} \boldsymbol{W} + \boldsymbol{W}^* \boldsymbol{\Omega}^* \boldsymbol{\Omega} \boldsymbol{W}\right)^{-1} | \, \widehat{\boldsymbol{H}}, \boldsymbol{W}, \widehat{\boldsymbol{R}}_n\right\} \rho_h \boldsymbol{W}^* \widehat{\boldsymbol{H}}^*$$

$$= \left(\frac{\boldsymbol{W}^* \widehat{\boldsymbol{H}}^* \widehat{\boldsymbol{H}} \boldsymbol{W}}{(1+\sigma_c^2)^{\mathbf{2}}} + S_i P_s \frac{\sigma_c^2}{1+\sigma_c^2} \boldsymbol{I} \right)^{-1} \frac{\boldsymbol{W}^* \widehat{\boldsymbol{H}}^*}{1+\sigma_c^2} \tag{98}$$

3.2.2 Modified SLNR Precoding with Imperfect CSIT

In the previous section we derived how the receiver processing matrices should be calculated at the transmitter in the iSLNR algorithm with imperfect CSIT. The next step of the algorithm is to use these matrices to update the effective leakage channels, so we must consider the impact of imperfect CSIT on this step as well.

The expression to derive the initial precoding weights follows from the newly derived SLNR precoding scheme with imperfect CSIT provided in equation 53 and restated below to remind the reader

$$\boldsymbol{W}_i \propto S_i \max eigenvectors\ of$$

$$\left(\left(\frac{\widehat{\widehat{\boldsymbol{H}}}_i^* \widehat{\widehat{\boldsymbol{H}}}_i}{(1+\sigma_c^2)^2} + \left(\sum_{k \neq i} M_k \frac{\sigma_c^2}{1+\sigma_c^2} + \frac{M_i}{S_i P_s} \sigma_n^2 \right) \boldsymbol{I} \right)^{-1} \left(\frac{\widehat{\boldsymbol{H}}_i^* \widehat{\boldsymbol{H}}_i}{(1+\sigma_c^2)^2} + \frac{\sigma_c^2}{1+\sigma_c^2} \boldsymbol{I} \right) \right) \tag{99}$$

Under the assumption of equal power per stream and unit total transmit power the result is then normalized such that

$$\|\boldsymbol{w}_s\|^2 = \frac{1}{\sum_{i=1}^{K} S_i} \quad \forall\, s \tag{100}$$

Where $\boldsymbol{w}_s$ is the s^{th} column in $\boldsymbol{W}$.

For each of the subsequent iterations in the iSLNR algorithm we update the precoding matrix using the modified SLNR metric which uses effective leakage channels as given in equation 39 and shown below.

$$mSLNR = \frac{\|\boldsymbol{H}_i \boldsymbol{W}_i\|^2}{S_i \sigma_n^2 + \|\bar{\boldsymbol{H}}_i \boldsymbol{W}_i\|^2} \tag{101}$$

With imperfect CSIT, the expression is conditioned on the user channel estimate and effective leakage channel estimate

$$= \frac{E\left\{Tr[\boldsymbol{W}_i^* \boldsymbol{H}_i^* \boldsymbol{H}_i \boldsymbol{W}_i] \mid \hat{\boldsymbol{H}}_i\right\}}{S_i \sigma_n^2 + E\left\{Tr[\boldsymbol{W}_i^* \bar{\boldsymbol{H}}_i^* \bar{\boldsymbol{H}}_i \boldsymbol{W}_i] \mid \hat{\bar{\boldsymbol{H}}}_i\right\}}$$

$$= \frac{Tr\left[E\left\{\boldsymbol{W}_i^* \boldsymbol{H}_i^* \boldsymbol{H}_i \boldsymbol{W}_i \mid \hat{\boldsymbol{H}}_i\right\}\right]}{S_i \sigma_n^2 + Tr\left[E\left\{\boldsymbol{W}_i^* \bar{\boldsymbol{H}}_i^* \bar{\boldsymbol{H}}_i \boldsymbol{W}_i \mid \hat{\bar{\boldsymbol{H}}}_i\right\}\right]} \tag{102}$$

We must now expand this expression and maximize it as we have in previous sections. Note that we have already simplified the expression in the numerator in our previous work, so we focus our attention on the leakage term in the denominator. Since $\boldsymbol{W}_i$ is not a random variable, but a chosen quantity it can be removed from the expectation.

$$E\left\{\boldsymbol{W}_i^* \bar{\boldsymbol{H}}_i^* \bar{\boldsymbol{H}}_i \boldsymbol{W}_i \mid \hat{\bar{\boldsymbol{H}}}_i\right\} = \boldsymbol{W}_i^* E\left\{\bar{\boldsymbol{H}}_i^* \bar{\boldsymbol{H}}_i \mid \hat{\bar{\boldsymbol{H}}}_i\right\} \boldsymbol{W}_i \tag{103}$$

So we are left to determine the expression for $E\left\{\bar{\boldsymbol{H}}_i^* \bar{\boldsymbol{H}}_i \mid \hat{\bar{\boldsymbol{H}}}_i\right\}$. To consider the imperfect CSIT we explicitly write out the operation used to update the entire effective channel using the normalized receiver processing matrices that are calculated at the transmitter as follows

$$\breve{\boldsymbol{H}} = \begin{bmatrix} \breve{\boldsymbol{T}}_1 & \boldsymbol{0} & \cdots & \boldsymbol{0} \\ \boldsymbol{0} & \boldsymbol{0} & \cdots & \boldsymbol{0} \\ \boldsymbol{0} & \breve{\boldsymbol{T}}_2 & \cdots & \boldsymbol{0} \\ \boldsymbol{0} & \boldsymbol{0} & \cdots & \boldsymbol{0} \\ \vdots & \vdots & \ddots & \vdots \\ \boldsymbol{0} & \boldsymbol{0} & \cdots & \breve{\boldsymbol{T}}_K \\ \boldsymbol{0} & \boldsymbol{0} & \cdots & \boldsymbol{0} \end{bmatrix} \begin{bmatrix} \boldsymbol{H}_1 \\ \boldsymbol{H}_2 \\ \vdots \\ \boldsymbol{H}_K \end{bmatrix} \tag{104}$$

As mentioned earlier, the rows containing all zeros are needed to ensure the dimension of $\breve{\boldsymbol{H}}$ is equal to the dimension of $\boldsymbol{H}$ since this scheme is only applicable for non-full-rank transmissions. The effective leakage channel for the i^{th} user is then of course

$$\bar{\boldsymbol{H}}_i = \left[\breve{\boldsymbol{T}}_1 \boldsymbol{H}_1, \boldsymbol{0}, \ldots, \breve{\boldsymbol{T}}_{i-1} \boldsymbol{H}_{i-1}, \boldsymbol{0}, \breve{\boldsymbol{T}}_{i+1} \boldsymbol{H}_{i+1}, \boldsymbol{0}, \ldots, \breve{\boldsymbol{T}}_K \boldsymbol{H}_K, \boldsymbol{0}\right]^T \tag{105}$$

Substituting this into the expectation we intend to evaluate, $E\left\{\overline{\boldsymbol{H}}_i^*\overline{\boldsymbol{H}}_i \mid \widehat{\overline{\boldsymbol{H}}}_i\right\}$, we may rewrite it using a summation as follows

$$E\left\{\overline{\boldsymbol{H}}_i^*\overline{\boldsymbol{H}}_i \mid \widehat{\overline{\boldsymbol{H}}}_i\right\} = E\left\{\left(\sum_{k=1,k\neq i}^{K} \boldsymbol{H}_k^*\breve{\boldsymbol{T}}_k^*\breve{\boldsymbol{T}}_k\boldsymbol{H}_k\right) \mid \widehat{\boldsymbol{H}}_k, \breve{\boldsymbol{T}}_k\right\} \tag{106}$$

With imperfect CSIT we substitute the distribution for $\boldsymbol{H}_k$ given $\widehat{\boldsymbol{H}}_k$ as in previous derivations

$$= E\left\{\left(\sum_{k=1,k\neq i}^{K} \left(\rho_h\widehat{\boldsymbol{H}}_k^* + \boldsymbol{\Omega}_k{}^*\right)\breve{\boldsymbol{T}}_k^*\breve{\boldsymbol{T}}_k\left(\rho_h\widehat{\boldsymbol{H}}_k + \boldsymbol{\Omega}_k\right)\right) \mid \widehat{\boldsymbol{H}}_k, \breve{\boldsymbol{T}}_k\right\} \tag{107}$$

Again noting independence between $\widehat{\boldsymbol{H}}_k$ and $\boldsymbol{\Omega}_k$ this can be expanded and simplified to

$$= E\left\{\left(\sum_{k=1,k\neq i}^{K} \rho_h^2\widehat{\boldsymbol{H}}_k^*\breve{\boldsymbol{T}}_k^*\breve{\boldsymbol{T}}_k\widehat{\boldsymbol{H}}_k + \boldsymbol{\Omega}_{\mathrm{k}}^*\breve{\boldsymbol{T}}_k^*\breve{\boldsymbol{T}}_k\boldsymbol{\Omega}_k\right) \mid \widehat{\boldsymbol{H}}_k, \breve{\boldsymbol{T}}_k\right\} \tag{108}$$

Noting that $Tr\left[\breve{\boldsymbol{T}}_k^*\breve{\boldsymbol{T}}_k\right] = S_k$ and that $\widehat{\boldsymbol{H}}_k$ and $\breve{\boldsymbol{T}}_k$ are given, this can be equivalently expressed

$$= \sum_{k=1,k\neq i}^{K} \frac{\widehat{\boldsymbol{H}}_k^*\breve{\boldsymbol{T}}_k^*\breve{\boldsymbol{T}}_k\widehat{\boldsymbol{H}}_k}{(1+\sigma_c^2)^2} + S_k\frac{\sigma_c^2}{1+\sigma_c^2}\boldsymbol{I} \tag{109}$$

Recognizing that the term on the left is just a scaled version of the original expression using the estimated effective leakage channels we can rewrite this as

$$= \left(\frac{\widehat{\overline{\boldsymbol{H}}}_i^*\widehat{\overline{\boldsymbol{H}}}_i}{(1+\sigma_c^2)^2} + \sum_{k\neq i} S_k\frac{\sigma_c^2}{1+\sigma_c^2}\boldsymbol{I}\right) \tag{110}$$

For a single stream per user this is of course

$$= \left(\frac{\widehat{\overline{\boldsymbol{H}}}_i^*\widehat{\overline{\boldsymbol{H}}}_i}{(1+\sigma_c^2)^2} + (K-1)\frac{\sigma_c^2}{1+\sigma_c^2}\boldsymbol{I}\right) \tag{111}$$

Substituting this back into equation 103 we have

$$E\left\{\boldsymbol{W}_i^*\bar{\boldsymbol{H}}_i^*\bar{\boldsymbol{H}}_i\boldsymbol{W}_i \mid \hat{\bar{\boldsymbol{H}}}_i\right\} = \boldsymbol{W}_i^*\left(\frac{\hat{\bar{\boldsymbol{H}}}_i^*\hat{\bar{\boldsymbol{H}}}_i}{(1+\sigma_c^2)^2} + \sum_{k\neq i} S_k \frac{\sigma_c^2}{1+\sigma_c^2}\boldsymbol{I}\right)\boldsymbol{W}_i \tag{112}$$

Now that we have determined the expression involving the effective leakage channel used by the mSLNR metric, we remind the reader that the expression in the numerator of the mSLNR expression in equation 102 simplifies to

$$= \frac{\hat{\boldsymbol{H}}_i^*\hat{\boldsymbol{H}}_i}{(1+\sigma_c^2)^2} + M_i \frac{\sigma_c^2}{1+\sigma_c^2}\boldsymbol{I} \tag{113}$$

With these two results we arrive at the expression for the modified SLNR metric as shown below.

$$= \frac{Tr\left[\boldsymbol{W}_i^*\left(\frac{\hat{\boldsymbol{H}}_i^*\hat{\boldsymbol{H}}_i}{(1+\sigma_c^2)^2} + M_i \frac{\sigma_c^2}{1+\sigma_c^2}\boldsymbol{I}\right)\boldsymbol{W}_i\right]}{Tr\left[\boldsymbol{W}_i^*\left(\frac{\hat{\bar{\boldsymbol{H}}}_i^*\hat{\bar{\boldsymbol{H}}}_i}{(1+\sigma_c^2)^2} + \left(\sum_{k\neq i} S_k \frac{\sigma_c^2}{1+\sigma_c^2} + \frac{1}{P_s}\sigma_n^2\right)\boldsymbol{I}\right)\boldsymbol{W}_i\right]} \tag{114}$$

Using the same eigenvalue decomposition approach as in previous derivations the precoding weights which will maximize the modified SLNR considering imperfect CSIT are given by

$\boldsymbol{W}_i \propto S_i \max eigenvectors\ of$

$$\left(\left(\frac{\hat{\bar{\boldsymbol{H}}}_i^*\hat{\bar{\boldsymbol{H}}}_i}{(1+\sigma_c^2)^2} + \left(\sum_{k\neq i} S_k \frac{\sigma_c^2}{1+\sigma_c^2} + \frac{1}{P_s}\sigma_n^2\right)\boldsymbol{I}\right)^{-1}\left(\frac{\hat{\boldsymbol{H}}_i^*\hat{\boldsymbol{H}}_i}{(1+\sigma_c^2)^2} + M_i \frac{\sigma_c^2}{1+\sigma_c^2}\boldsymbol{I}\right)\right) \tag{115}$$

3.2.3 Simulation Results

In section 2.3 we saw that there was very little difference in the achieved sum-rate using the iSLNR algorithm with ZF or IRC receivers with perfect CSIT. On the other hand, Figure 3.4 highlights the significant gap in performance between the ZF and IRC receivers

when CSIT is imperfect. This particular simulation is of a 4x(2x4) system operating at 30 dB SNR and 10 dB CSIT. The converged solution using IRC receivers improves the system sum-rate by approximately 27% compared to the converged solution using ZF receivers. So while there is little to no benefit to using the IRC receiver in an idealized setting, the quality of the CSIT must be considered. Further, we observe that the iSLNR algorithm which considers the CSIT error converges to only a slightly better solution than the one that doesn't, but it converges much more quickly, within just a few iterations. So we observe that there is a gain of about 1 bits/s/hz at a few iterations by considering the imperfect CSIT. This is a good result since a practical system might realistically be able to perform several iterations, but performing on the order of 100's of iterations is more than likely infeasible given the resource and time constraints of a practical system.

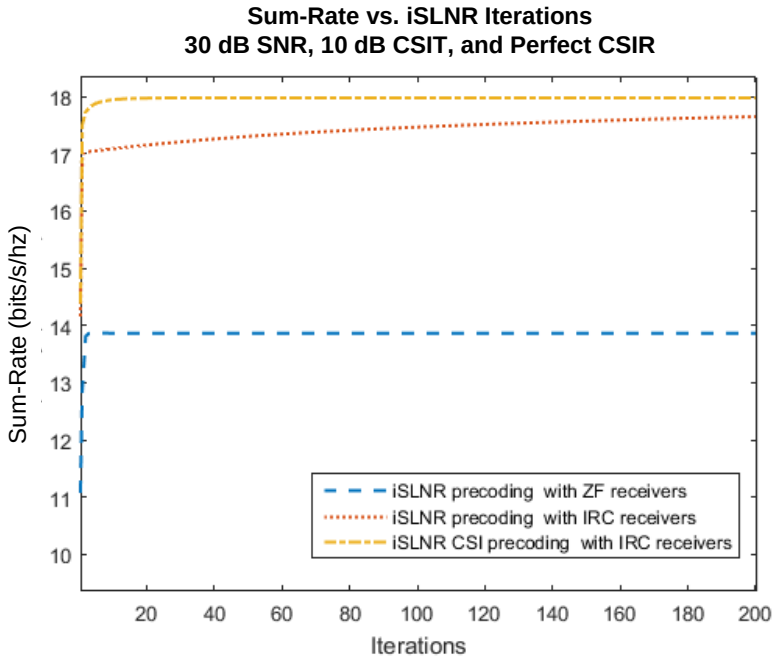

Figure 3.4 Sum-rate achieved using iSLNR in a 4x(2x4) system with 30 dB SNR and 10 dB CSIT

Figure 3.5 shows the uncoded error rate of a 8x(4x4) system using iSLNR for 64 QAM transmission operating at 10 dB CSIT. In this case the imperfect CSIT causes additional MUI, but the receivers have sufficient degrees of freedom to suppress it. This results in a consistently improving BER with increased SNR. Considering the CSIT error in the iSLNR algorithm provides considerable gain, particularly in the high SNR regime. At ten

iterations the iSLNR algorithm considering CSIT error provides about 11.5 dB of gain at an error rate of 1e-3 compared to the standard iSLNR algorithm.

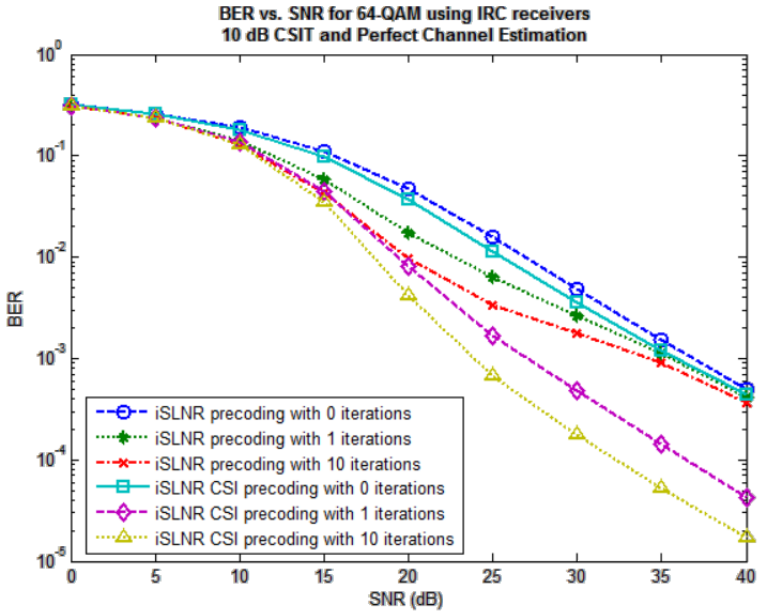

Figure 3.5: BER of a 8x(4x4) system using iSLNR for 64 QAM transmission operating with 10 dB CSIT

Figure 3.6 shows a similar simulation with a 8x(2x4) system. In this case the receivers do not have sufficient degrees of freedom to suppress the residual MUI that results from imperfect CSIT. The result of this deficiency is an error floor at high SNR. The iSLNR algorithm considering the CSIT error will significantly reduce the error floor however, in this case by between one to two orders of magnitude at the tenth iteration. The iSLNR algorithm not considering the CSIT error exhibits some interesting behavior, where the performance at mid-range SNR is actually better than the final error floor at high SNR. The reason for this is rather intuitive though. Consider the method by which the CSIT error is accounted for in the iSLNR algorithm. We have increased diagonal-loading in the interference-plus-noise covariance matrix calculation as well as in the precoding matrix calculation. At low SNR, the diagonal loading due to CSIT error is insignificant compared to that due to the noise power, so the schemes produce nearly identical results. In the mid-range SNR the two terms become the same order of magnitude and we see the algorithm which does not consider the CSIT error begin to diverge from the algorithm which does. As SNR continues to increase the diagonal loading is dominated by the term due to CSIT error and the algorithm which considers this levels off at an error floor. The

algorithm which does not consider the CSIT however, continues to reduce its diagonal loading as the noise power approaches zero. This solution is overly optimistic and causes performance to actually degrade despite a higher SNR.

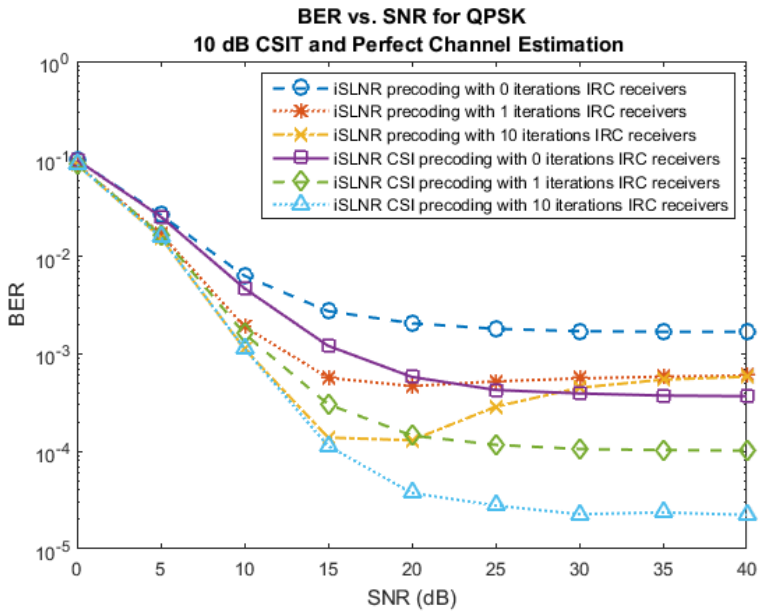

Figure 3.6: BER of a 8x(2x4) system using iSLNR for QPSK transmission operating with 10 dB CSIT

We also note that the sum-rate gains of accounting for the CSIT error are magnified for larger systems with more users. In Figure 3.7 we show sum-rate of a 16x(2x8) system operating at 30 dB SNR and with 10 dB CSIT. In this case the difference between the algorithm which considers the CSIT error and the algorithm which does not is more significant compared to the results shown earlier. At just a few iterations there is a gain of approximately 15% or 5 bits/s/Hz in achieved sum-rate.

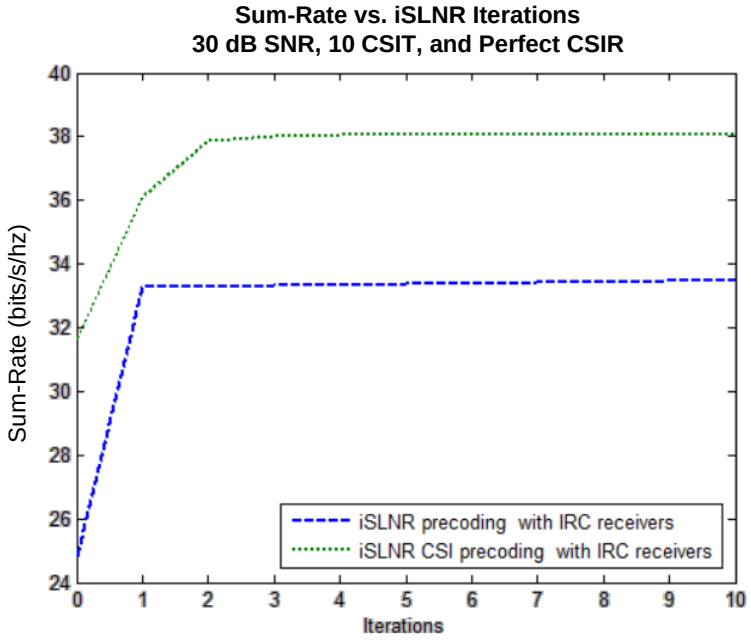

Figure 3.7: Sum-rate of a 16x(2x8) system using iSLNR operating at 30 dB SNR and 10 dB CSIT

3.2.4 MMSE Modification of CSIT for iSLNR Precoding

In the interest of being complete we might also consider applying the MMSE modification of CSIT as discussed in section 3.1.2. The initial precoding would then be given as in equation 72. The subsequent iterations of precoding would be given by substituting the modified channel estimates and error variance into equation 115 which yields

$$\boldsymbol{W}_i \propto S_i \max eigenvectors\ of$$

$$\left(\left(\frac{\overline{\boldsymbol{H}}_i'^{*}\overline{\boldsymbol{H}}_i'}{(1+\sigma_c^{2\prime})^2}+\left(\sum_{k\neq i}S_k\frac{\sigma_c^{2\prime}}{1+\sigma_c^{2\prime}}+\frac{1}{P_s}\sigma_n^2\right)\boldsymbol{I}\right)^{-1}\left(\frac{\boldsymbol{H}_i'^{*}\boldsymbol{H}_i'}{(1+\sigma_c^{2\prime})^2}+M_i\frac{\sigma_c^{2\prime}}{1+\sigma_c^{2\prime}}\boldsymbol{I}\right)\right) \tag{116}$$

Furthermore we substitute the modified channel estimates and error variance into the receiver processing calculation as

$$\widehat{\boldsymbol{T}}_{IRC}=\frac{\boldsymbol{W}^{*}\boldsymbol{H}'^{*}\widehat{\boldsymbol{R}}_n^{-1}}{1+\sigma_c^{2\prime}}\cdot\left(\frac{\boldsymbol{W}^{*}\boldsymbol{H}'^{*}\widehat{\boldsymbol{R}}_n^{-1}\boldsymbol{H}'\boldsymbol{W}}{(1+\sigma_c^{2\prime})^{\mathbf{2}}}+S_iP_sTr\left[\widehat{\boldsymbol{R}}_n^{-1}\right]\frac{\sigma_c^{2\prime}}{1+\sigma_c^{2\prime}}\boldsymbol{I}\right)^{-1} \tag{117}$$

Where $\widehat{\boldsymbol{R}}_n^{-1}$ is also calculated using the modified quantities as below

$$\widehat{\boldsymbol{R}}_n = \frac{\boldsymbol{H}'\boldsymbol{W}_n\boldsymbol{W}_n^*\boldsymbol{H}'^*}{(1+\sigma_c^{2\prime})^2} + \left(\left(P_s\sum_{k\neq i}S_k\right)\frac{\sigma_c^{2\prime}}{1+\sigma_c^{2\prime}} + \sigma_n^2\right)\boldsymbol{I} \tag{118}$$

In Figure 3.8 we show the effect of using the MMSE modified CSIT in the iSLNR algorithm as described in equations 116-118. We note that the zeroth iteration is identical to the result shown for the non-iterative SLNR precoding in Figure 3.3. At this point the MMSE modification provides a marginal, though non-negligible gain of 0.4 dB at an error rate of 1e-3. We note that with increased iterations this marginal gain is diminished to the point where it is considered negligible. We therefore conclude that applying a practical MMSE modification to the CSIT is not useful for the iSLNR algorithm.

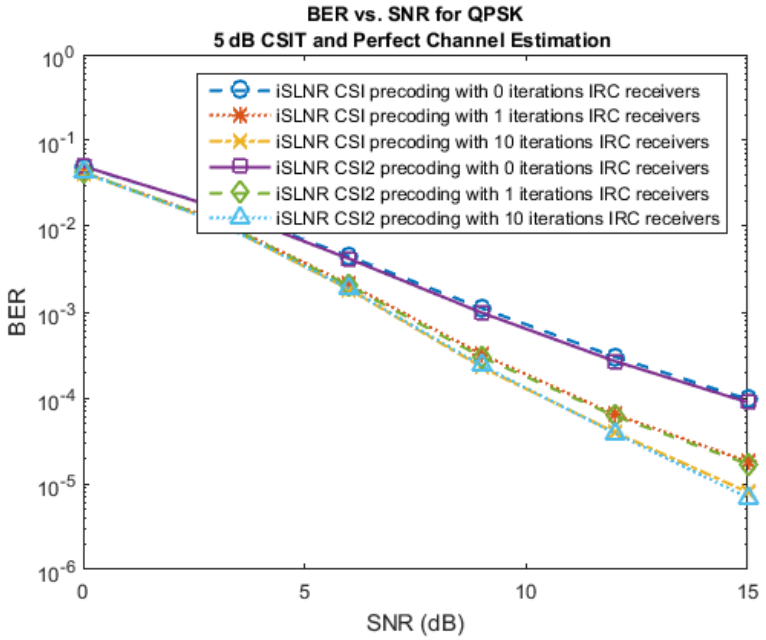

Figure 3.8: BER using iSLNR precoding with and without the MMSE modified CSIT

3.3 iSLNR Precoding with Imperfect CSIR

Up until this point we have assumed perfect CSIR. Imperfect CSIR presents a potential problem to the iSLNR algorithm, which relies on calculating the receiver processing at

each user to make better use of the receiver subspace. We therefore aim to determine the effect of imperfect CSIR.

Similar to the imperfect CSIT model, we model imperfect CSIR with

$$\acute{\boldsymbol{G}} \triangleq \boldsymbol{G} + \boldsymbol{\Theta} \tag{119}$$

Where $\acute{\boldsymbol{G}}$ is the channel estimate at the receiver, $\boldsymbol{G}$ is the true channel, and $\boldsymbol{\Theta}$ is a matrix of i.i.d. complex Gaussian random variables with zero mean and variance σ_e^2.

Figures 3.10 and 3.11 we see the sum-rate achieved by a 9x(3x3) system using the iSLNR algorithm and operating at 20 and 10 dB SNR respectively. Each figure shows a family of curves which varies the quality of CSIR. From these results we first observe that CSIR error at the receiver can significantly degrade the system sum-rate. Further, we observe that the gain achieved by the iSLNR algorithm decreases as the CSIR degrades. In fact, there comes a point where the CSIR quality is so prohibitive that the iSLNR algorithm actually produces worse performance than the cSLNR solution (shown as the zeroth iteration of the iSLNR algorithm). This is an intuitive result since the iSLNR algorithm depends on knowledge of the receiver processing whereas the cSLNR scheme does not. Looking more closely we note that the point at which the iSLNR algorithm stops being beneficial consistently occurs where the CSIR quality is less than the SNR. We therefore conclude that as a rule of thumb the iSLNR algorithm should not be applied if the CSIR quality is worse than the SNR in a system with sufficient degrees of freedom at the transmitter. To achieve significant gains it should really be at least several dB greater.

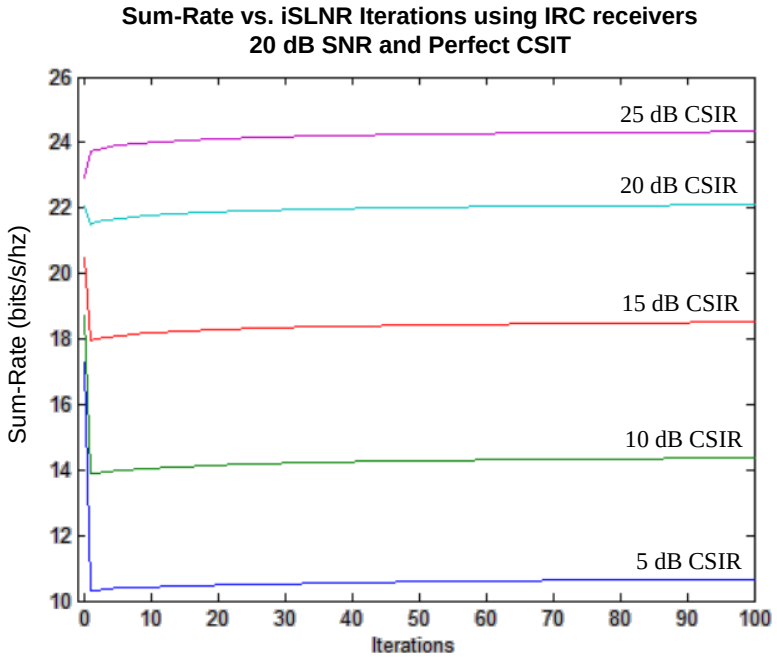

Figure 3.9: Sum-rate achieved in a 9x(3x3) system operating at 20 dB SNR and with varying quality of CSIR

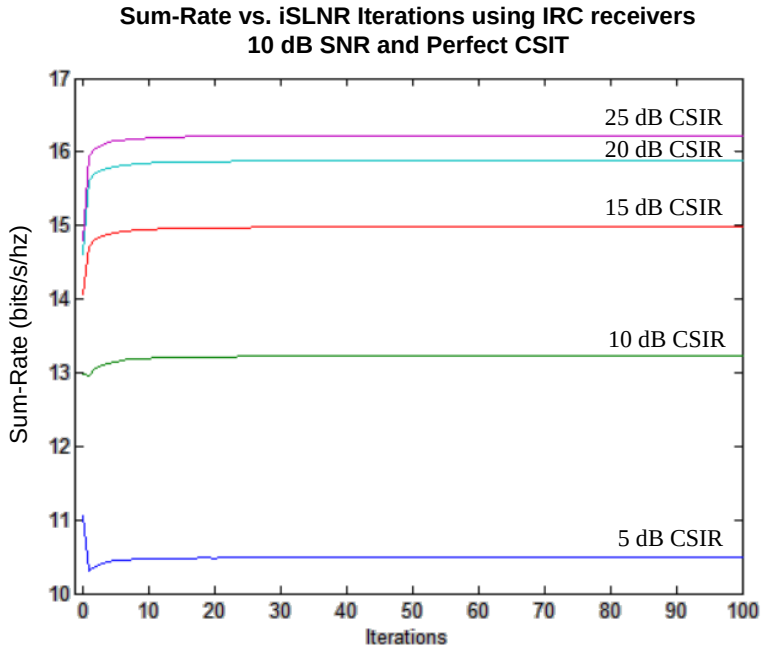

Figure 3.10: Sum-rate achieved in a 9x(3x3) system operating at 10 dB SNR with varying quality of CSIR

With this result in mind, recall that the gain achieved by the iSLNR algorithm is greater when there are insufficient degrees of freedom at the transmitter. This is because the iSLNR algorithm effectively reduces the required degrees of freedom for a system using non-full rank transmission. So while the previous results showed that the iSLNR

algorithm did not produce significant system gain when the CSIR quality was equal to or less than the SNR, we must also consider the case of a system with insufficient degrees of freedom at the transmitter. In this case we expect the gain of the iSLNR algorithm to be greater which may lead us to a different conclusion than in the previous cases studied.

Figures 3.12 and 3.13 show the sum-rate achieved by a 6x(3x3) system using the iSLNR algorithm and operating at 20 dB and 10 dB SNR respectively. In this case we observe that the iSLNR algorithm will continue to provide system sum-rate gain even when the CSIR quality is slightly worse than the SNR. With sufficiently low CSIR quality however, the iSLNR algorithm will degrade sum-rate compared to the cSLNR scheme as we observed in the earlier cases.

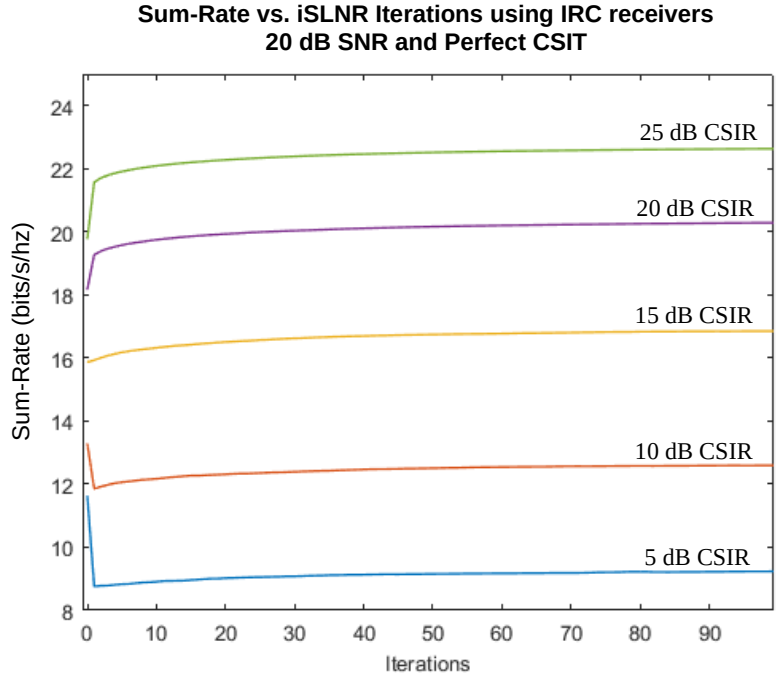

Figure 3.11: Sum-rate achieved in a 6x(3x3) system operating at 20 dB SNR and with varying quality of CSIR

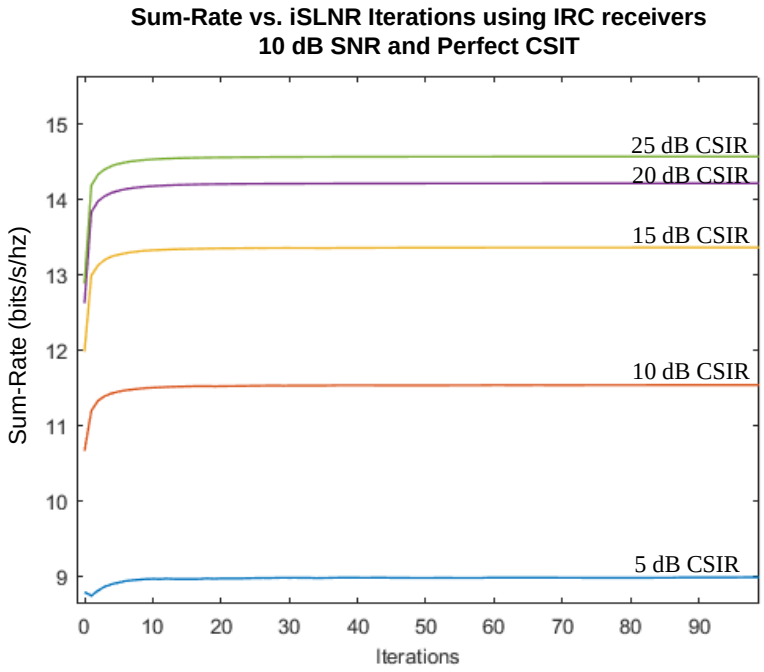

Figure 3.12: Sum-rate achieved in a 6x(3x3) system operating at 10 dB SNR and with varying quality of CSIR

Based on these results we have drawn several conclusions. First, the iSLNR algorithm requires a certain quality of CSIR to be effective. This requirement can change based on the system configuration. Specifically, systems with sufficient degrees of freedom, that is, $N_t \geq \sum M_i$, generally require a quality of CSIR that is greater than the SNR to achieve significant gains using the iSLNR algorithm. For systems which do not have enough degrees of freedom at the transmitter, the algorithm can still be useful even with lower CSIR quality.

3.4 Chapter Summary

In this chapter we have looked at the effects of CSIT and CSIR when employing either the cSLNR precoding or the iSLNR precoding schemes. We also proposed several solutions to mitigate the impact of imperfect CSIT and demonstrated the gain they achieve.

With regard to the cSLNR scheme we derived a new solution to consider imperfect CSIT which was shown to be superior to the solution previously suggested in [7]. We then investigated the effect of a linear modification to the CSIT to meet the MMSE criterion which was motivated by the work in [12]. To this end, we derived the MMSE

modification which avoids relying on the true channel value; an impractical requirement. It was shown that applying this MMSE modification can provide a marginal though non-negligible gain for the cSLNR scheme.

For the iSLNR algorithm we derived a method to calculate the receiver processing matrices and the precoding matrices in a manner that accounts for the CSIT error. Using these newly derived expressions showed improved performance in terms of system sum-rate and error rate compared to the original iSLNR algorithm. We then applied the same MMSE modification as used for the cSLNR scheme. Ultimately the gain achieved by applying this modification was diminished after several iterations of the algorithm to the point where it was considered negligible and removed from consideration.

We then went on to investigate the effects of CSIR error. From simulation we showed first that with high CSIR error the iSLNR algorithm can actually reduce system performance compared to the cSLNR solution. We demonstrated that when a system has sufficient degrees of freedom to fully suppress the multiuser-interference, the iSLNR algorithm will only provide system gain when the quality of the CSIR is greater than the SNR. On the other hand in a system with insufficient degrees of freedom, the iSLNR algorithm may provide non-trivial system gains even when the quality of the CSIR is less than the SNR.

We also want to mention a fundamental tradeoff that exists between the iSLNR algorithm and other joint transmit/receive processing design algorithms mentioned in the initial introduction to the iSLNR algorithm in Chapter 2. This tradeoff is highlighted by the work regarding CSIR error. A nice benefit of the iSLNR algorithm is that it considers the receiver processing with no additional overhead; neither sending calculated processing matrices to the users nor receiving user processing matrices to consider in the precoding formulation. The drawback is that this makes the system performance more susceptible to degradation due to CSIR error. If the receiver processing matrices were sent explicitly then the precoding could be designed with full confidence in the receiver processing. Of course, using explicitly signaled receiver processing matrices would also suffer from

being limited to a quantized codebook besides the additional overhead signaling. All of these tradeoffs must be considered to achieve the best system design.

Chapter 4
Additional Considerations

In this chapter we investigate several other practical considerations for the iSLNR algorithm. We begin by discussing the impact of transmit antenna correlation on the achievable sum-rate. We then move on to consider the impact of time-varying channels and how the iSLNR algorithm considering imperfect CSIT might be applied in this setting. We then propose a method to improve the convergence of the iSLNR algorithm with IRC receivers. Finally, we investigate tradeoffs in selecting the number of co-scheduled users for the iSLNR algorithm.

4.1 The Effect of Transmit Antenna Correlation

In the previous analysis we have assumed the channel to be spatially white. This is a reasonable assumption when the angles-of-arrival/departure for the multi-path scatterers are uniformly distributed around both the transmit and receive antenna arrays, but if the angles-of-arrival/departure follow a more narrow distribution then the channel will exhibit spatial correlation. In a practical system it is common for the angles-of-arrival/departure to follow a more narrow distribution at the base station than at the mobile since the base station antennas will typically be placed high, away from significant nearby scatterers. The angles-of-arrival/departure at the mobile will be closer to a uniform distribution due to its low physical placement among many potential scatterers. With this in mind, the effects of transmit antenna correlation at the base station is of interest since this work focuses on the downlink.

A system with N transmit antennas and M receive antennas will have an NMxNM channel correlation matrix denoted $\boldsymbol{R}$. In general each element of this matrix, $r_{i,j}$, is unique with the exception that $r_{i,j} = r_{j,i}^{*}$ since correlation matrices must be Hermitian, and the elements along the diagonal must be equal to one since each channel is perfectly correlated with itself. For the purpose of simplified analysis, the Kronecker assumption is

often made. The Kronecker assumption considers the channel correlations to be separable into receive and transmit side correlations, *i.e.*, the correlation between channel h_{ij} and h_{km} is the product of the correlation between the i and k receive antennas and the correlation between the j and m transmit antennas. Using this approximation the antenna correlation matrix is given by

$$\boldsymbol{R} = \boldsymbol{R}_{tx} \otimes \boldsymbol{R}_{rx} \tag{120}$$

Where $\otimes$ denotes the Kronecker product. Using this assumption the MIMO channel is modeled as

$$\boldsymbol{H} = \boldsymbol{R}_{rx}^{1/2} \boldsymbol{A} \boldsymbol{R}_{tx}^{1/2} \tag{121}$$

Where $\boldsymbol{A}$ is the independent MIMO channel as used in other sections. In this analysis we will conintue to assume independence at the receive antennas, so the MIMO channel is simply

$$\boldsymbol{H} = \boldsymbol{A} \boldsymbol{R}_{tx}^{1/2} \tag{122}$$

Further, we assume a uniformly spaced linear array at the transmitter. As such, the correlation between any two adjacent transmit antennas is given by ρ_{tx}, and the transmit correlation matrix is given by

$$\boldsymbol{R}_{tx} = \begin{bmatrix} 1 & \rho_{tx} & \rho_{tx}^2 & \cdots & \rho_{tx}^{N-1} \\ \rho_{tx} & 1 & \rho_{tx} & \cdots & \rho_{tx}^{N-2} \\ \rho_{tx}^2 & \rho_{tx} & 1 & \cdots & \rho_{tx}^{N-3} \\ \vdots & \vdots & \vdots & \ddots & \vdots \\ \rho_{tx}^{N-1} & \rho_{tx}^{N-2} & \rho_{tx}^{N-3} & \cdots & 1 \end{bmatrix} \tag{123}$$

With this model, we examine the performance of the iSLNR algorithm via simulation. Figure 4.1 shows the sum-rate achieved using the iSLNR algorithm in an 8x(2x4) system operating at 20 dB SNR and with varying ρ_{tx}. We observe that sum-rate is significantly degraded for higher correlation, though the iSLNR consistently shows improvement compared to the cSLNR solution in all but the completely correlated case ($\rho_{tx} = 1$). We

further note that sum-rate appears to be monotonically increasing per iteration of the iSLNR algorithm for all values of ρ_{tx}.

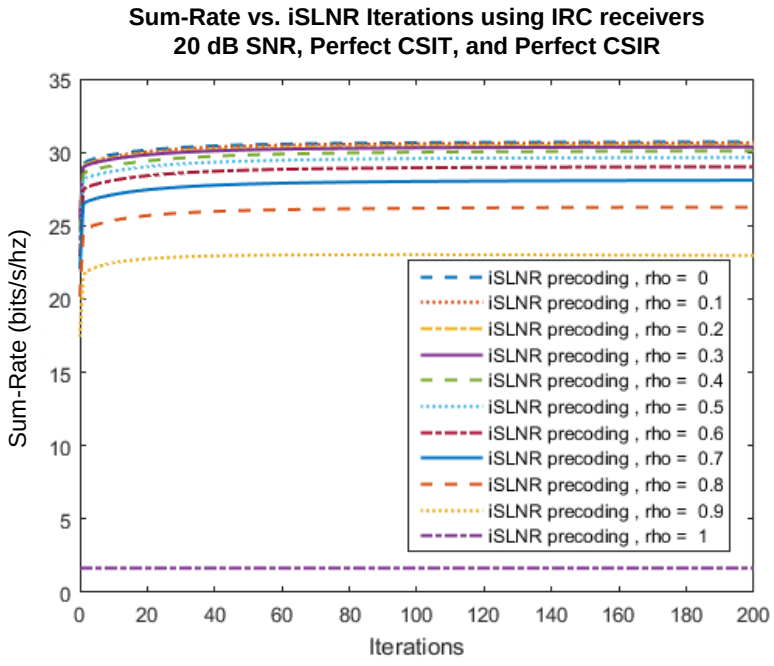

Figure 4.1: Sum-rate of 8x(2x4) system with varying transmit correlation

Figure 4.2 shows a similar simulation for a 4x(2x4) system. Again we observe degraded sum-rate for increasing transmit correlation. Interestingly, we also observe that at high correlation the sum-rate appears to no longer be monotonically increasing. After about 20 iterations, the sum-rate actually begins to decrease. This is the first simulation where we have observed this behavior. Figure 4.3 shows the same results but with ZF receivers. In this case we don't observe the issue of non-monotonically increasing sum-rate. To try to pinpoint the cause of this issue, we performed a number of additional simulations with different system configurations. The results are included in the appendix to avoid repetitive figures in the main text. In summary, we observed that this issue occurs for any system which employs IRC receivers and operates with high transmit antenna correlation. We also observed that the effect is much more significant when $N < \sum M_i$, which is why it was not initially observed in Figure 4.1.

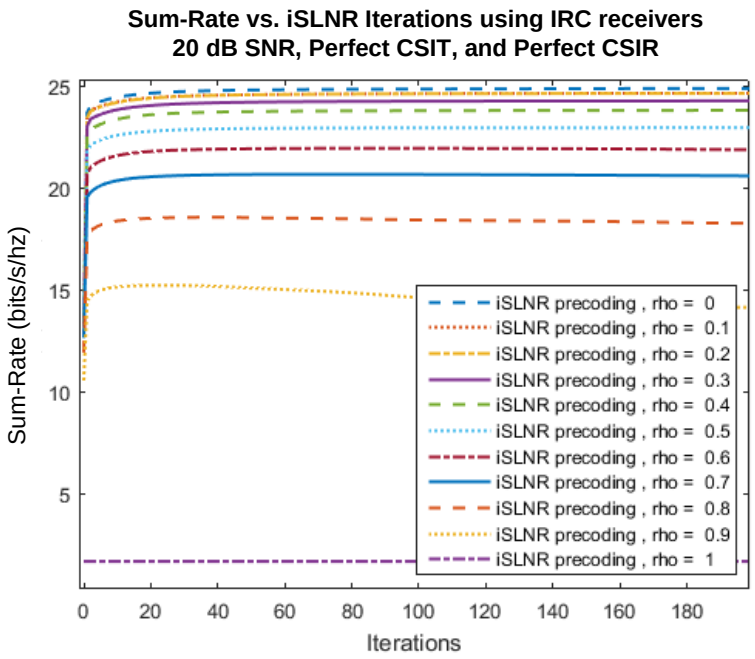

Figure 4.2: Sum-rate of 4x(2x4) system with varying transmit correlation

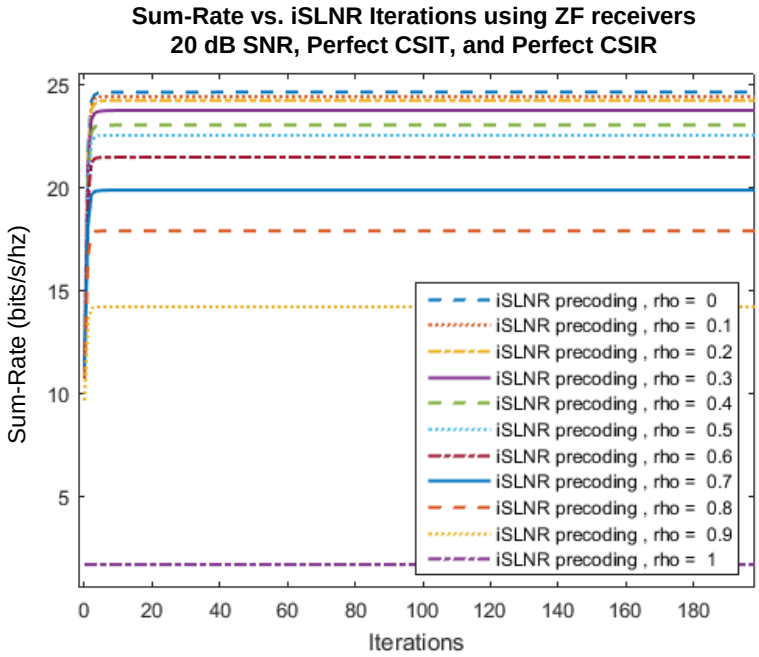

Figure 4.3: Sum-rate of 4x(2x4) system using ZF receivers with varying transmit correlation

Unfortunately, we cannot offer a mathematically rigorous proof as to why this issue occurs. We speculate that it results from the approximation that is made by the mSLNR metric. Recall that the mSLNR metric considers the signal power at the receive antennas

but the noise and leakage are considered after the receiver processing. There is no guarantee that maximizing this metric will in fact maximize the SINR at the output of the receiver. In most cases simulations have shown that it will, but it appears that the approximation may break down with high transmit antenna correlation and IRC receivers. From what we've seen, even in this case the algorithm will provide a substantial initial gain.

In this section we investigated the impact of transmit antenna correlation on the achieved sum-rate using the iSLNR algorithm. We first observed that increased transmit antenna correlation will degrade the system sum-rate. We further observed that the iSLNR algorithm will consistently provide gain in system sum-rate with two caveats: (1) no observable gain is achieved when the transmit antennas are perfectly correlated and (2) the gain provided may not be monotonically increasing per iteration with high transmit antenna correlation. From our simulations the latter caveat appears to be limited to the case where IRC receivers are used and is most prominent when $N < \sum M_i$.

4.2 Time-Varying Channels

So far we have assumed a static channel for the duration of each transmission. While this is useful to compare the effect of imperfect CSIT and CSIR, and indeed may be a reasonable approximation in low-mobility scenarios, real world systems will often exhibit time-variance in the channel due to user mobility and/or changes in the environment. It is therefore worthwhile to consider how this will affect the system. In a time-varying channel, the quality of CSIT will degrade over time, though the CSIR will track the changes. Time-varying channels are therefore a natural extension of the previously described iSLNR algorithm considering CSIT error.

In this work we use Jake's model for narrowband time-varying channels. Jake's model assumes some number (typically around 50) of multi-path scatterers with angles-of-arrival that are uniformly distributed around the antennas and which have experienced Doppler

shifts following a cosine distribution scaled by the maximum Doppler shift *i.e.*, the Doppler shift for the i^{th} multi-path component will be given by

$$f_i = f_{dmax} \cos(2\pi f) \tag{124}$$

With f_{dmax} being the maximum Doppler shift and f being uniformly distributed between 0 and 1. In this situation it can be shown that the time correlation of the channel between times t_0 and t_1 is given by

$$\rho_t = J_o\big(2\pi f_d(t_1 - t_0)\big) \tag{125}$$

Where J_o is a zero[th] order Bessel function of the first kind. Using the timing structure defined in section 2.2 and with a max Doppler of 10 Hz we can expect the channel correlation and the resulting CSIT error variance shown in Figures 4.1 and 4.2. As you can see, by the end of the frame transmission, the CSIT quality has degraded significantly.

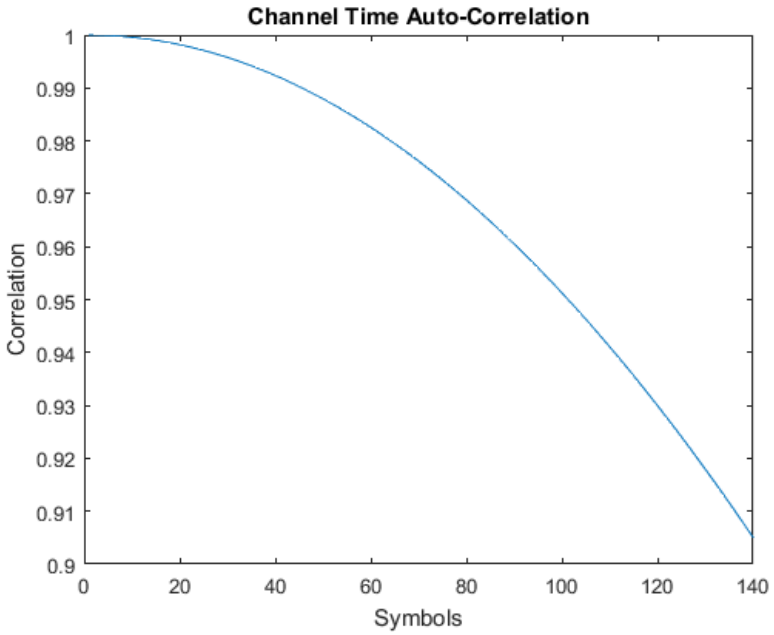

Figure 4.4: 10 Hz max Doppler channel correlation over a 140 symbol frame with a duration of 10 ms.

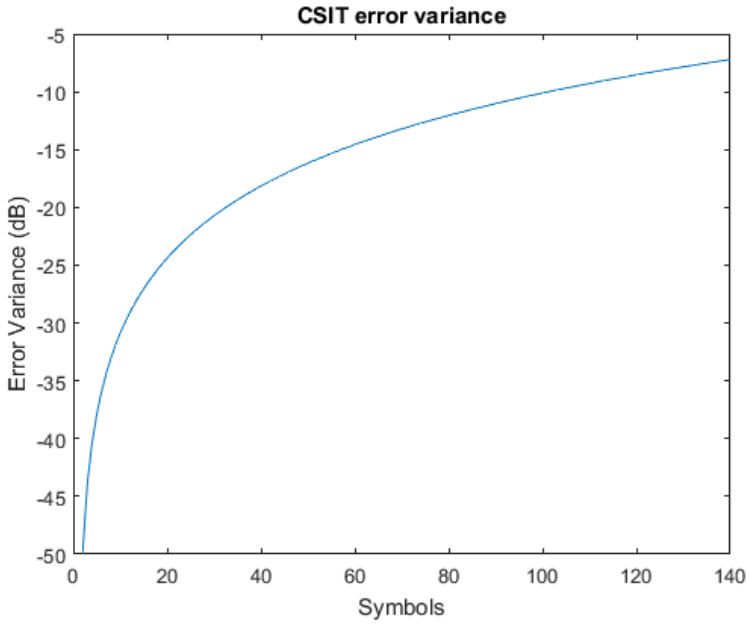

Figure 4.5: 10 Hz max Doppler CSIT error variance due to a time-varying channel.

Since the time-varying channel will degrade the CSIT quality over time, we first consider an 'optimal' approach in which the iSLNR algorithm is applied per symbol where the specific CSIT quality for each symbol is considered. In chapter three we saw that considering the CSIT quality led to improved convergence of the algorithm, so when we say this is an optimal approach, we mean that this approach will have good convergence properties while still converging to the best possible solution.

The complexity of performing the iSLNR algorithm for each symbol is almost certainly prohibitive, so we also investigate approaches wherein a single precoding matrix is calculated and applied for the duration of the transmission. In other words, we use the iSLNR solution considering CSIT error from equation 115 but choose a single value, denoted $\hat{\sigma}_c^2$, to represent the CSIT error variance despite it being a function of time across the transmission. So the precoding matrix will be calculated using equation 126.

$\boldsymbol{W}_i \propto S_i \max eigenvectors\ of$

$$\left(\left(\frac{\widehat{\widehat{\boldsymbol{H}}}_i^{*}\widehat{\widehat{\boldsymbol{H}}}_i}{(1+\hat{\sigma}_c^2)^2}+\left(\sum_{k\neq i}S_k\frac{\hat{\sigma}_c^2}{1+\hat{\sigma}_c^2}+\frac{1}{P_s}\sigma_n^2\right)\boldsymbol{I}\right)^{-1}\left(\frac{\widehat{\boldsymbol{H}}_i^{*}\widehat{\boldsymbol{H}}_i}{(1+\hat{\sigma}_c^2)^2}+M_i\frac{\hat{\sigma}_c^2}{1+\hat{\sigma}_c^2}\boldsymbol{I}\right)\right) \quad (126)$$

There are several criteria we might consider for selecting $\hat{\sigma}_c^2$. We might for example, use the CSIT quality of the first or last symbol. Based on our understanding of the problem from chapter 3 we would expect that using the CSIT of the first symbol will converge to roughly the best possible solution, but would not take advantage of the degraded CSIT quality of the later symbols which will improve the algorithms convergence. On the other hand, using the CSIT quality of the last symbol will converge quickly but will limit the solution by not taking advantage of the good CSIT in the first symbols. A tradeoff between these two approaches could be to take the mean of the CSIT quality to achieve better convergence but not quite the optimal converged solution.

Figure 4.7 shows sum-rate achieved by a 4x(2x4) system when applying the proposed solutions for the iSLNR algorithm in a time-varying channel. The simulation uses a timing structure similar to LTE; 140 symbols over a period of 10 ms. The results match our expectations well. The iSLNR algorithm with no consideration to the degrading CSIT converges rather slowly, but to nearly the best possible solution. Recall that we observed a similar result when investigating block-fading channels with imperfect CSIT. The solution which considered the CSIT quality provided significant gain in terms of its convergence, but the converged solution was only slightly better than that of the original algorithm. Returning to Figure 4.7, we see that the iSLNR algorithm considering the CSIT error per symbol converges faster compared to the original iSLNR algorithm. The iSLNR algorithm using the CSIT error of the last symbol is overly pessimistic which leads to a solution that does not take advantage of the high CSIT quality of the earlier symbols; it therefore achieves a much lower sum-rate. Finally, by taking the mean CSIT quality the solution converges quickly, but doesn't quite converge to the best possible solution. In this case the difference is rather small though.

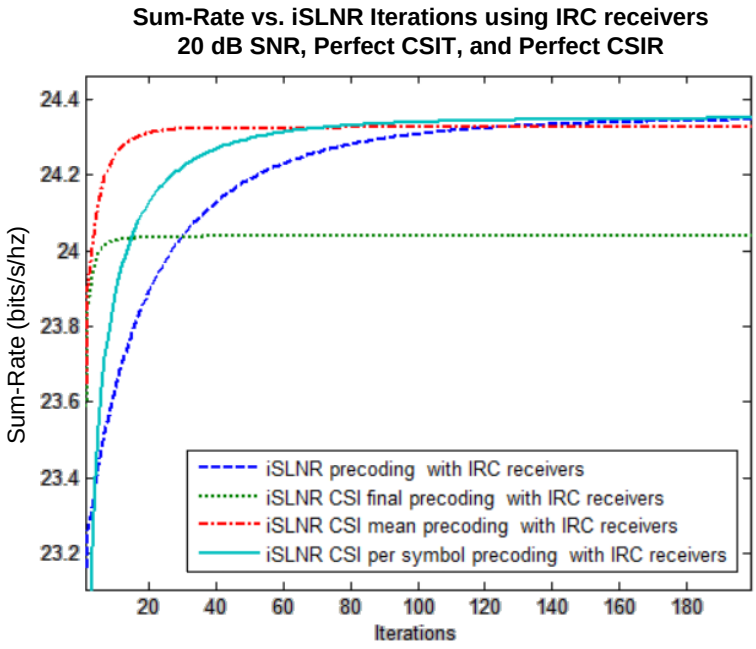

Figure 4.6: Sum-rate of a 4x(2x4) system in a time-varying channel

Figure 4.8 shows similar results for a 16x(2x8) system when applying the proposed solutions for the iSLNR algorithm in a time-varying channel. In this case the differences are more pronounced. Using the CSIT quality based on the last symbol severely limits the achieved sum-rate. Even using the mean limits the solution non-trivially. Using the per-symbol precoding provides a nice improvement in convergence while achieving a solution slightly better than the single solution with no consideration to the degrading CSIT.

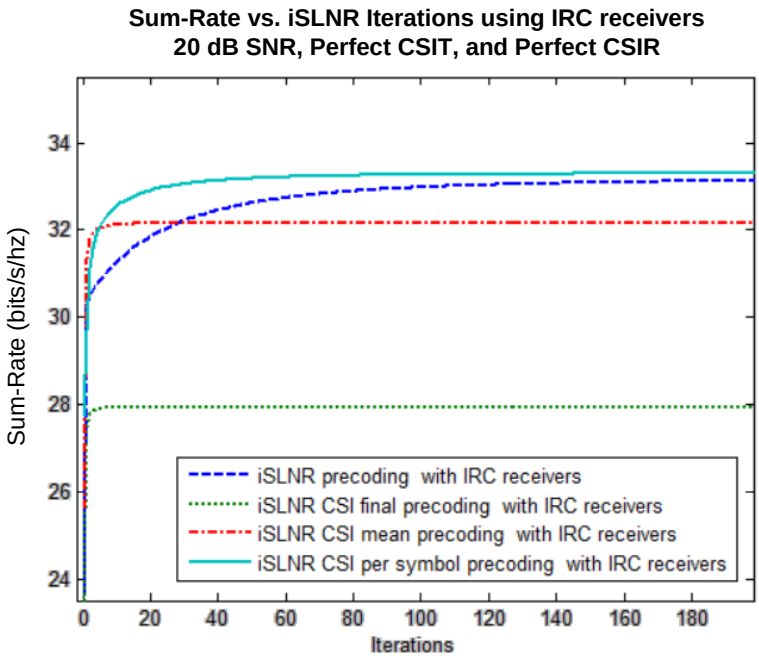

Figure 4.7: Sum-rate of a 16x(2x8) system in a time-varying channel

In this section we considered how the iSLNR algorithm might be applied in a time-varying channel. We proposed several intuitive solutions based on the degradation of CSIT over the transmission interval: to apply the iSLNR algorithm for each individual symbol with consideration to the CSIT quality at that specific symbol, or to apply a single solution based on the initial CSIT error, the final CSIT error, or the mean CSIT error. We observed that these solutions lead to a tradeoff between convergence rate and the optimality of the converged solution.

4.3 Improved Convergence of the iSLNR Algorithm for IRC Receivers

One of the main concerns expressed in [8] was the slow convergence of the iSLNR algorithm when using IRC receivers compared to MF receivers, especially since the gain provided by using IRC receivers is marginal (under the assumption of perfect CSIT). In the previous chapter we extended this work and made two important observations: (1) in a system with imperfect CSIT the IRC receiver may drastically outperform the ZF receiver and (2) convergence is improved when consideration is given to the CSIT error. This is particularly true for systems involving many users and transmit antennas. In the previous section of this chapter we investigated the use of the iSLNR algorithm in time-varying

channels, which effectively degrades the CSIT and so can be approached in a similar manner. Seeing how this work led to quicker convergence for the IRC receiver, we wanted to explore other methods that might further improve its convergence.

This exploration began by considering the reason for the IRC receiver's slow convergence. In general we know that the IRC receiver will provide suppression of interfering signals whereas the ZF receiver will not. Since we use the receiver output to update the effective leakage channels this implies that

$$E\left\{\left\|\widehat{\boldsymbol{T}}_{j,IRC}\boldsymbol{H}_i\right\|^2\right\} < E\left\{\left\|\widehat{\boldsymbol{T}}_{j,ZF}\boldsymbol{H}_i\right\|^2\right\} \quad \forall\, i \neq j \tag{127}$$

which implies,

$$E\left\{\left\|\bar{\boldsymbol{H}}_{i,IRC}\right\|^2\right\} < E\left\{\left\|\bar{\boldsymbol{H}}_{i,ZF}\right\|^2\right\} \tag{128}$$

Looking at the modified SLNR expression used by the iterative algorithm, we can see that this is effectively putting a lower priority on minimizing leakage. In a sense, the IRC receiver structure masks significant interference from the precoder calculation, causing it to converge more slowly. On the other hand, the iSLNR algorithm using ZF receivers converges much more quickly so as to mitigate the significant interference at the output of the receiver.

From previous results we know that the ZF and IRC receivers will achieve similar performance using the iSLNR algorithm (under the assumption of perfect CSIT). We also know that for a given precoding matrix $\boldsymbol{W}$, we should expect the IRC receiver to outperform the ZF receiver (assuming perfect channel estimation). It stands to reason then, that given the solution for $\boldsymbol{W}$ found by executing several iterations of the iSLNR algorithm for ZF receivers, performance should be equivalent or improved by using IRC receivers.

This hypothesis is verified by simulation and provides some interesting insight into the problem. The plot below shows the convergence behavior of a 4x(2x4) system using the

iSLNR algorithm operating at 30 dB SNR and with perfect CSIT and channel estimation at the receiver. The first curve shows the iSLNR algorithm for ZF receivers, but in a system employing IRC receivers, and the second curve shows the standard iSLNR algorithm for IRC receivers. You can see that the former converges very quickly, though the latter ultimately converges to a better solution. So while considering the IRC structure will eventually provide some benefit, a significant portion of the achievable gain can be realized in the first several iterations by using the ZF receiver structure to update the effective leakage channels.

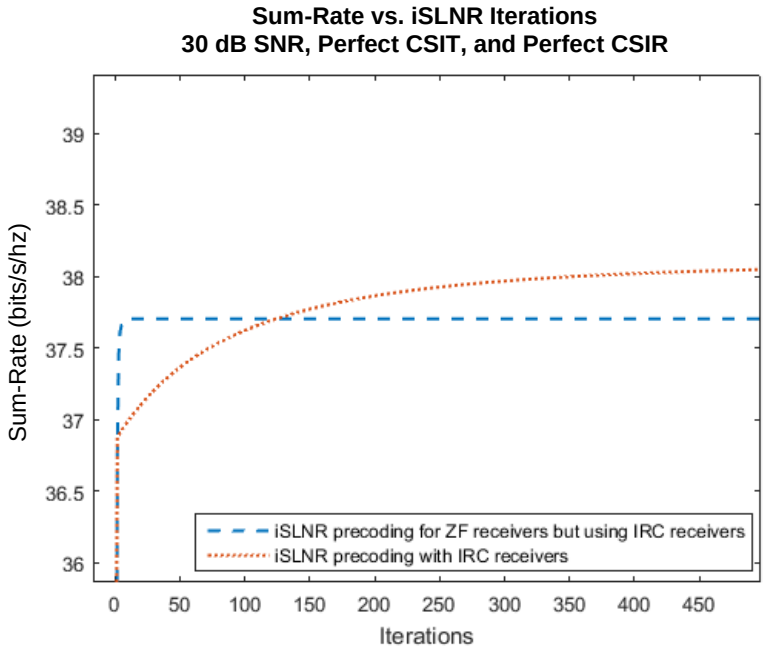

Figure 4.8: Sum-rate using the iSLNR algorithm for IRC and ZF receivers but employing IRC receivers

It stands to reason then, that an algorithm could be devised which achieves very quick convergence and the full potential of the IRC receiver. Indeed this can be accomplished by a implementing a simple state machine. The algorithm begins by using the ZF receiver structure and then switches to the IRC receiver structure after some defined number of iterations, here denoted as n_{ZF}. This concept is shown below, with $n_{ZF} = 50$. You can see that the solution converges very quickly when using the ZF receiver structure, stays there until the switching point, and then continues to converge to the best possible solution by using the IRC receiver structure.

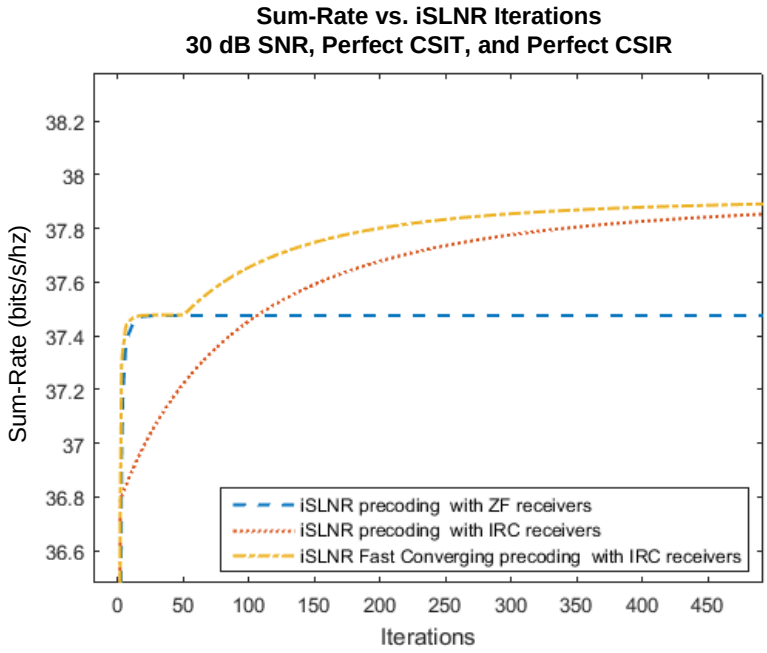

Figure 4.9: Sum-rate of a 4x(2x4) system using the fast-converging iSLNR algorithm with $n_{ZF} = 50$

There is a question of how to select n_{ZF}. In the previous plot, the system wastes its effort performing many iterations where nothing is gained (roughly iterations 5 to 50). Optimally, the algorithm would perform some number of iterations using the ZF structure until converged, then immediately switch to the IRC structure to achieve additional gain without wasted effort. As there is currently no known expression for the converged sum-rate using this algorithm, a closed form solution is unlikely. There are however several possible approaches that could be used for a practical system.

The most straightforward approach would be to simply always perform some set number of iterations using the ZF receiver before switching. This would be inefficient at low SNR though, where the ZF portion of the algorithm will converge in just one or two iterations. Another approach would be to utilize a lookup table which defines how many iterations should be performed in a given channel condition based on simulated results. A final method would be to examine the change in the precoding matrix after each iteration. If the total change is less than some threshold, consider the solution to have converged and switch to assuming the IRC structure. In the subsequent results we determine the

switching point based on simulated results. Using this approach we can achieve performance as shown in Figure 4.10 below.

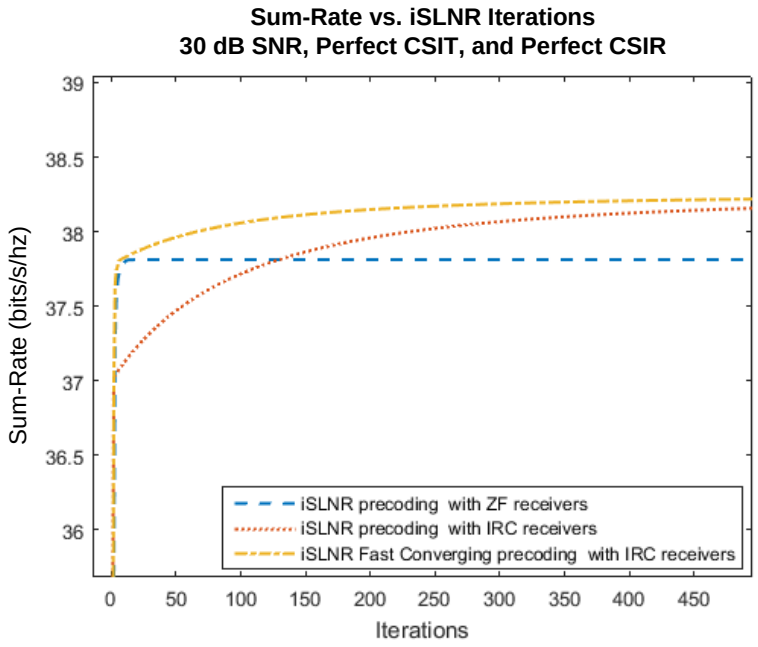

Figure 4.10: Sum-rate of a 4x(2x4) system using the fast-converging iSLNR algorithm with $n_{ZF} = 5$

This result holds equally for the case of imperfect CSIT and channel estimation at the receiver. Figure 4.11 shows a combination of several of the algorithms discussed in this work: the standard iSLNR algorithm, the iSLNR algorithm modified for imperfect CSIT, the fast converging iSLNR algorithm, and the fast converging iSLNR algorithm considering imperfect CSIT. You can see that the work in chapter 3 still holds true, that is, once the fast converging algorithms switch to using the IRC structure to update the effective leakage channels, the iSLNR algorithm proposed in Chapter 3 which considers CSIT error still performs better than the algorithm which does not. It is noteworthy however that most of the gain is achieved by the initial iterations using the ZF structure.

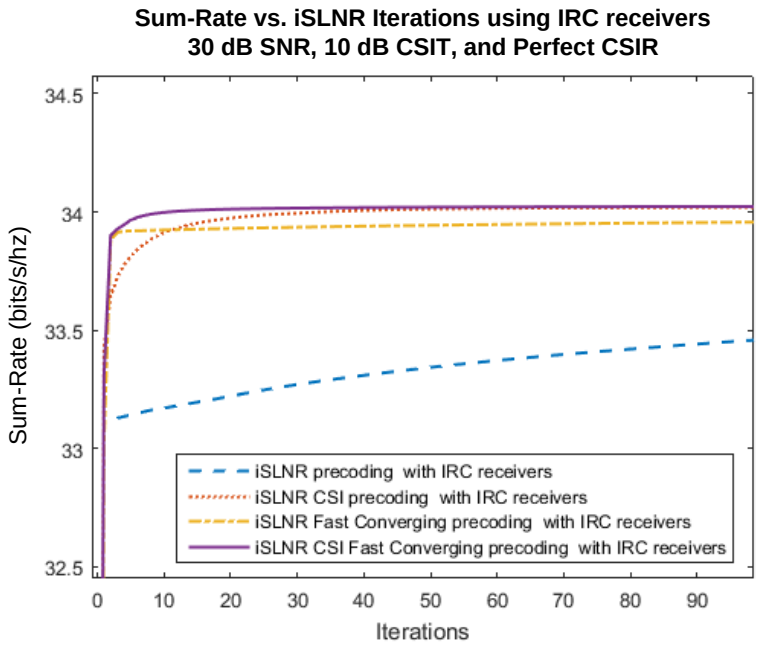

Figure 4.11: Sum-rate of a 9x(3x3) system using both the standard and fast-converging iSLNR algorithms with and without consideration to CSIT error

The results are similar even for systems with a large number of transmit antennas and users. Previously we had shown tremendous improvement for a system of this configuration by considering the CSIT error. It turns out that nearly all of the gain can be had in just a few iterations using this fast-converging approach. Figure 4.12 shows sum-rate of a 16x(2x8) system using the standard iSLNR algorithm, the iSLNR algorithm modified for imperfect CSIT, the fast converging iSLNR algorithm, and the fast converging iSLNR algorithm modified for imperfect CSIT.

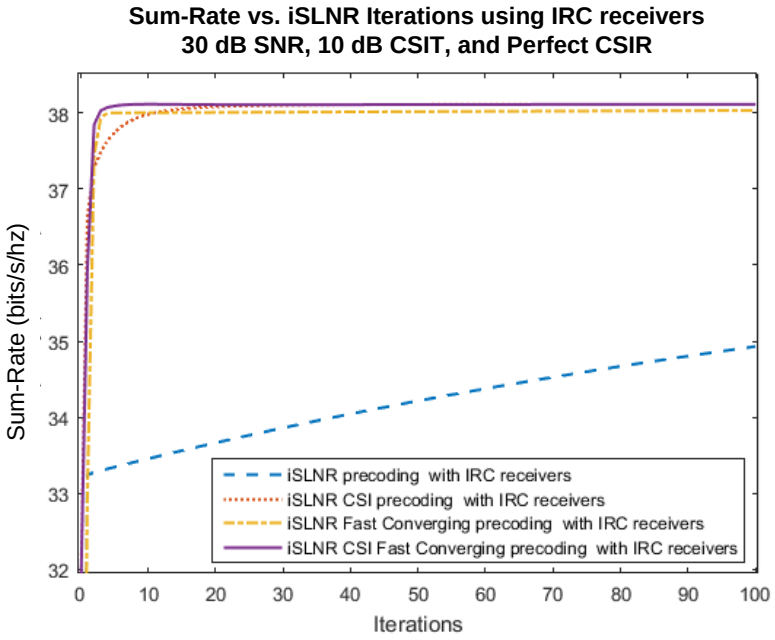

Figure 4.12: Sum-rate of a 16x(2x8) system using both the standard and fast-converging iSLNR algorithms with and without consideration to CSIT error

In this section we investigated a method to improve the convergence of the iSLNR algorithm when using IRC receivers, which proved to be rather effective. From simulations we saw that by using this algorithm nearly all of the gain is achieved in just a few iterations using the ZF receiver structure. The additional gain achievable using the IRC structure is comparatively small and may require many more iterations. We therefore conclude that a practical system would almost certainly avoid using the IRC structure altogether in the iSLNR algorithm. We further conclude that this proposed modification makes the pairing of the iSLNR algorithm and IRC receivers much more attractive. In such a system you can achieve good performance even with lower quality CSIT as we observed in chapter 3, as well as good convergence in a more ideal setting.

4.4 Selecting the Number of Co-Scheduled Users

In the previous sections we assumed a fixed system configuration, that is, a fixed number of transmit antennas and users. In a practical system users should be co-scheduled only when advantageous. So the question we wish to address in this section is, under what conditions is it better to co-schedule more users?

Figures 4.13 shows the sum-rate of a 4x(2xK) system employing IRC receivers where K is varied and CSIT is perfect. In this case we see that the system sum-rate will be greater using the iSLNR algorithm with four co-scheduled users for all SNR regimes. In the low SNR regime the sum-rate achieved by the iSLNR algorithm with two co-scheduled users and the SLNR precoding with four co-scheduled users are roughly the same, and only slightly better than the SLNR precoding with two co-scheduled users. In the high SNR regime, the sum-rate achieved with SLNR precoding for four users flattens out because the transmitter does not have sufficient degrees of freedom to suppress the MUI, which limits performance. Each of the other configurations has sufficient degrees of freedom so the sum-rate continues to improve with increasing SNR.

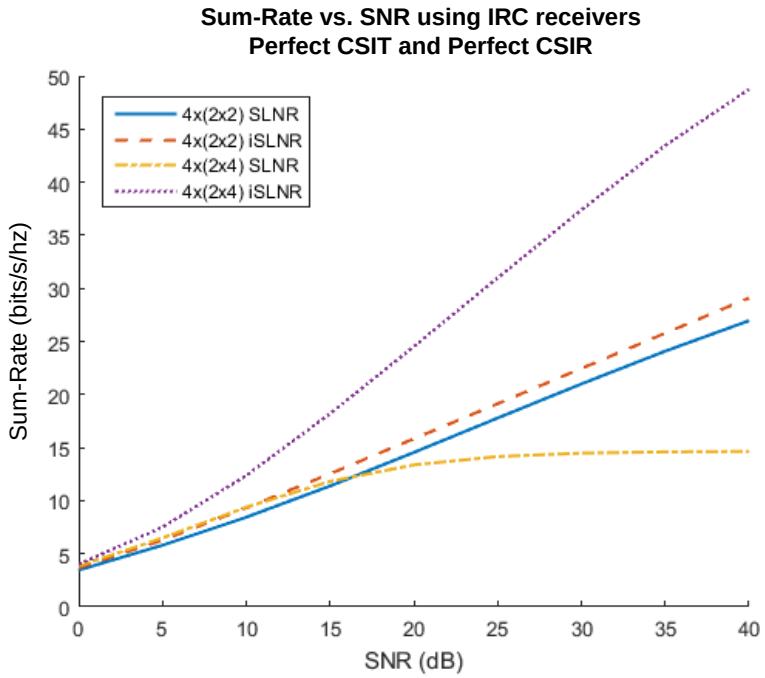

Figure 4.13: Sum-rate vs. SNR of a 4x(2xK) system operating with perfect CSIT with IRC receivers

Figure 4.14 shows a similar comparison but with the system operating at 10 dB CSIT. In this case we observe that using the iSLNR algorithm with four co-scheduled users is not the best solution for all SNR regimes in terms of providing the maximum system sum-rate. The imperfect CSIT causes the transmit precoding to be unable to completely suppress the MUI. In the case of two co-scheduled users with two receive antennas each, this residual MUI is suppressed at the receiver which allows sum-rate to continue to

improve at high SNR. On the other hand with four co-scheduled users each with two receive antennas the residual MUI cannot be fully suppressed at the receiver. This causes the achievable sum-rate to flatten out in the high SNR regime. We observe however that in the low SNR regime the residual MUI is not the dominant impairment, so having more users leads to improved sum-rate. So we see that the CSIT quality should be considered when deciding how many users are to be co-scheduled.

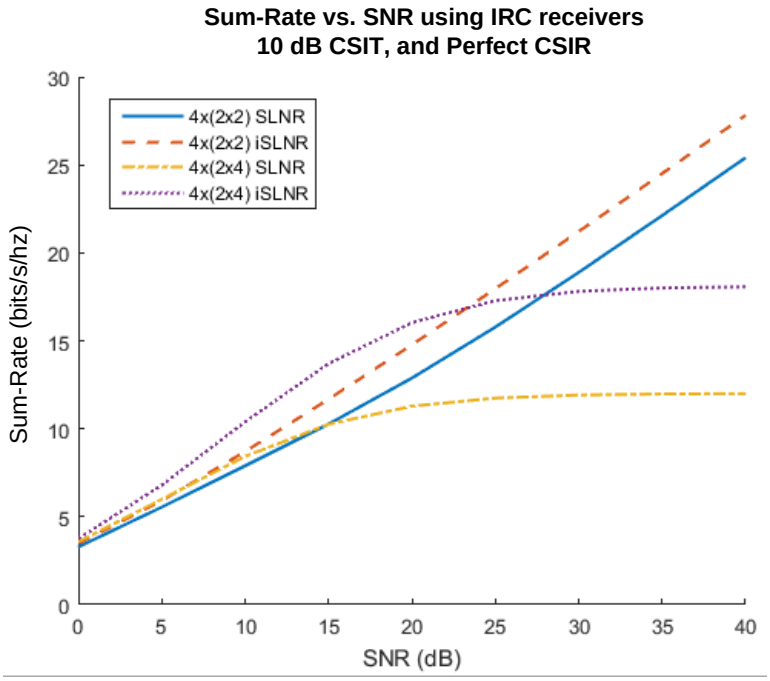

Figure 4.14: Sum-rate vs. SNR of a 4x(2xK) system operating with 10 dB CSIT with IRC receivers

Figure 4.15 shows a 4x(2xK) system employing ZF receivers operating at 10 dB CSIT. Note that in this case the receivers are unable to suppress the residual MUI. This means that the sum-rate will reach a maximum even for the two user case. So we observe that with ZF receivers the system sum-rate will always be best by using the iSLNR algorithm with four users.

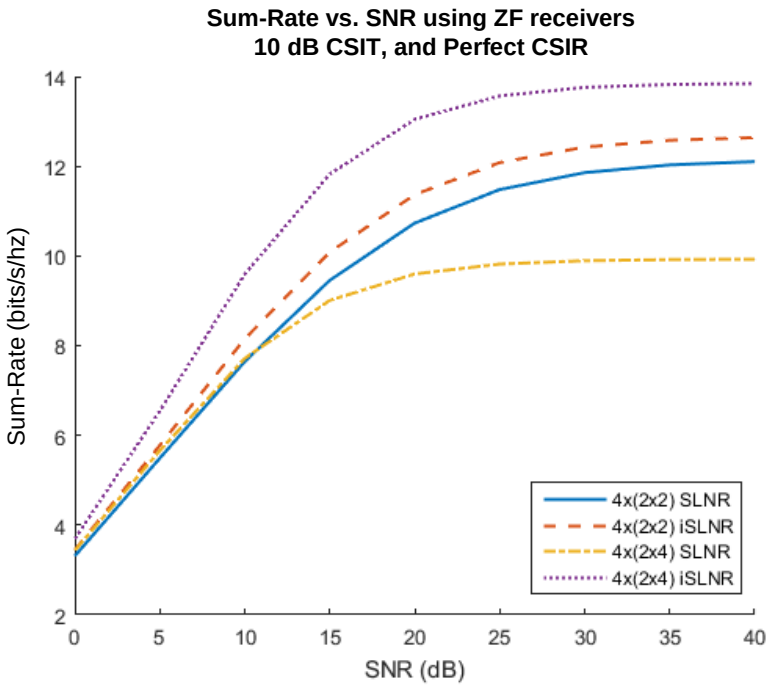

Figure 4.15: Sum-rate vs. SNR of a 4x(2xK) system operating with 10 dB CSIT

We can make similar comparisons for a system with eight transmit antennas. Figure 4.16 shows the sum-rate achieved by a 8x(2xK) system with perfect CSIT and for varying K. We observe that as in the four transmit antenna case, the system sum-rate is maximized by using the iSLNR algorithm with a large number of users, in this case eight. Figure 4.17 shows the sum-rate achieved by a 8x(2xK) system with 10 dB CSIT and for varying K. Again we observe that in the low SNR regime the sum-rate is maximized by co-scheduling eight users. And again we observe that the schemes with more than two users are unable to suppress the residual MUI resulting from the CSIT error, so the two user case achieves the greatest sum-rate in the high SNR regime. We note however, that the transition between these two operating regimes occurs at a higher SNR than in the 4x(2xK) case.

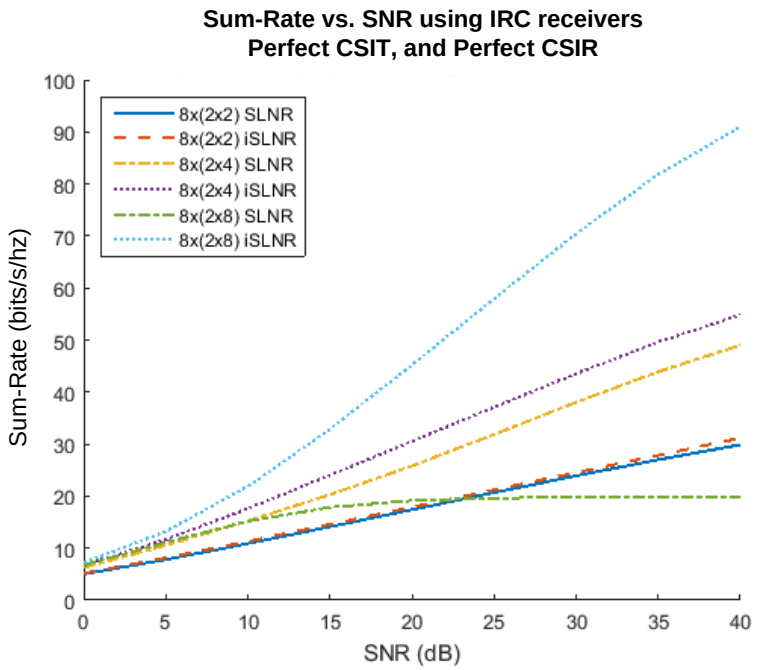

Figure 4.16: Sum-rate vs. SNR of a 8x(2xK) system operating with Perfect CSIT

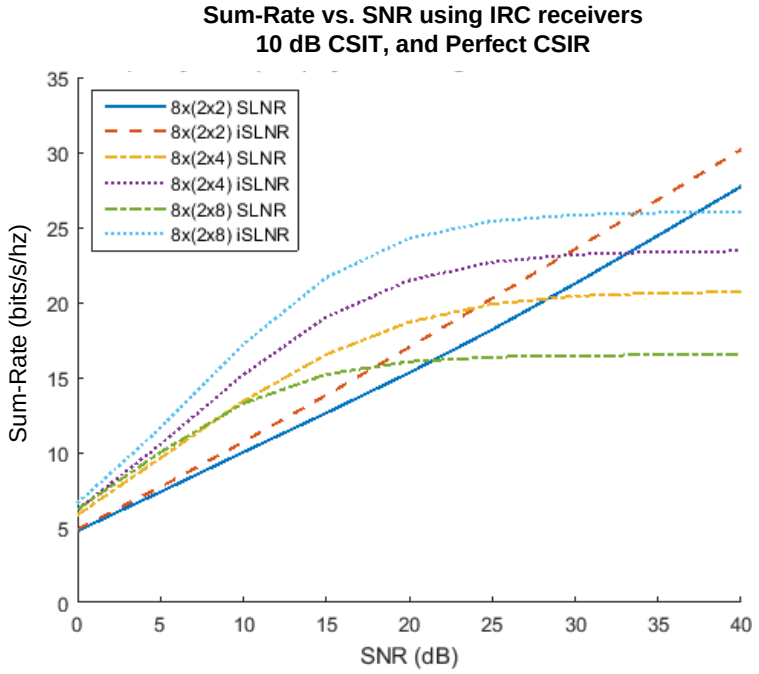

Figure 4.17: Sum-rate vs. SNR of a 8x(2xK) system operating with 10 dB CSIT

4.5 Conclusions

In this chapter we investigated several practical considerations of the iSLNR algorithm. We began by looking at achieved performance with transmit antenna correlation. The two

key observations were as follows: (1) system sum-rate decreases with increased transmit antenna correlation and (2) sum-rate may not be monotonically increasing per iteration of the algorithm when transmit antenna correlation is high and IRC receivers are used. We continued by examining performance of the iSLNR algorithm in time-varying channels using several possible approaches based on our previous analysis on imperfect CSIT. We showed that there is an inherent tradeoff between achieving fast convergence and achieving the best possible converged solution. We then proposed a modification to the algorithm which can drastically improve its convergence when IRC receivers are employed. It was shown that using this approach coupled with the solution which considers CSIT error provides the best convergence. With this modification in mind the advantage of the IRC receiver is clear as it will achieve the same performance as the ZF receiver even at just a few iterations in ideal conditions besides also achieving significantly better performance with imperfect CSIT as we saw in the previous chapter. Finally, we examined the sum-rate achieved by a system with a fixed number of transmit antennas but with a varied number of co-scheduled users and operating with various qualities of CSIT. From this work we observed that in the ideal case it is always best to co-schedule the maximum number of users supported by the degrees of freedom achieved with the iSLNR algorithm, but with imperfect CSIT the number of users which will maximize the system sum-rate may depend on the SNR. At low SNR it is best to co-schedule the maximum number of users with the iSLNR algorithm, but at high SNR the imperfect CSIT causes residual MUI which dominates performance, making it better to co-schedule fewer users.

Chapter 5

iSLNR for LTE-A

In this chapter we demonstrate the application of the iSLNR algorithm to one of the most prominent modern day wireless standards, LTE-A. There are several key distinctions between the previous analysis and an implementation for LTE-A which will be discussed later. In the first section of this chapter we provide the necessary background on the LTE-A standard. The second section presents the simulated performance of the algorithm, and finally we draw conclusions on the utility of the iSLNR algorithm for LTE-A.

5.1 MU-MIMO in LTE-A

In this section we go over the details of the implementation of MU-MIMO in LTE-A. Specifically, we desire to understand how the waveforms are modulated, how precoding is accomplished at the base station, how channel estimation may be performed at the user, and how these considerations may impact the iSLNR algorithm.

5.1.1 Downlink Waveform

The LTE-A downlink uses orthogonal frequency division multiplexing (OFDM), wherein many narrowband carriers are transmitted in parallel. This provides several nice features: (1) each subcarrier experiences frequency flat fading (2) inter-symbol-interference can be mitigated by the insertion of a cyclic-prefix and (3) the FFT and IFFT provide efficient means of implementing the OFDM modem in hardware/software. Precoding can be performed simply by multiplying each symbol by the precoding weights prior to the IFFT operation. A block diagram of a MIMO-OFDM system is included below in Figure 5.1. In this case there is only one user.

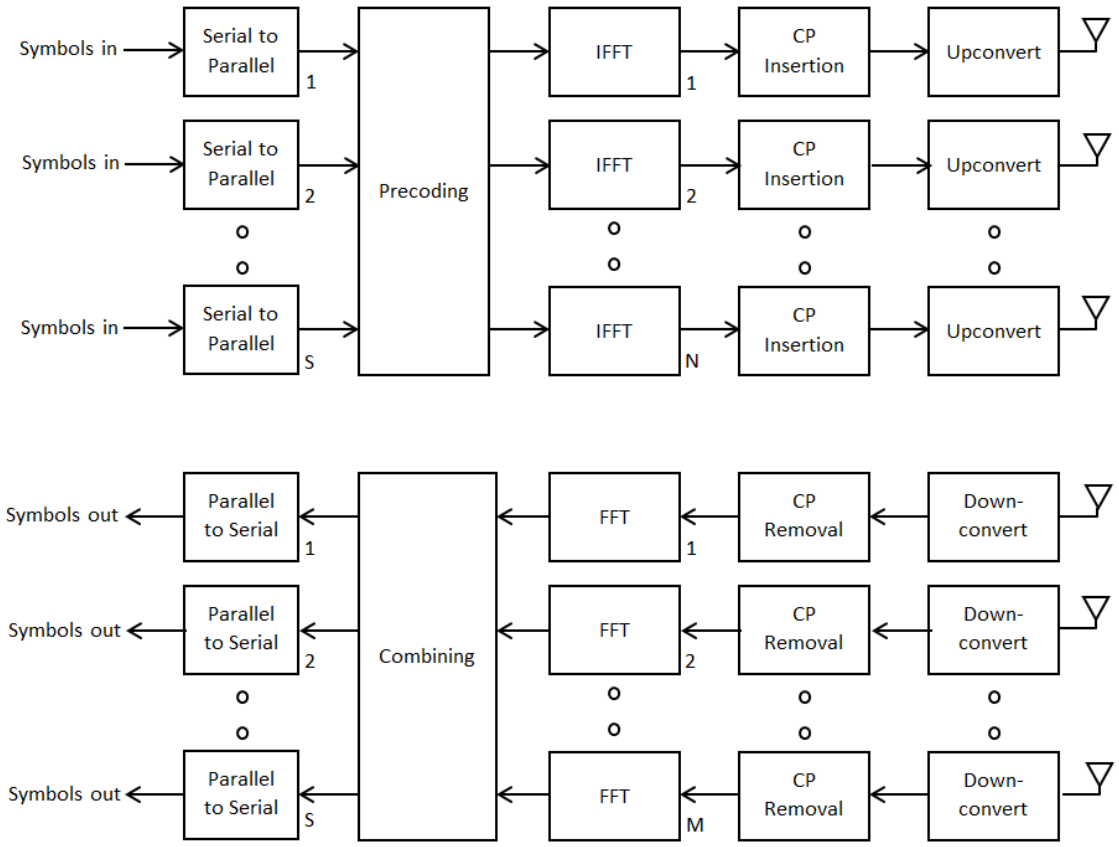

Figure 5.1: Block diagram of MIMO-OFDM system

5.1.2 MU-MIMO Transmission Modes

The LTE downlink supports a number of MIMO techniques including transmit diversity, beamforming, spatial-multiplexing, and MU-MIMO. Currently there are ten different transmission modes (TM) defined for LTE which are shown in Table 5.1. MU-MIMO was originally added to the LTE standard in release 8 as defined by TM5. This mode allowed an eNB to transmit to two users simultaneously using the same resource blocks provided each user's transmission used a different precoding matrix. The gain of this scheme was severely limited due to the precoding matrices being restricted to a finite codebook. This limitation was overcome in TM8 and TM9 which were defined in release 10. In these transmission modes, arbitrary precoding can be employed at the eNB. Channel estimation is performed at the UE using the demodulation reference signals (DMRS) which are UE-specific reference signals that are precoded using the same precoding matrix as the data symbols. This effectively makes the precoding transparent to

the UE, that is, the UE does not require knowledge of the precoding matrix employed at the eNB. This added flexibility allows the eNB to choose much better precoding matrices in terms of reducing the MUI at the UE. The standard makes no requirements for how these precoding matrices should be formulated other than that the finest precoding granularity is per resource block (RB), which is a unit of radio resources consisting of 12 subcarriers and 7 OFDM symbols. TM8 allows the eNB to transmit two spatial streams which can be for a single UE or two separate UE. TM9 allows for up to 8 layer transmission and up to four co-scheduled users. TM10 is an extension to TM9 which supports Cooperative Multi-Point transmission.

Downlink Transmission modes in LTE Release 12			
Transmission modes	**Description**	**DCI** (Main)	**Comment**
1	Single transmit antenna	1/1A	single antenna port port 0
2	Transmit diversity	1/1A	2 or 4 antennas ports 0,1 (…3)
3	Open loop spatial multiplexing with cyclic delay diversity (CDD)	2A	2 or 4 antennas ports 0,1 (…3)
4	Closed loop spatial multiplexing	2	2 or 4 antennas ports 0,1 (…3)
5	Multi-user MIMO	1D	2 or 4 antennas ports 0,1 (…3)
6	Closed loop spatial multiplexing using a single transmission layer	1B	1 layer (rank 1), 2 or 4 antennas ports 0,1 (…3)
7	Beamforming	1	single antenna port, port 5 (virtual antenna port, actual antenna configuration depends on implementation)
8	Dual-layer beamforming	2B	dual-layer transmission, antenna ports 7 and 8
9	8 layer transmission	2C	Up to 8 layers, antenna ports 7 - 14
10	8 layer transmission	2D	Up to 8 layers, antenna ports 7 - 14

Table 5.1: LTE-A Downlink Transmission Modes

5.1.3 MU-MIMO Channel Estimation

As mentioned in the previous section, TM9 uses the DMRS for channel estimation at the UE. There is a unique DMRS for each of the transmitted spatial layers, which are referred to as antenna ports in the LTE standard. Channel estimation is performed independently

per RB since the precoding may be unique for each. The DMRS for each antenna port uses the same complex sequence r defined below, where c is a pseudo-random sequence.

$$r(m) = \frac{1}{\sqrt{2}}\left(1-2\cdot c(2m)\right) + j\frac{1}{\sqrt{2}}\left(1-2\cdot c(2m+1)\right), \qquad m = \begin{cases} 0,1,\ldots,12N_{\mathrm{RB}}^{\max,\mathrm{DL}}-1 & \text{normal cyclic prefix} \\ 0,1,\ldots,16N_{\mathrm{RB}}^{\max,\mathrm{DL}}-1 & \text{extended cyclic prefix} \end{cases}.$$

The final complex signal is spread by port specific sequences which orthogonalize the reference signals on different layers so they can be differentiated at the receiver. The sequences are shown below.

Antenna port p	$[\overline{w}_p(0) \quad \overline{w}_p(1) \quad \overline{w}_p(2) \quad \overline{w}_p(3)]$
7	$[+1 \quad +1 \quad +1 \quad +1]$
8	$[+1 \quad -1 \quad +1 \quad -1]$
9	$[+1 \quad +1 \quad +1 \quad +1]$
10	$[+1 \quad -1 \quad +1 \quad -1]$
11	$[+1 \quad +1 \quad -1 \quad -1]$
12	$[-1 \quad -1 \quad +1 \quad +1]$
13	$[+1 \quad -1 \quad -1 \quad +1]$
14	$[-1 \quad +1 \quad +1 \quad -1]$

Table 5.2: Spreading sequences for DMRS

The resulting complex signals are then mapped to the resource grid as shown in Figure 5.2. When 3-8 spatial layers are used, the DMRS is allocated an additional 3 dB of power [24]. The reference signal spreading occurs in the time domain; the necessary assumption being that the channel can be considered static over the symbols corresponding to one element of the non-spread reference sequence.

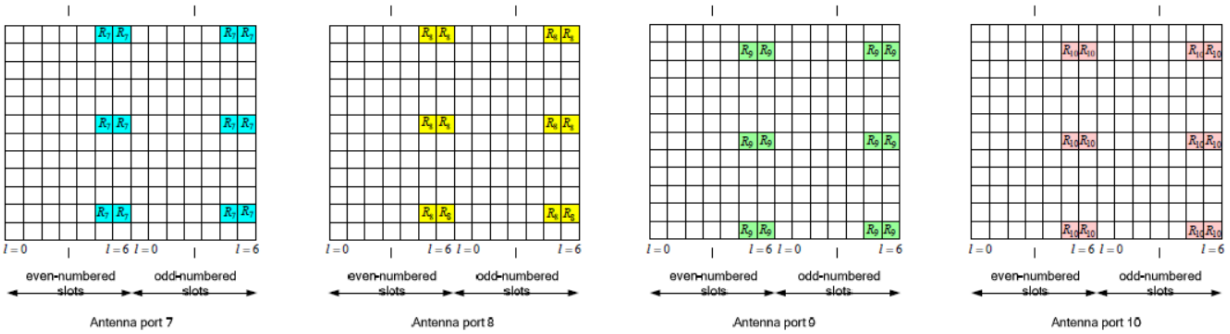

Figure 5.2: DMRS mapping to the resource grid

There are a number of approaches that the UE might use for channel estimation. Two of the more conventional approaches are the least squares (LS) and minimum-mean-square-error (MMSE) estimates [26]. The MMSE estimate provides better performance at the cost of additional complexity. We show simulations using both of these channel estimation techniques so we can compare how effective the iSLNR algorithm is in each case.

5.2 Simulated Performance

In this section we present results from simulations conducted for the LTE-A MU-MIMO downlink using the iSLNR algorithm. The algorithm is applied per RB based on the mean channel across each subcarrier. A single receive filter is then calculated to update the leakage channel. Of course in reality, the receive filters will be unique for each resource element, so this is a simplification. We simulate a 4x(2x2) system operating with 10 MHz of bandwidth where all RB's are allocated to the two users. The channel is modeled using the Extended Pedestrian A model with zero Doppler. The transmission uses 64 QAM with a coding rate of $1/2$. The channel is estimated using the LS estimator. This simulation does not include HARQ. Figure 5.3 shows the uncoded BER, Figure 5.4 shows the BLER, and Figure 5.5 shows the throughput achieved by the system. You can see that at a BLER of 1e-1 we achieve around 4.25 dB of gain, and similar gain is seen in terms of the throughput curve.

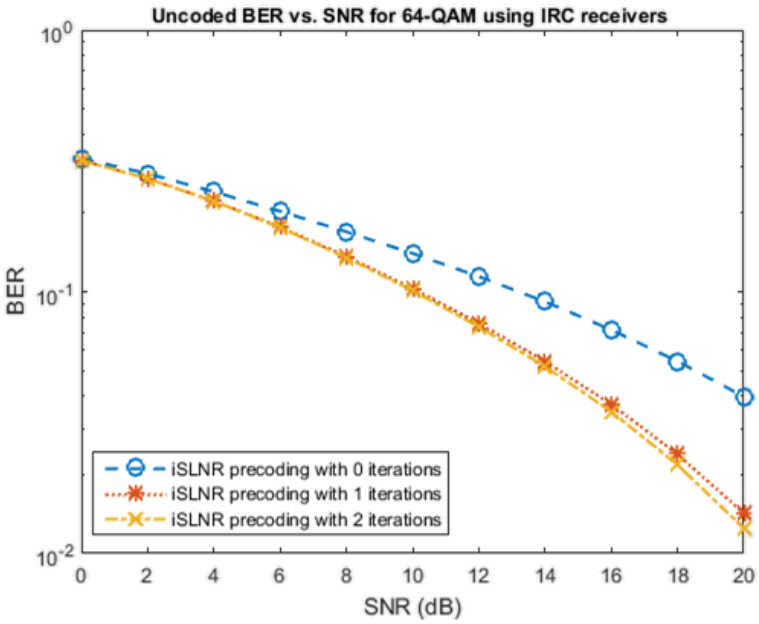

Figure 5.3: Uncoded BER of LTE-A using iSLNR with LS channel estimation

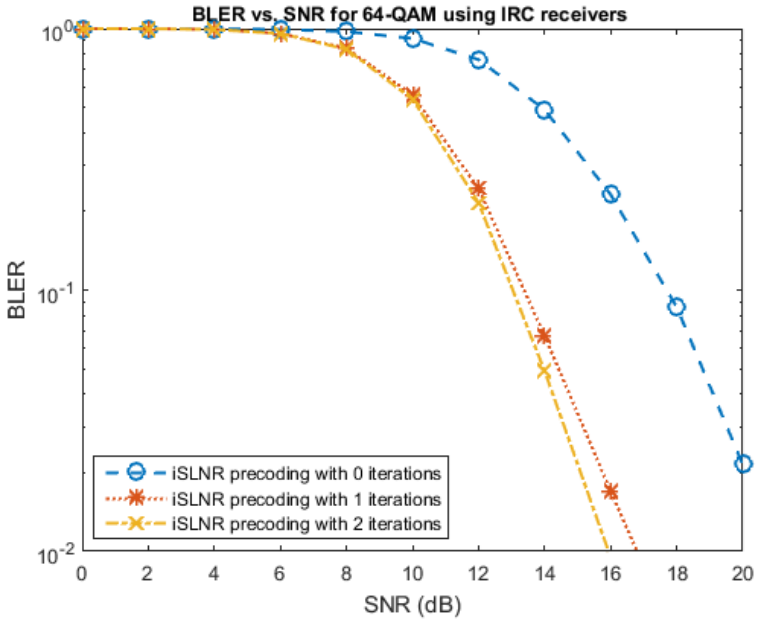

Figure 5.4: BLER of LTE-A using iSLNR with LS channel estimation

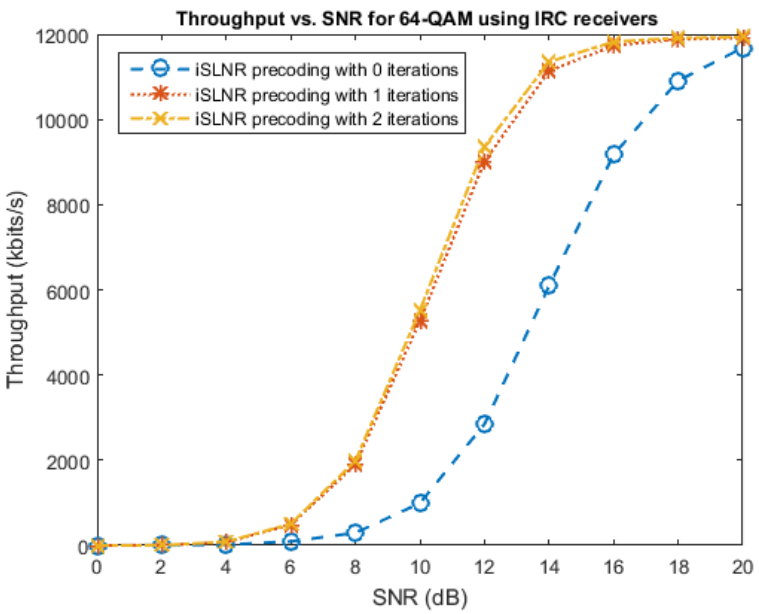

Figure 5.5: Throughput of LTE-A using iSLNR with LS channel estimation

Figures 5.6 to 5.8 show a similar simulation with the only difference being that the UE use the MMSE channel estimate rather than the LS channel estimate. There are two key things to note here. First, the performance is improved using the MMSE estimate even for the cSLNR scheme (zeroth iteration of the iSLNR algorithm). We further observe that the gains achieved by the iSLNR algorithm are greater in this case. At a BLER of 1e-1 the iSLNR algorithm provides about 5 dB of gain compared to the 4.25 dB that was achieved when the LS channel estimate was used. This aligns with our observations in chapter 3; that the gain achieved by the iSLNR algorithm will decrease with degraded CSIR.

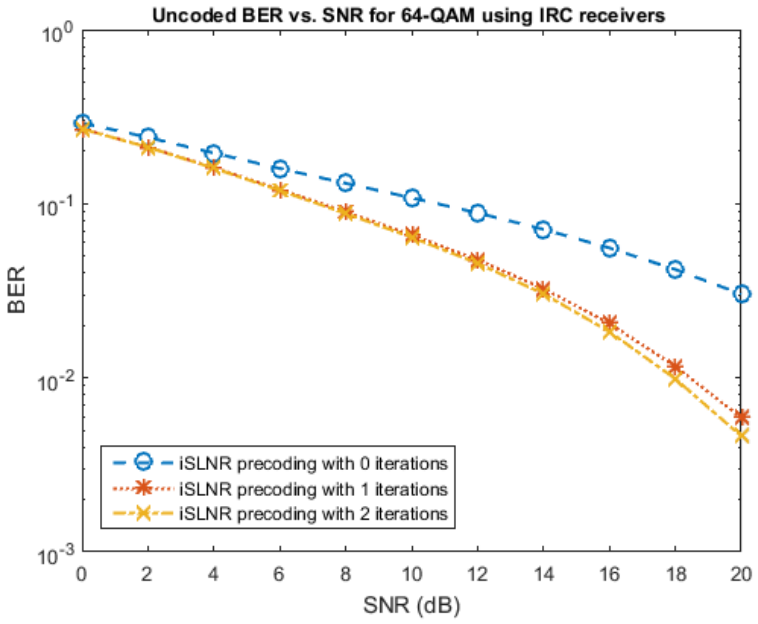

Figure 5.6: Uncoded BER of LTE-A using iSLNR with MMSE channel estimation

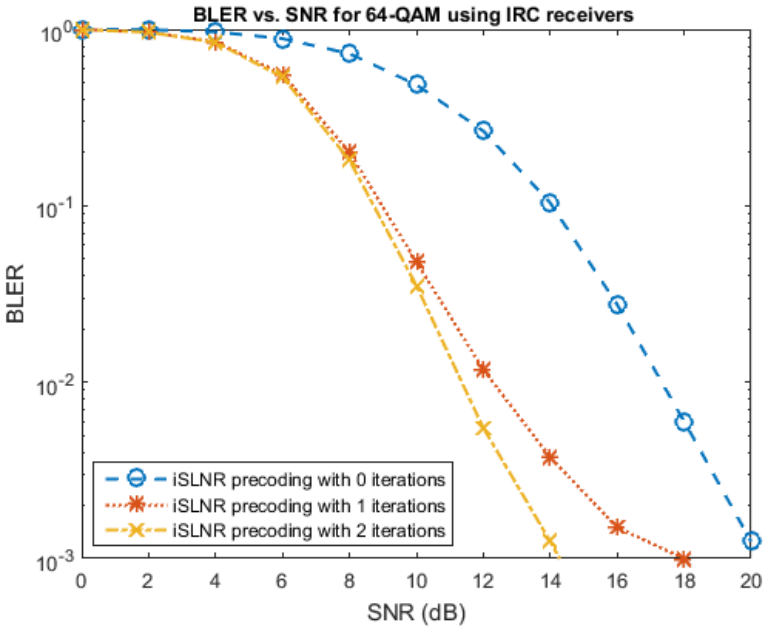

Figure 5.7: BLER of LTE-A using iSLNR with MMSE channel estimation

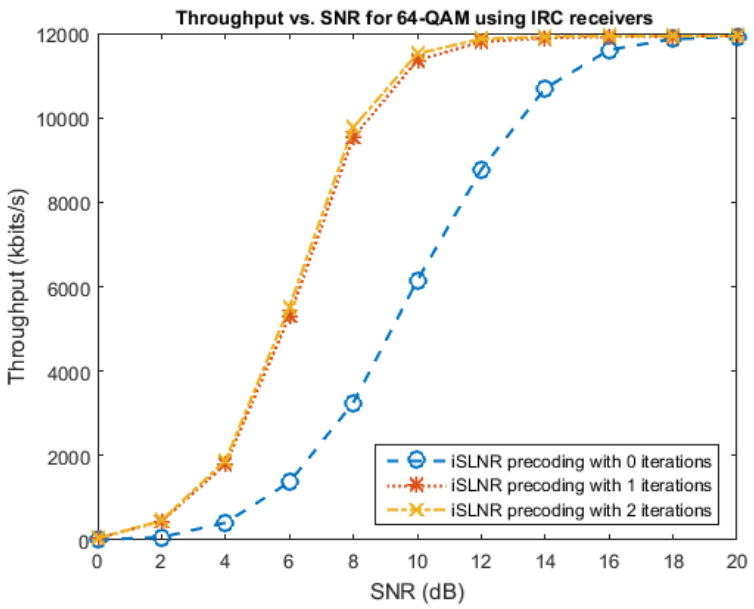

Figure 5.8: Throughput of LTE-A using iSLNR with MMSE channel estimation

5.3 Conclusions

In this chapter we applied the iSLNR algorithm to the LTE-A downlink. Simulations showed significant improvements in BER, BLER, and throughput. Using the MMSE estimate provided better performance than the LS estimate and enabled the iSLNR algorithm to provide slightly greater gain. This aligned with our analysis in Chapter 3 where we saw that the gains of the iSLNR algorithm will degrade with lower quality CSIR.

Chapter 6

Conclusion

In this thesis we have examined a number of practical aspects of leakage-based precoding for the MU-MIMO downlink. We began by considering the impact of imperfect CSIT and proposing solutions which mitigate the performance degradation. We also investigated the impact of imperfect CSIR. We then continued by examining the impact of other practical considerations such as transmit antenna correlation and time-varying channels. We also proposed a simple modification which can improve convergence of the algorithm with IRC receivers and examined the problem of selecting the number of co-scheduled users. Finally, we demonstrated performance of the algorithm when applied to the LTE-A framework for MU-MIMO.

Our analysis of imperfect CSI began by deriving an expression for the precoding matrices which will maximize the SLNR in the presence of imperfect CSIT. Simulations showed that the derived solution was superior to the one previously proposed in [7] which used the same error model. We then went on to examine the impact of modifying the CSIT to meet the MMSE criteria without relying on knowledge of the true channel as in [12]. This showed a marginal though non-negligible performance gain for the cSLNR precoding scheme. Next, we applied similar analysis to the iSLNR algorithm. The derivation of the precoding solution follows the same approach as with the cSLNR scheme, but we also had to consider the effect that the CSIT error had on the receive filter calculations. Simulations showed that the proposed solutions can provide substantial gains compared to the iSLNR algorithm which does not consider imperfect CSIT. We also observed that with imperfect CSIT, the sum-rate achieved with IRC receivers can be much greater than that achieved with ZF receivers. We then investigated the same MMSE modification for the iSLNR algorithm and found that after several iterations the gain had become negligible. We also showed the performance degradation due to imperfect CSIR. It was shown that the CSIR quality must be sufficiently high for the iSLNR algorithm to provide substantial performance gains.

Through simulation we demonstrated the performance degradations experienced due to transmit antenna correlation and time-varying channels. We observed that the sum-rate achieved using the iSLNR algorithm may not be monotonically increasing per iteration when IRC receivers are used and transmit antenna correlation is high. We demonstrated how our work on imperfect CSIT is relevant to the case of time-varying channels and that there is a tradeoff between achieving fast converging and the optimal solution. We then showed how a trivial modification of the iSLNR algorithm can greatly improve its convergence with IRC receivers. With this modification, the performance-complexity tradeoff seems to favor IRC receivers, whereas the authors of [8] concluded that ZF receivers were the better choice. We observed that the choice of how many users should be co-scheduled may depend on the CSIT quality and the SNR. With perfect CSIT it is always best to schedule the maximum number of users supported by the iSLNR algorithm. On the other hand, with imperfect CSIT it may be beneficial to reduce the number of users at high SNR due to insufficient suppression of the MUI at the receiver.

In Chapter 5 it was shown that the iSLNR algorithm can provide significant gain for LTE-A. The simulations were performed for a 4x(2x2) system with a single stream per user, whereas TM9 supports up to eight spatial streams. Based on our previous analysis the achievable gains should be even greater for a system with more antennas and users. We compared the algorithm's performance with LS and MMSE channel estimators at the UE and showed that greater gain is achieved using the MMSE estimate, which aligns with our analysis in Chapter 3.

References

[1] B. Schulz, “LTE Transmission Modes and Beamforming,” Rohde & Schwarz White Paper, July 2015.

[2] Bejarano, Oscar, Edward W. Knightly, and Minyoung Park. "IEEE 802.11 ac: from channelization to multi-user MIMO." *IEEE Communications Magazine*51.10 (2013): 84-90.

[3] G. Caire and S. Shamai, "On the achievable throughput of a multiantenna Gaussian broadcast channel," in *IEEE Transactions on Information Theory*, vol. 49, no. 7, pp. 1691-1706, July 2003

[4] Q. H. Spencer, A. L. Swindlehurst, M. Haardt, "Zero-forcing methods for downlink spatial multiplexing in multiuser MIMO channels," in *IEEE Transactions on Signal Processing*, 2004, vol. 52, no. 2, pp. 461-471.

[5] H. Lee, K. Lee, B. M. Hochwald and I. Lee, "Regularized Channel Inversion for Multiple-Antenna users in Multiuser MIMO Downlink," *Communications, 2008. ICC '08. IEEE International Conference on*, Beijing, 2008, pp. 3501-3505.

[6] A. Tarighat, M. Sadek, A.H. Sayed, "A multi user beamforming scheme for downlink MIMO channels based on maximizing signal-to-leakage ratios," in *Acoustics, Speech, and Signal Processing, 2005. Proceedings. (ICASSP '05). IEEE International Conference on* , 2003, vol.3, no., pp.iii/1129-iii/1132.

[7] M. Sadek, A. Tarighat, A.H. Sayed, "A Leakage-Based Precoding Scheme for Downlink Multi-User MIMO Channels," in *Wireless Communications, IEEE Transactions on* , 2007, vol.6, no.5, pp.1711-1721.

[8] P. Patcharamaneepakorn, S. Armour, A. Doufexi, "A modified leakage-based transmit filter design for multi-user MIMO systems," in *Personal Indoor and Mobile Radio Communications (PIMRC), 2013 IEEE 24th International Symposium on* , 2013, pp.912-916.

[9] G. Xiangchuan, F. Xiong, L. Song, "A successive iterative optimization precoding method for downlink multi-user MIMO system," in *Wireless Communications and Signal Processing (WCSP), 2010 International Conference on* , 2010, pp.1-5.

[10] Z. Bai, S. Iwelski, G. Bruck, P. Jung,; B. Badic, T. Scholand, R. Balraj, "Receiver performance-complexity tradeoff in LTE MU-MIMO transmission," in *Ultra Modern Telecommunications and Control Systems and Workshops (ICUMT), 2011 3rd International Congress on*, Budapest, 2011, pp.1-7.

[11] P. Karunakaran, T. Wagner, A. Scherb, W. Gerstacker, "On Interference Rejection Combining for LTE-A Systems: Analysis of Covariance Estimators and an Iterative Algorithm for Frequency-Selective Channels," in *Vehicular Technology Conference (VTC Spring)*, Glasgow, 2015, pp. 1-5.

[12] P. Cao, G. Kang, N. Zhang and P. Zhang, "A modified precoding scheme for MIMO downlink channel with imperfect CSIT," *Communication Systems, 2008. ICCS 2008. 11th IEEE Singapore International Conference on*, Guangzhou, 2008, pp. 841-845.

[13] J. Wang, S. Jin, X. Gao, K. K. Wong and E. Au, "Statistical eigenmode SDMA transmission for a two-user downlink," *Communications (ICC), 2012 IEEE International Conference on*, Ottawa, ON, 2012, pp. 3872-3877

[14] Qing Huang and Yingmin Wang, "Linear receivers for multi-cell MIMO transmission in LTE-advanced downlink," *Communications and Networking in China (CHINACOM), 2013 8th International ICST Conference on*, Guilin, 2013, pp. 286-290

[15] M. S. Dastgahian and H. Khoshbin, "A novel vector perturbation based on joint transceiver algorithm in cooperative mu-MIMO," *Electrical Engineering (ICEE), 2011 19th Iranian Conference on*, Tehran, Iran, 2011, pp. 1-6

[16] A. Bourdoux and N. Khaled, "Joint TX-RX optimisation for MIMO-SDMA based on a -space constraint," *Vehicular Technology Conference, 2002. Proceedings. VTC 2002-Fall. 2002 IEEE 56th*, 2002, pp. 171-174 vol.1

[17] Joint Tx-Rx MMSE Design for MIMO Multicarrier Systems with Tomlinson-Harashima Precoding," in *IEEE Transactions on Wireless Communications*, vol. 7, no. 8, pp. 3118-3127, August 2008.

[18] P. Patcharamaneepakorn, A. Doufexi and S. Armour, "Equivalent Expressions and Performance Analysis of SLNR Precoding Schemes: A Generalisation to Multi-Antenna Receivers," in *IEEE Communications Letters*, vol. 17, no. 6, pp. 1196-1199, June 2013.

[19] H. Wang, X. Xu, M. Zhao, W. Wu and Y. Yao, "Robust Transmission for Multiuser MIMO Downlink Systems with Imperfect CSIT," *Wireless Communications and Networking Conference, 2008. WCNC 2008. IEEE*, Las Vegas, NV, 2008, pp. 340-344.

[20] D. Debbarma, Qing Wang, S. H. de Groot and A. Lo, "Effects of imperfect CSIT on downlink MU-MIMO fair SLNR scheduling algorithm," *Communications and Vehicular Technology in the Benelux (SCVT), 2013 IEEE 20th Symposium on*, Namur, 2013, pp. 1-6.

[21] J. Zhang, M. Haardt and F. Roemer, "Robust design of block diagonalization using perturbation analysis," *Acoustics, Speech and Signal Processing (ICASSP), 2013 IEEE International Conference on*, Vancouver, BC, 2013, pp. 4192-4196

[22] P. Chang, T. Lv, T. Wang, H. Gao and Y. Li, "MMSE Modified Multi-User MIMO Downlink Transmission with Imperfect CSI," *Vehicular Technology Conference (VTC Spring), 2011 IEEE 73rd*, Budapest, 2011, pp. 1-5

[23] Leon-Garcia, A., “Probability, Statistics, ad Random Processes for Electrical Engineering,” pp. 334

[24] 3GPP 36.213, “Evolved Universal Terrestrial Radio Access (E-UTRA); Physical layer procedures,” 3GPP, Sophia Antipolis, Technical Specification 36.213 v12.5.0, Mar. 2015.

[25] X. Zhang, X. Zhou, “LTE-Advanced Air Interface Technology,” CRC Press, Boca Raton, FL, 2013, pp. 116.

[26] J. J. van de Beek, O. Edfors, M. Sandell, S. K. Wilson and P. O. Borjesson, "On channel estimation in OFDM systems," *Vehicular Technology Conference, 1995 IEEE 45th*, Chicago, IL, 1995, pp. 815-819 vol.2.

[27] D. Bai *et al.*, "LTE-advanced modem design: challenges and perspectives," in *IEEE Communications Magazine*, vol. 50, no. 2, pp. 178-186, February 2012.

[28] P. Patcharamaneepakorn, A. Doufexi and S. M. D. Armour, "Weighted Sum Sum-rate Maximization Using a Modified Leakage-Based Transmit Filter Design," in *IEEE Transactions on Vehicular Technology*, March 2013, vol. 62, no. 3, pp. 1177-1188.

Appendix A: Additional Transmit Antenna Correlation Simulations

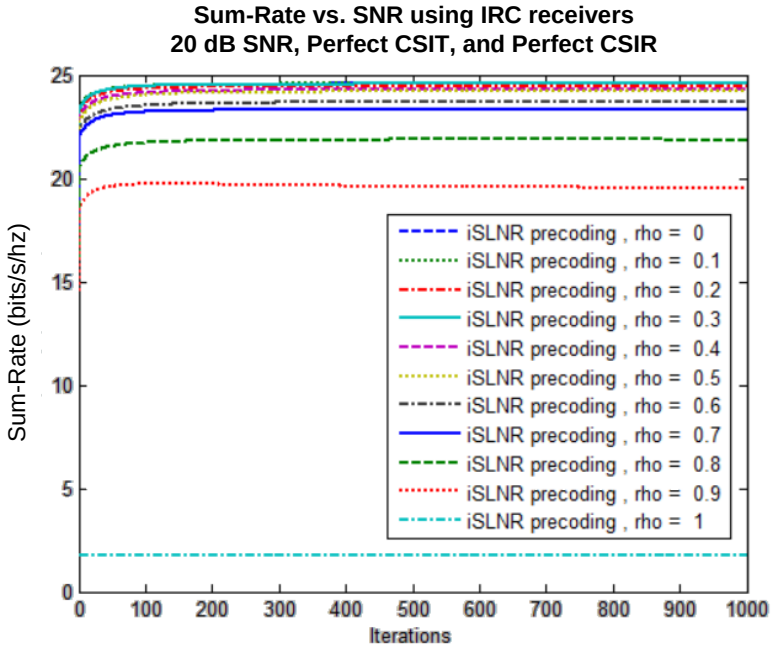

Figure 8.1: Sum-rate of 6x(3x3) system with varying transmit correlation

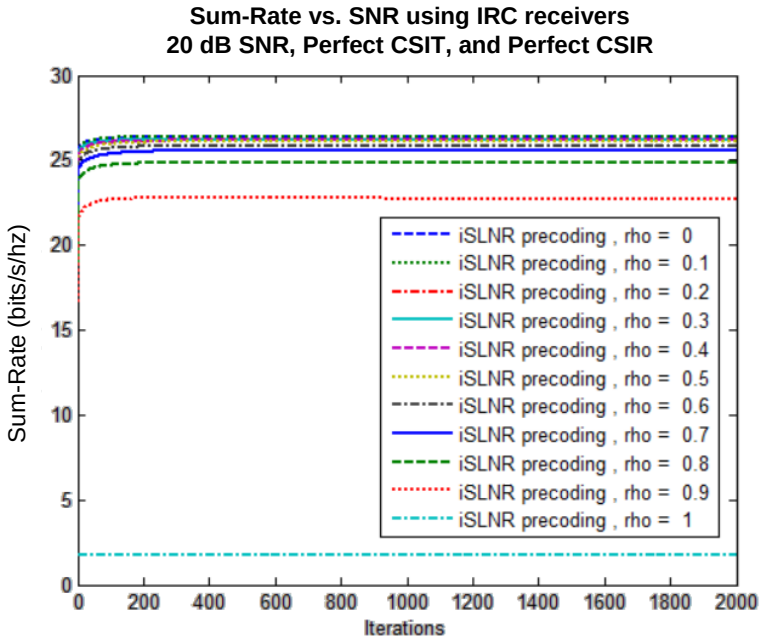

Figure 8.2: Sum-rate of 9x(3x3) system with varying transmit correlation

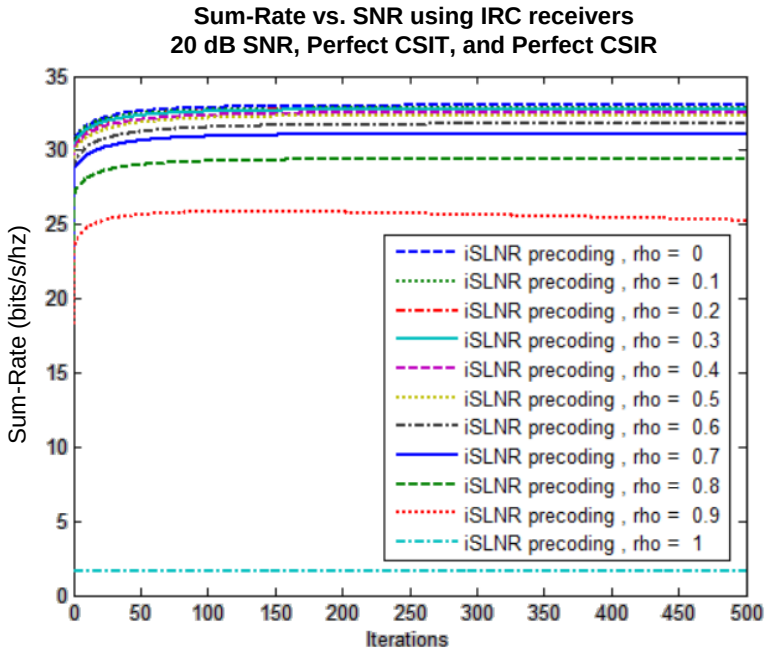

Figure 8.3: Sum-rate of 9x(3x4) system with varying transmit correlation

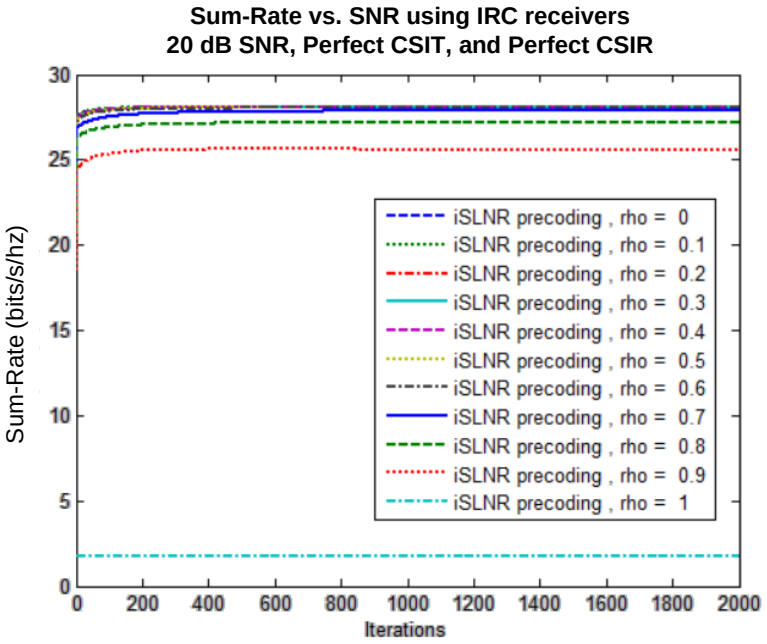

Figure 8.4: Sum-rate of 12x(3x4) system with varying transmit correlation

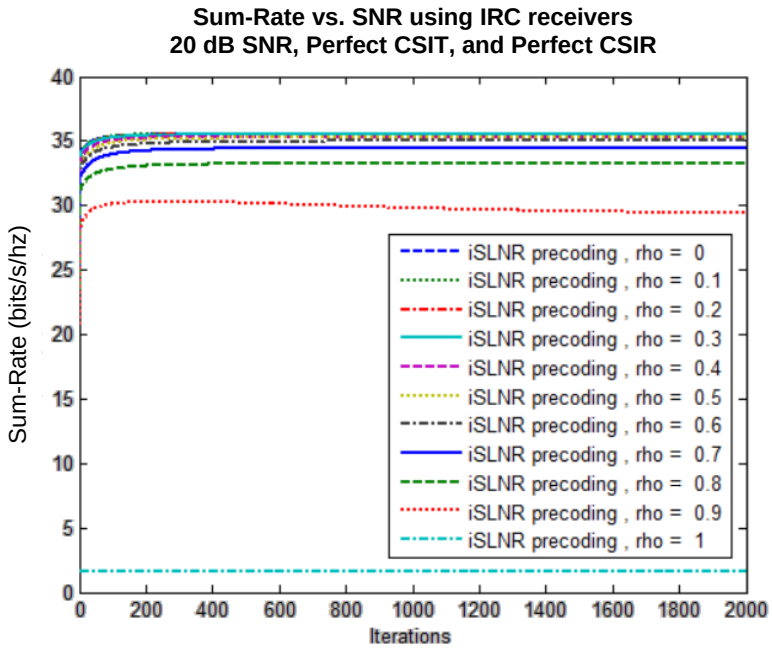

Figure 8.5: Sum-rate of 12x(4x4) system with varying transmit correlation

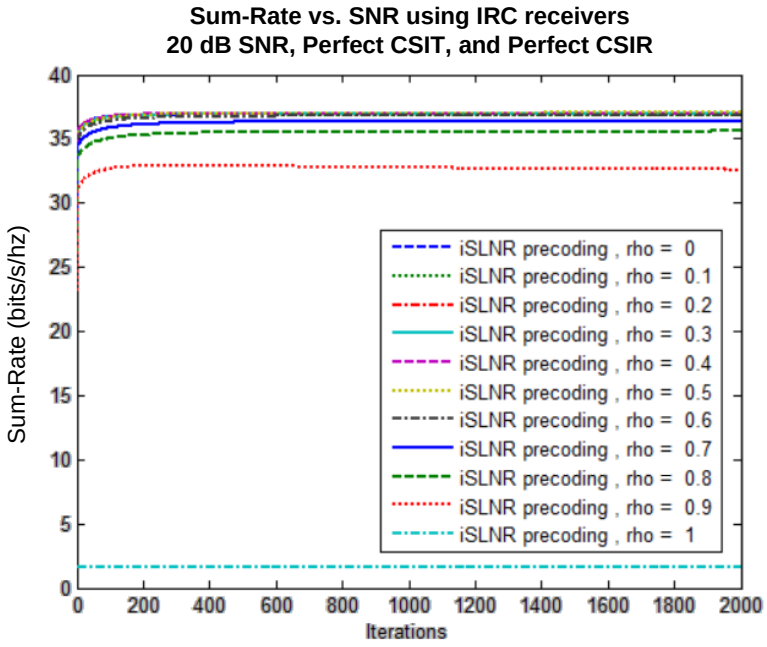

Figure 8.6: Sum-rate of 16x(4x4) system with varying transmit correlation

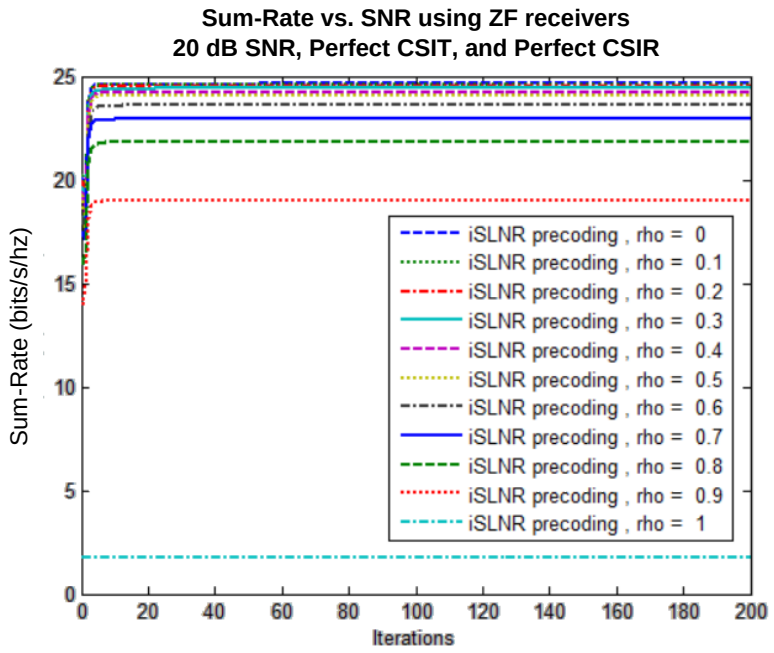

Figure 8.7: Sum-rate of 6x(3x3) system with ZF receivers and varying transmit correlation

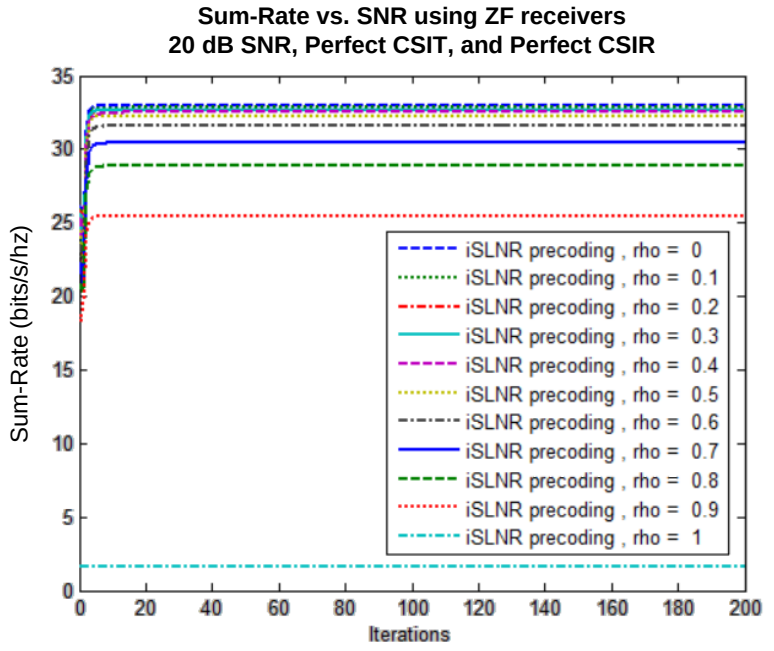

Figure 8.8: Sum-rate of 9x(3x4) system with ZF receivers and varying transmit correlation

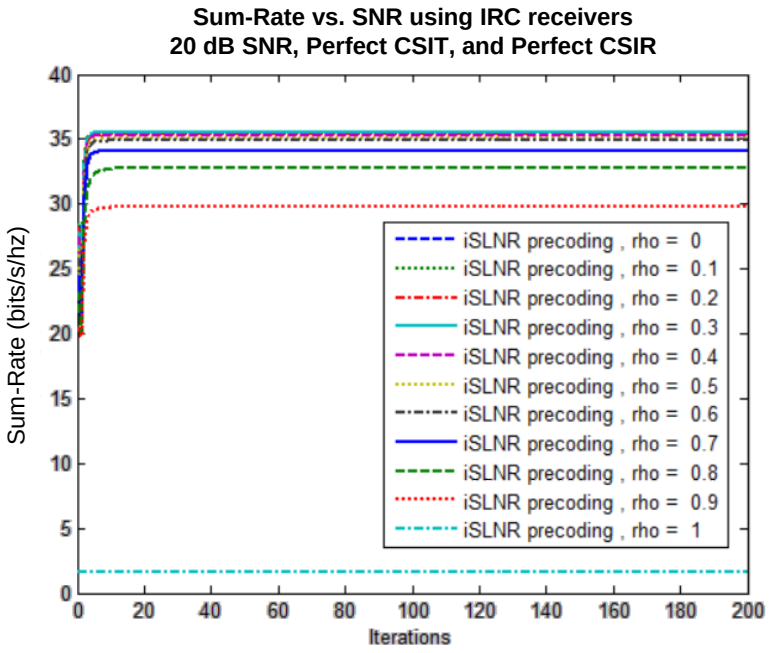

Figure 8.9: Sum-rate of 12x(4x4) system with ZF receivers and varying transmit correlation